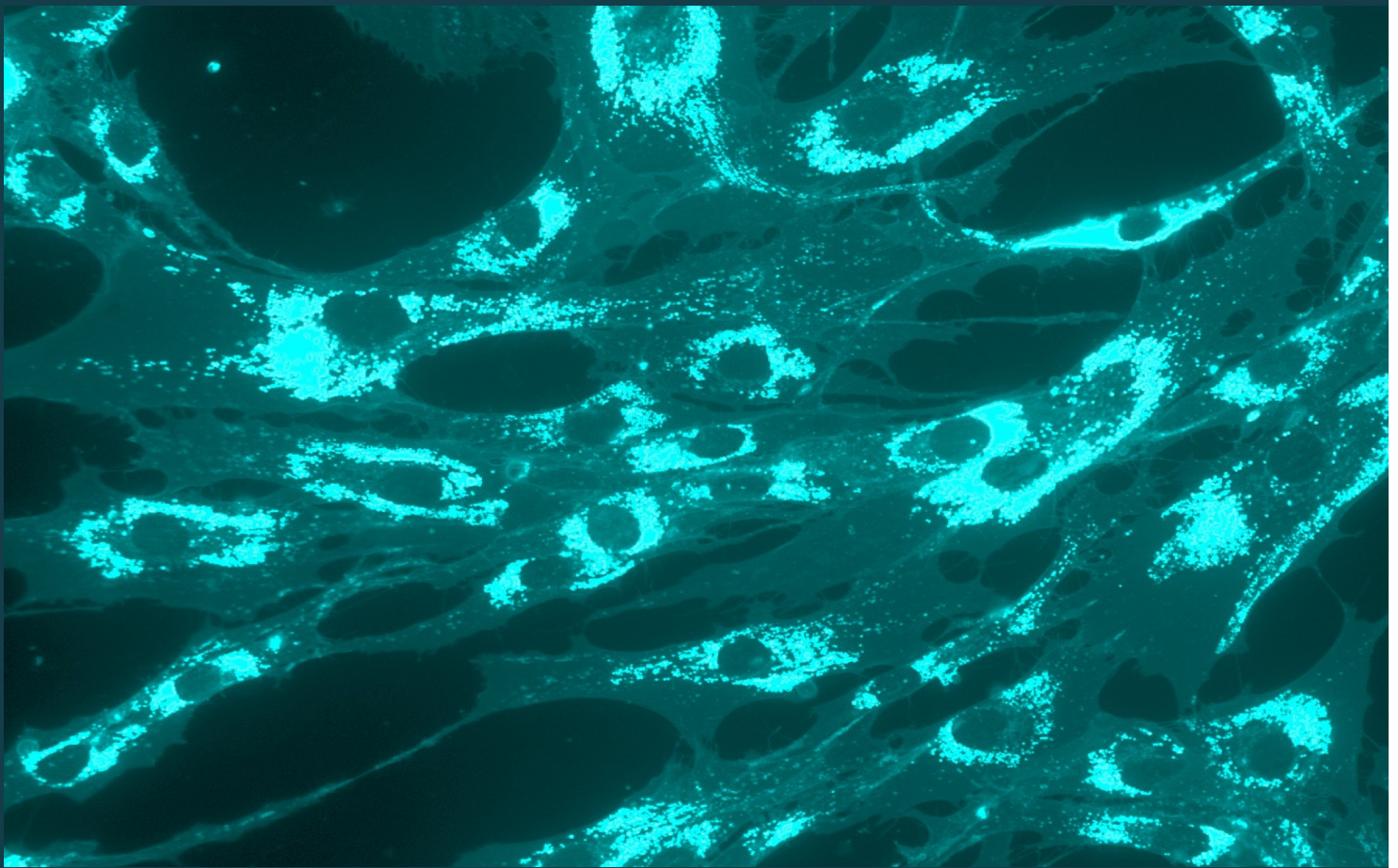


Viral Gene Therapy to Brain Capillary Endothelial Cells for Protein Secretion of Recombinant Niemann-Pick Type C2 Protein

– A Novel Strategy for Delivery of NPC2 to the Brain



Master's Thesis

Eva Hede Olsen
Medicine with industrial Specialization
Biomedicine

Aalborg University

**Medicine with Industrial
Specialization
Department of Health Science and
Technology**

**Aalborg University
Frederik Bajers Vej 7
9220 Aalborg Denmark**

Project title:

*“Viral Gene Therapy to Brain
Capillary Endothelial Cells for
Protein Secretion of Recombinant
Niemann-Pick Type C2 Protein
– A Novel Strategy for Delivery of
NPC2 to the Brain.”*

Project group:

17gr9031

Author:

Eva Hede Olsen

Supervisor:

Annette Burkhart Larsen
Assistant Professor

Co. Supervisor:

Torben Moos
Professor

Project delivery:

December 2nd 2017

Number of pages: 65

Number of Appendices: 2

Abstract

Secretion of recombinant protein towards the central nervous system (CNS) induced by viral gene modification of brain endothelial cells (BCECs), represents a novel strategy for drug delivery to the CNS, by circumventing the blood-brain-barrier (BBB). A relevant application of the strategy is the lysosomal storage disease, Niemann-Picks type C2, as it is a genetic disease caused by a deficiency of the soluble protein NPC2, resulting in accumulation of intracellular cholesterol, which causes both visceral symptoms and progressive neurodegeneration. Furthermore, the lysosomal storage has been observed to cause increased lysosomal biogenesis, with increased expression of lysosomal genes. Intravenous NPC2 replacement has been observed to reverse visceral but not CNS symptoms, due to an inability to cross the BBB. The aim of this study was, therefore, to investigate if BCECs could be genetically modified using a viral vector to induce secretion of recombinant NPC2 protein towards both the CNS and the circulation without compromising the barrier integrity in an *in vitro* BBB model and whether this could reverse cholesterol accumulations in NPC2 mutant fibroblasts.

NPC2 expression lentiviral vectors were produced and used to for gene modification of and *in vitro* BBB model. Gene modification efficiency was evaluated based on flow cytometry and immunocytochemical staining of NPC2. The barrier integrity was continuously measured based on trans-endothelial electrical resistance (TEER). Conditioned medium from transduced cells was used to treat NPC2 mutant human fibroblasts and cholesterol accumulations were examined by Filipin III staining of cholesterol. Furthermore, the relative gene expression of the lysosomal genes Lamp1 and MCOLN1 was examined in wildtype and NPC2 mutant fibroblast with or without NPC2 replacement. The *in vitro* BBB model was successfully transduced with produced NPC2 expression lentivira without compromising the barrier integrity in BBB model. Furthermore, the lentiviral vector seemed to induce a more stable long-term recombinant NPC2 expression compared to a non-viral vector. Cholesterol accumulations in NPC2 mutant fibroblasts were reversed following treatment with conditioned medium from genetically modified cells but a similar effect was observed following treatment with conditioned medium from non-modified cell due to an unexpectedly high natural secretion of endogenous NPC2. Signs of a therapeutic effect from secreted recombinant NPC2 was, however, seen from treatment with conditioned medium from the top chamber of the genetically modified BBB model. Moreover, MCOLN1 gene expression was increased in NPC2 mutant fibroblasts compared to wildtype, and seemed to decrease following NPC2 replacement, while no significant differences were observed for Lamp1 expression.

Preface

This master's thesis was based on original experimental data, generated at the Laboratory of Neurobiology at Aalborg University. The studies implemented in this thesis were based on previous studies of non-viral gene modifications of an *in vitro* BBB model based on primary rat brain endothelial cells (RBECS) at the Laboratory of Neurobiology at Aalborg University. However, this study represented the first attempts to genetically modify an *in vitro* BBB model using a viral approach in the Laboratory of Neurobiology at Aalborg University.

Acknowledgements

I would like to express my greatest acknowledgement to my main supervisor Annette Burkhart Larsen, for her invaluable professional and personal guidance throughout the entire project period. Her engagement and interest in this study has been both very inspirational and motivating and without her guidance and skilled advice with isolation of primary rat brain endothelial cells, constructions of *in vitro* BBB models, and flow cytometric analysis and microscopy this study would not have been possible. I would also like to thank my fellow student Christine Bodelund Christiansen for both relevant and interesting discussions concerning the study. Moreover, I would like to thank Hanne Krone Nielsen for her helpful advices with cell culturing and Merete Fredsgaard for her advice with quantitative polymerase chain reactions. A special thank goes to Esben Christensen for his skilled advice regarding the cloning procedures. Lastly, I would like to thank the entire group in Laboratory of Neurobiology at Aalborg University for their feedback and guidance at several group meetings as well as for their general helpfulness in the lab.

List of Abbreviations

AAV	Adeno-associated virus
BBB	Blood-brain barrier
BCEC	Brain capillary endothelial cell
bFGF	Basic fibroblast growth factor
CAG	Cytomegalovirus / β -actin
cAMP	Cyclic adenosine monophosphate
CBFA2T2	Core binding factor, alpha subunit 2, translocation partner 2
CHO	Chinese hamster ovary
CI-M6PR	Cation independent mannose-6-phosphate receptor
CLEAR	Coordinated Lysosomal Expression and Regulation
CMV	Cytomegalovirus
CNS	Central nervous system
DMEM	Dulbecco's Modified Eagle Medium
DMSO	Dimethylsulfoxid
DPEC	Diethylpyrocarbonate
ELISA	Enzyme-linked immunosorbent assay
ERT	Ezyme replacement therapy
FBS	Fetal bovine serum
GOLGA1	Golgin A1
HC	Hydrocortisone
HIV-1	Human immunodeficiency virus type 1
HPRT1	Hypoxanthine Phosphoribosyltransferase 1
HSV	Herpes simplex virus
HUVEC	Human umbilical vein endothelial cell
ICC	Immunocytochemistry
Lamp1	Lysosomal membrane protein 1
LTR	Long terminal repeat
MCOLN1	Mucolipin-1
MOI	Multiplicity of Infection
NEAA	Non-Essential Amino Acids
NPC1	Niemann-Pick type C1 protein
NPC2	Niemann-Pick type C2 protein
OPF	Orange fluorescent protein
PBS	Phosphate- buffered saline
PCR	Polymerase chain reaction
PRPF31	Pre-mRNA processing factor 3
RBEC	Primary rat brain endothelial cell
RG	Reference gene
RO	4-(3-Butoxy-4-methoxybenzyl)-2-imidazolidinone
RT-qPCR	Reverse Transcriptase Quantitative Polymerase Chain Reaction
TEER	Trans-endothelial electrical resistance
TFEB	Transcription factor EB
TJ	Tight junction
VSGP	Vertical supranuclear gaze palsy
VSV-G	Vesicular stomatitis virus G
ZNF5	Zinc finger protein 5
ZO-1	Zona occludens 1
α -SMA	α -smooth muscle actin

Table of Contents

1	Introduction.....	9
1.1	The Blood-Brain-Barrier	9
1.2	Gene Delivery to the Bran Capillary Endothelial Cells	11
1.3	Niemann-Picks disease type C2.....	14
2	Hypothesis.....	17
3	Materials	18
4	Methods.....	19
4.1	Cell growth.....	19
4.2	Production of NPC2 Lentiviral Vectors	22
4.3	Gene modification of <i>in vitro</i> Blood Brain Barrier Models	27
4.4	Flow Cytometry	28
4.5	Immunocytochemistry	28
4.6	NPC2 Replacement Assay.....	29
4.7	Reverse Transcriptase Quantitative Polymerase Chain Reaction.....	30
4.8	Statistics.....	31
5	Results	32
5.1	Production of NPC2 expression virus.....	32
5.2	Gene Modification of Primary Rat Brain Endothelial Cells	34
5.3	Integrity of <i>in-vitro</i> Blood-Brian-Barrier Model During Gene Modification	38
5.4	Characterization of Human Skin Fibroblasts.....	39
5.5	NPC2 Replacement Assays	40
6	Discussion	44
6.1	Production of NPC2 Lentiviral vectors	44
6.2	Lentiviral Gene Modification of Rat Brain Endothelial Cells	45
6.3	Possibly Stable Long-term Expression Following Lentiviral Gene Modification	47
6.4	Intact <i>in vitro</i> Blood-Brain-Barrier Integrity Following Lentiviral Gene Modification.....	48
6.5	Reversed Cholesterol Accumulation in NPC2 Mutant Fibroblasts Following Addition of Conditioned Medium from both Genetically Modified and Non-Modified Cells.....	49
6.6	Potential Quantitative Evaluation of the Therapeutic Effect of NPC2 Replacement Based on Relative Lysosomal Gene Expression	50
6.7	Future Perspectives – From <i>in vitro</i> to <i>in vivo</i>	51
6.8	Other Relevant Applications of the Proposed Strategy	52
7	Conclusion	53
8	References.....	53
	Appendix I	64
	Appendix II.....	65

1 Introduction

The need for new treatment options is highly relevant in several diseases affecting the central nervous system (CNS), including neurodegenerative disorders, CNS tumours, neurovascular diseases and neurological infections. However, development of such new treatments is complicated by the blood-brain-barrier (BBB) restricting the entry of substances into the CNS (1). The BBB is formed by brain capillary endothelial cells (BCECs) lining the microvasculature of the CNS. In close contact with pericytes and astrocytic end-feet, these comprise a physical and biological barrier separating the CNS from the circulation. The BBB is essential for the maintenance of a stable microenvironment within the CNS, which is required for optimal neuronal function, as well as for the protection from entry of potentially harmful substances (2–6). Due to the BBB, passive transport to the CNS is limited to small lipid-soluble molecules and gasses like oxygen and carbon dioxide, which comprises a major obstacle in the development of new therapeutics for CNS diseases (1,7,8).

Several different approaches to circumvent this obstacle have been explored, including temporarily increasing BBB permeability to increase the possibility of passive diffusion, completely by-passing the BBB by intraventricular administration, as well as exploiting existing transport mechanisms through BCECs (9,10). Temporarily increasing the permeability of the BBB may involve a risk of severe adverse events, due to a lack of specificity, while the use of intraventricular injections involves risks related to the surgery and anesthesia needed for this approach (1,11). In addition to that, limited diffusion within the extracellular space of the CNS, often lead to a poor distribution following such injections (9,12). Exploiting existing transcellular transport mechanisms thus seems more promising (1,9,11). However, these methods can be compromised by the efflux transport system of the BCECs, which transports a broad variety of molecules from the CNS to the circulation, ultimately causing transport of the therapeutics back into the circulation (11).

Rather than trying to circumvent the limitations caused by the BBB, another approach has been to genetically modify the BCECs comprising the BBB to produce and secrete therapeutic molecules to the CNS (10,13–15). Both viral and non-viral vectors have been investigated. Thomsen et al. used two different non-viral vectors to genetically modify monocultures of an immortalized human brain microvascular endothelial cell line (HBMEC) and a rat brain endothelial cell line (RBE4) to secrete human recombinant growth hormone 1, after which they were able to detect the recombinant growth hormone 1 in the medium (14). In addition to that, Jiang et al. were able to detect glial-derived neurotrophic factor (GDNF) secretion following transfection of a mouse brain endothelial cell line (MBEC4). In this study, MBEC4s monocultures were used as an *in vitro* BBB model in which they found secretion primarily to the brain side (13). Moreover, they were able to detect increased GDNF levels in the brain of mice following intracarotid injections of a non-viral GDNF gene therapy (13). On the contrary, Larsen et al. observed secretion of recombinant Erythropoietin mainly to the blood side following transfection of primary rat brain endothelial cells (RBECs) co-cultured with primary astrocytes in an *in vitro* BBB model (10). A viral approach was tried by Chen et al. who used an adeno associated virus (AAV) vector to induce expression of the protein, absent in a lysosomal storage disease mouse model, after which they observed disease improvement in some models (15). Genetically modifying the BCECs thus may represent a new potential route for drug delivery to the CNS.

1.1 The Blood-Brain-Barrier

As mentioned, the BBB comprises a physical and biological barrier separating the CNS from the circulation. The physical barrier is mainly formed by the BCECs, which differ from other endothelial cells due to their lack of fenestrations and formation of tight junctions (TJs) (3,9). TJs are located between adjacent BCECs towards the luminal side and entails blocking of the paracellular transport of large or hydrophilic molecules (3,16). As a result of the blocked transport of hydrophilic ions, the

BBB has a high transendothelial electrical resistance (TEER) compared to peripheral endothelial cells (3,17). The TJs are comprised of transmembrane proteins, including claudins, occludins and junction adhesion molecules, which are linked to the cytoskeleton by cytoplasmic plaque proteins including zona occludens (ZO) 1, 2 and 3, afadin and cingulin, see Figure 1(3,18). In addition to tight junctions, adherent junctions are connecting adjacent BCECs towards the abluminal side, contributing to the maintenance of TJs (11). Adherent junctions are comprised of the transmembrane cadherins, which are linked to the cytoskeleton via catenins and vinculin (11,19). In addition to the passive physical barrier formed primarily by TJs, the BCECs constitutes a biological barrier by expressing a large number of efflux transporter proteins restricting the unspecific passage of molecules that are able to penetrate the BCEC, by exporting such molecules from the CNS to the circulation (11). Furthermore, BCECs show a very low rate of pinocytotic activity (9).

Apart from BCECs, the BBB is also comprised of astrocytic end-feet and pericytes which, together with the perivascular neurons, constitutes the so-called neurovascular unit (20). Both astrocytic end-feet and pericytes have been shown to be important for the formation and maintenance of the BBB integrity (2,6,16,21). *In vitro* studies with BCECs have demonstrated induction of tight junction formation resulting from the presence of astrocytes or astrocyte conditioned medium (16). Moreover astrocytes secrete GDNF, transforming growth factor- β , basic fibroblast growth factor (bFGF) and angiopoitin-1, which are important for induction of the BBB phenotype (16). The importance of pericytes has also been demonstrated, as the reduced presence of pericytes has been shown to increase BBB permeability *in vivo* (6).

1.1.1.1 *In vitro* BBB models

Several *in vitro* BBB models have been developed in order to be able to investigate the characteristics and regulatory properties of the BBB. With the purpose of being able to mimic the *in vivo* situation as closely as possible, development of BBB models based on primary or low passage BCECs have been made using BCECs from rat (21,22), murine (23,24), porcine (25,26), bovine (27), and human brains (28). By cultivating BCECs on semipermeable hanging culture inserts a polarization can be induced with a defined apical membrane towards the top chamber, representing the blood side, as well as a basal membrane towards the bottom chamber, representing the brain side of the BBB (16,29). Furthermore, culturing the BCECs on hanging culture inserts, allows for co-culturing with astrocytes or triple-culturing with astrocytes and pericytes in order to increase the similarity to the *in vivo* conditions even more. Co-culturing with astrocytes has been shown to increase TEER and induce the BBB phenotype of BCECs (30,31), while the triple-culture mimics the *in vivo* condition even more and the addition of pericytes has been shown to moderately increase TEER values when compared to co-cultures with astrocytes (21,32).

To further increase the BBB integrity in the *in vitro* BBB models, a number of different soluble factors have been added to the culture medium. Addition of cyclic adenosine monophosphate (cAMP) have been shown to increase TEER. This effect can be even further improved by addition of the cAMP-specific phosphodiesterase type IV inhibitor 4-(3-Butoxy-4-methoxybenzyl)-2-imidazolidinone (RO) (30,33–35). Also, bFGF and hydrocortisone (HC) have been shown to increase *in vitro* barrier properties (34,36–39). The applicability of these models can be evaluated by assessment of the BCEC expression of characteristic transporters and TJ proteins like ZOs, claudins and occludin, as well as an assessment of the TEER and permeability to molecules like mannitol, sucrose, sodium fluorescein, and fluorescein-isothiocyanate (FITC)-dextran with different molecular weights (29). As TEER measurements may be influenced by several different factors, it can not necessarily be directly correlated to paracellular transport. Hence, TEER measurements alone cannot be used to determine the permeability of an *in vitro* BBB model (29,40).

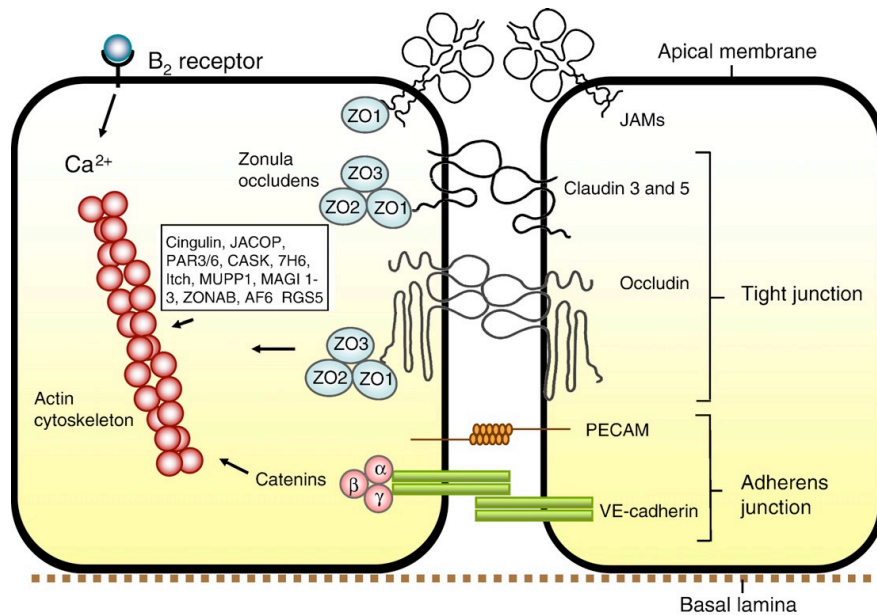


Figure 1. Tight junctions (TJ) and adherent junctions (AJ) connection the brain capillary endothelial cells (BCECs) in the Blood-Brain Barrier (BBB). TJs are formed by transmembrane proteins, including claudins, occludins and junction adhesion molecules (JAMs) which are anchored to the cytoskeleton by cytoplasmic plaque proteins including zona occludens (ZO) 1, 2 and 3, afadin (AF-6) and cingulin. AJs supports the maintenance of TJs, and are composed of platelet endothelial cell adhesion molecules (PECAMs) and Vascular endothelial (VE) cadherins linked to the cytoskeleton by catenins. Adapted from (3).

1.2 Gene Delivery to the Brain Capillary Endothelial Cells

As mentioned previously, gene modification of the BCECs has been proposed as a strategy for circumventing the limitations of drug delivery to the CNS, caused by the BBB (10,13–15). However, this strategy is highly dependent on the use of an optimal vector for gene delivery. The vector must be able to induce efficient delivery and transcription of genetic material as well as protection from degradation by nucleases and phagocytosis within the circulation. In addition to that, the gene delivery vector should be efficient enough to induce a large proportion of genetically modified BCECs in order to ensure a high biodistribution of the therapeutic molecule throughout the entire CNS. Furthermore, BCECs within the mature BBB are non-dividing which comprise an additional challenge, specific for this approach, as many vectors are dependent on cell division for effective gene modification (10,41).

Both viral and non-viral vectors have been studied extensively throughout the years of which viral vectors have dominated the field due to a low efficiency of the non-viral vectors (41,42). Although improvements have been made within the non-viral vector approach, non-viral vector gene therapy is still associated with significant drawbacks when compared to viral gene therapy. Viral gene therapy generally results in a higher proportion of genetically modified cells and thus a higher gene expression (41,42). Furthermore, some viral vectors possess a natural ability to efficiently by-pass cellular membranes in order to transport their genetic material to the cell nucleus, making such vectors less dependent on cell division. Non-viral vectors are on the contrary typically transported to the endosomes upon cell internalization and must be capable of endosomal escape for cytoplasmic delivery of the genetic material (43). However, transport to the cell nucleus is still needed in order to induce subsequent gene expression. Furthermore, some viral vectors are capable of integrating into the host genome and thereby induce long-term gene expression (41,42). A major advantage of non-viral vectors however, is their low immunogenicity (10,41,44). Nevertheless, the higher gene modification efficiency combined with a possible stable long-term gene expression of some viral vectors, make these particularly attractive in relation to gene delivery to the BCECs (45,46).

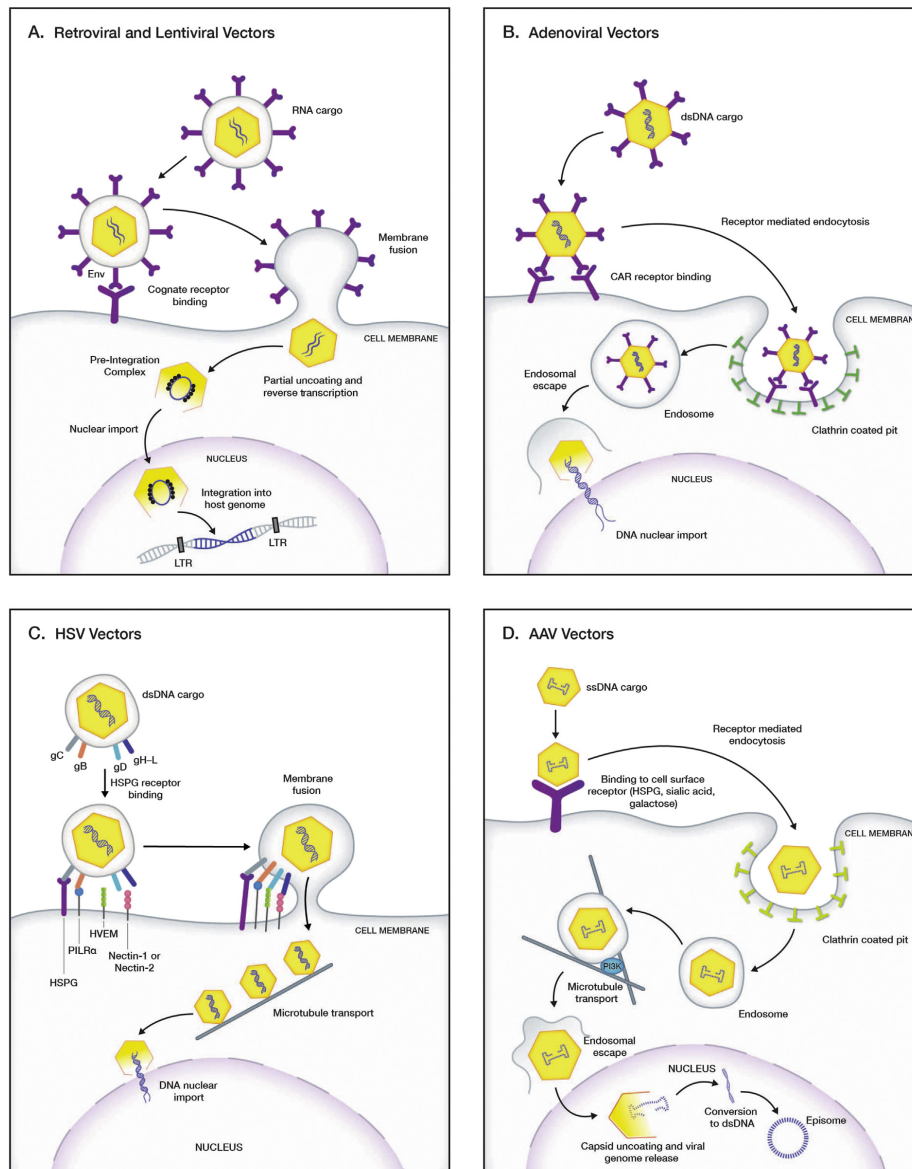


Figure 2. Schematic overview of the viral mechanisms for cell entering and delivery of genetic material into host cells. **A: Mechanism used by retro- and lentiviral vectors.** Vectors bind to the cell surface via glycoproteins expressed on the lipid envelope surrounding the viral capsid, which induces fusion of the envelope with the cellular membrane and release of the viral capsid into the cytoplasm. The RNA transgene is then reverse transcribed into DNA which is then released from the capsid and transported into the nucleus where it integrates into the host cell genome, to induce transgene expression. **B: Mechanism used by adenoviral vectors.** Fiber knobs on the capsid surface are used to bind to the cell surface to induce endocytosis. Endosomal escape of the partially degraded viral capsid is triggered by a decreased pH in the endosome, after which the double-stranded DNA transgene is delivered to the cell nucleus from the viral capsid through nuclear pores, to induce a transient transgene expression. **C: Mechanism used by HSV vectors.** The viral vector attaches to the cell surface through specific glycoproteins on the surface of the viral envelope, which induces fusion with the cell membrane and release of the viral capsid to the cytoplasm. Subsequently, the viral capsid is transported to the cell nucleus via microtubules within the cytoplasm followed by release of the double-stranded DNA into the nucleus through nuclear pores in order to finally induce transgene expression. **D: Mechanism used by AAV vectors.** The viral capsid is attached to the cell surface via different cell surface receptor ligands, which vary among different AAV serotypes. Receptor binding then induces endocytosis followed by a release of the partially degraded capsid from the endosome, in response to a decreased pH. The released partially degraded capsid is then transported into the cell nucleus where viral double-stranded DNA is preserved, to induce stable episomal transgene expression. CAR – coxsackievirus and adenovirus receptor, Env - envelope glycoprotein, HSPG – heparin sulfate glycoprotein, HVEM – herpesvirus entry mediator, LTR – long terminal repeats, PI3K – phosphatidylinositol-3 kinase, PILRa – paired immunoglobulin-like type 2 receptor- α . Adapted from (42).

The natural mechanism by which viruses are able to efficiently deliver their genetic material to a host cell varies between different classes of virus, see Figure 2. Viruses like adenoviruses and AAVs contain a protein capsid, which is internalized by receptor-mediated endocytosis for which reason they have developed refined methods for endosomal escape and subsequent delivery of their DNA to the cell nucleus (42,46). Other viruses like, retrovirus, lentivirus and herpes simplex virus (HSV) have a protein capsid sealed in a lipid membrane envelope, enabling fusion with the cell membrane after which their genetic material is released into the cytoplasm for either direct delivery of DNA to the nucleus, for HSV, or reverse transcription to DNA, in the case of retro- or lentiviruses, followed by transport to the nucleus (42). Yet, it is exactly these mechanisms that are exploited when using viral vectors for gene delivery. By removing the viral genes to keep only the packaging signals, viral vectors can be packaged *in vitro* in the presence of helper plasmids, containing the viral genes for virus structure and replication. In this way, the finally packaged viral vectors do not contain any viral genes. Several potential viral gene therapy vectors have been investigated throughout the years, but in clinical trials, the most commonly used viral vectors include adenoviral vectors, HSV type 1 vectors, AAV vectors, retroviral vectors, and lentiviral vectors (41,42).

Adenoviral vectors can be produced with high viral titers with a large packaging capacity of up to 36 kb after removal of viral genes, which constitutes one of the major advantages of using these for gene delivery (41,42,46). Furthermore, they have been shown to be able to induce a stable gene expression in the brain for up to one year, even though they do not integrate their genetic material into the host cell genome (47). However, adenovirus possess an ability to provoke a strong immune response, which can result in severe adverse events (48–50). In a clinical trial with ornithine transcarbamylase (OTC) deficient patients, an adenoviral vector was used to deliver the normal OTC gene, which led the death of one patient due to severe inflammation and cytotoxicity (51). The use of adenoviral vectors for gene delivery to the CNS have therefore been limited due to the high immunogenicity (41,42).

HSV-1 vectors are on the contrary considered attractive candidates for neurological gene therapy due to a natural affinity towards neurons (52,53). They entail both recombinant HSV-1 vectors and HSV-1 amplicons, of which HSV-1 vectors can be produced with high titers but with relatively low loading capacities, while HSV-1 amplicons have a high loading capacity but are in turn difficult to generate with high titers (54,55). Despite the relatively low loading capacity, recombinant HSV-1 vectors have however been used in a wide range of neurological disorders (56).

AAV vectors are currently among the most commonly used viral vectors for CNS clinical trials (41,42). They are based on the non-pathogenic AAVs and express a very low immunogenicity which, is one of the major advantages of these vectors (57). AAV vectors include a large number of serotypes with different tissue tropism (45). Furthermore, AAV vectors are able to induce gene expression in both dividing and non-dividing cells and stable expression have been observed for more than 10 years in human brain following administration of an AAV vector based on AAV serotype 2 (58). AAV vectors can generally be produced at very high titers (59,60). However, the major drawback of AAV vectors is a very small packaging capacity which constitutes considerable limitations regarding possible applications (41,42). Furthermore, AAV neutralizing antibodies are found in up to 70 % of healthy individuals, depending on the AAV serotype and ethnography, which constitutes a major limitation to these vectors (61,62).

Retroviral vectors possess a relatively large loading capacity, but can only be produced with fairly low titers. Moreover, they are not considered as relevant candidates for CNS gene therapy as they are unable to genetically modify non-dividing cells. Gene expression following retroviral vector delivery implies integration into the host genome, which may be considered as an advantage due to the possibility of long-term expression. However, retroviral integration involves a significant risk of mutagenesis, due to a combination of the presence of long terminal repeat (LTR) regions with

enhancer properties and a tendency to integrate into promoter regions of genes (63). In a clinical trial with children suffering from X-linked severe combined immune deficiency, administration of retroviral gene therapy resulted in development of leukemia in some patients due to activation of a pro-oncogene caused by viral integration (64).

Lentiviral vectors are developed from human immunodeficiency virus type 1 (HIV-1), but with several modifications (41). Lentiviral vectors also integrate into the host genome, but contrary to retroviral vectors they are designed to eradicate LTR regions by self-inactivation and preferentially integrate into introns of active genes, which leads to a markedly reduced risk of mutagenesis (65,66). Similar to retroviral vectors, lentiviral vectors are produced with moderately low titers, however by pseudotyping with the vesicular stomatitis virus G (VSV-G) envelope protein they can be purified with higher titers than retroviral vectors (42,67). Due to the relatively large size of lentiviral vectors, the tissue distribution following direct injections to the brain is limited (42,46). However, this is considered less relevant in case of administration via the circulation. Like AAV vectors, lentiviral vectors are able to infect both dividing and non-dividing cells (41,42). However, the long-term expression resulting from viral integration of genetic material delivered by lentiviral vectors makes these more advantageous in case of chronic and genetic diseases in which permanent gene modification would be preferred.

1.3 Niemann-Picks disease type C2

Niemann-Picks disease type C2 is a lysosomal storage disease, which constitutes a group of diseases caused by lysosomal dysfunctions due to enzymatic or non-enzymatic deficiencies (68). In Niemann-Picks disease type C2, the lysosomal dysfunction is caused by deficiency of the soluble lysosomal cholesterol transporter NPC2, due to mutations in the NPC2 gene (68–71). The disease is inherited in an autosomal recessive manner and is considered a very rare disease (72). The clinical incidence of Niemann-Picks disease type C is estimated to be 1:104.000, of which mutations in the NPC2 gene comprises 5% of the cases, while 95 % of the cases are caused by mutations in the NPC1 gene (72). The NPC2 gene is located on chromosome 14 and is 13.5 kb long including five exons. Several different mutations have been observed leading to phenotypes with varying severity (69). In combination with NPC1, the NPC2 protein is involved in the lysosomal transport of cholesterol. However, the exact function of the proteins remains unclear (71,73–75). While NPC1 is a large membrane-bound protein, NPC2 is a small soluble protein consisting of 132 amino acids (71). Upon folding, NPC2 consists of two beta-sheets, formed by a total of seven beta-strands, which constitutes a beta-sandwich as depicted in Figure 4. Within the beta-sandwich, a cholesterol-binding pocket is formed by amino acids with hydrophobic sides chains. Three of these have been found essential for cholesterol binding (71,76,77). NPC2 is a highly preserved protein, which is illustrated by alignment of protein sequences from different species showing a minimal variation between species, see Figure 4. Functionally essential regions are all similar between human, bovine, mouse and rat NPC2 protein, with a few exceptions for rat and bovine NPC2. However, in these cases hydrophobic amino acids included in the formation of the cholesterol-binding pocket are substituted with other hydrophobic amino acids, hence the implication on protein function is considered minimal.

Newly synthesized NPC2 is phosphorylated within the Golgi apparatus by addition of mannose-6-phosphate residues. Phosphorylated NPC2 then binds to the 300 kDa cation-independent-mannose-6-phosphate receptor (CI-M6PR) within the Golgi apparatus after which it is either transported to the lysosomes or secreted from the cell (71,78). Secreted NPC2 can then be taken up by CI-M6PRs located in the cell membranes after which it is transported to the lysosomes (78). Within the cells, NPC2 mediates the transport of endocytosed cholesterol from the lysosomes in combination with NPC1, as illustrated in Figure 3. Both NPC1 and NPC2 must be present for processing of endocytosed cholesterol, as NPC2 appears to be responsible for effective binding of cholesterol to NPC1 (79,80).

Thus mutations in any of the two proteins result in similar cellular dysfunctions, which include cholesterol accumulations as well as altered sphingomyelin metabolism and accumulation of glycolipids and free sphingomyosine (72). The cellular dysfunctions lead to heterogeneous presentations of both visceral symptoms, including hepato- and splenomegaly, and progressive neurodegeneration, which is the most common cause of death (72). However, the severity of symptoms varies greatly and the survival is varying from a few days to over 60 years of age (73,81). The neurodegeneration leads to the development of a severe neurologic disease with neurological symptoms including cerebellar ataxia, dysplasia, dysarthria, progressive dementia, and a characteristic vertical supranuclear gaze palsy (VSGP) (72,82). Due to the heterogenic presentation of symptoms and varying severity, the disease has been classified into an early infantile, late infantile, juvenile and adult form based on the age of onset of neurological symptoms (72). In addition to the accumulation of cholesterol and sphingolipids, increased expression of lysosomal genes has been observed in response to lysosomal accumulation. Lysosomal gene expression has been found to be coordinated via a Coordinated Lysosomal Expression and Regulation (CLEAR) consensus sequence, which is regulated by the transcription factor EB (TFEB) (83,84). Furthermore, TFEB has been found to translocate from the cytoplasm to the cell nucleus in response to accumulation of undegraded molecules within the lysosomes, leading to the transcription of different lysosomal genes, including lysosomal membrane protein 1 (Lamp1) and mucopolin-1 (MCOLN1) (84). Lamp1 is considered a marker for lysosomal biogenesis and MCOLN1 comprises a lysosomal calcium channel, which is believed to be involved in the late endocytic pathway and regulation of lysosomal exocytosis (84,85). Niemann-Picks disease type C2 is believed to be significantly underdiagnosed due to a lack of clinical awareness (72). However, when Niemann-Picks disease is suspected, initial testing implies a Filipin III staining of cholesterol in cultured skin fibroblasts from a biopsy, to investigate the presence of perinuclear cholesterol accumulations. Subsequently, the NPC1 and NPC2 genes can be sequenced to further investigate the presence of mutations within these (81).

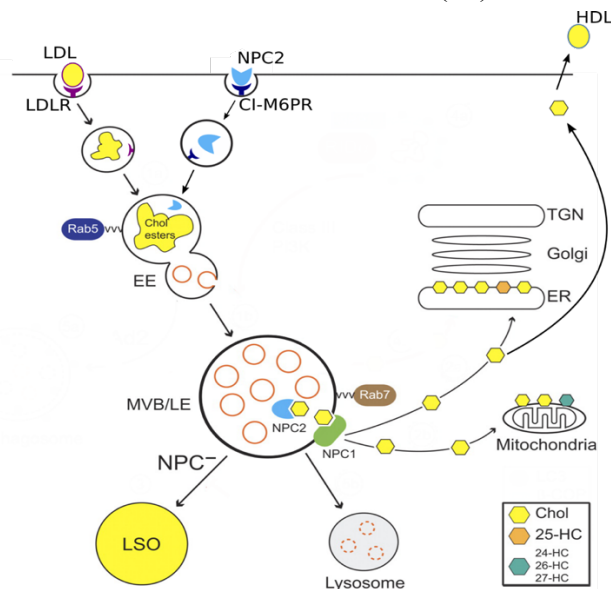


Figure 3: Intracellular cholesterol transport. Cholesterol (Chol) esters from low density lipoproteins (LDL) are endocytosed via the LDL-receptor (LDLR), un-esterified and transported to the multivesicular body (MVB)/late endosome (LE). Membrane bound NPC1 and soluble NPC2, which has either been synthesized by the cell itself or internalized via the CI-M6PR, then transports cholesterol to the mitochondria where it is converted to other oxysterols, to the endoplasmic reticulum (ER) where it is sensed by the cholesterol homeostatic machinery, or to the plasma membrane from which it can be transported by high density lipoproteins (HDL). Mutations in either NPC1 or NPC2 inhibits this transport of cholesterol, resulting in the formation of lysosomal storage organelles (LSO). Modified and adapted from (86).

The current treatment of NPC2 is however mainly symptomatic (72). The only specific treatment which has been approved is the glucosylceramide synthase inhibitor, Miglustat which can delay the onset of symptoms and thus increase survival, but without curing the disease (72,87). The only way to cure the disease would be by efficiently delivering the lacking NPC2 protein to especially the neuronal cells. In other lysosomal storage disorders, enzyme replacement therapy (ERT) has been used, however with varying results (82,88,89). Efficient ERT relies on the ability of cells to take up extracellular lysosomal enzymes and subsequently transport these to the lysosomes (90). This approach has previously been tested in a mouse model of Niemann-Picks disease type C2 (91). While several visceral improvements were observed upon systemic delivery of bovine NPC2 protein, purified from milk, no significant effects could be observed in the CNS, probably due to the BBB (91). Furthermore, it has previously been suggested that correction of the protein deficiency by gene therapy in some cells might result in correction of the deficiency in neighbouring cells too. A process referred to as cross-correction, which is possible due to the ability of cells to take up extracellular lysosomal enzymes and subsequently transport these to the lysosomes (78).

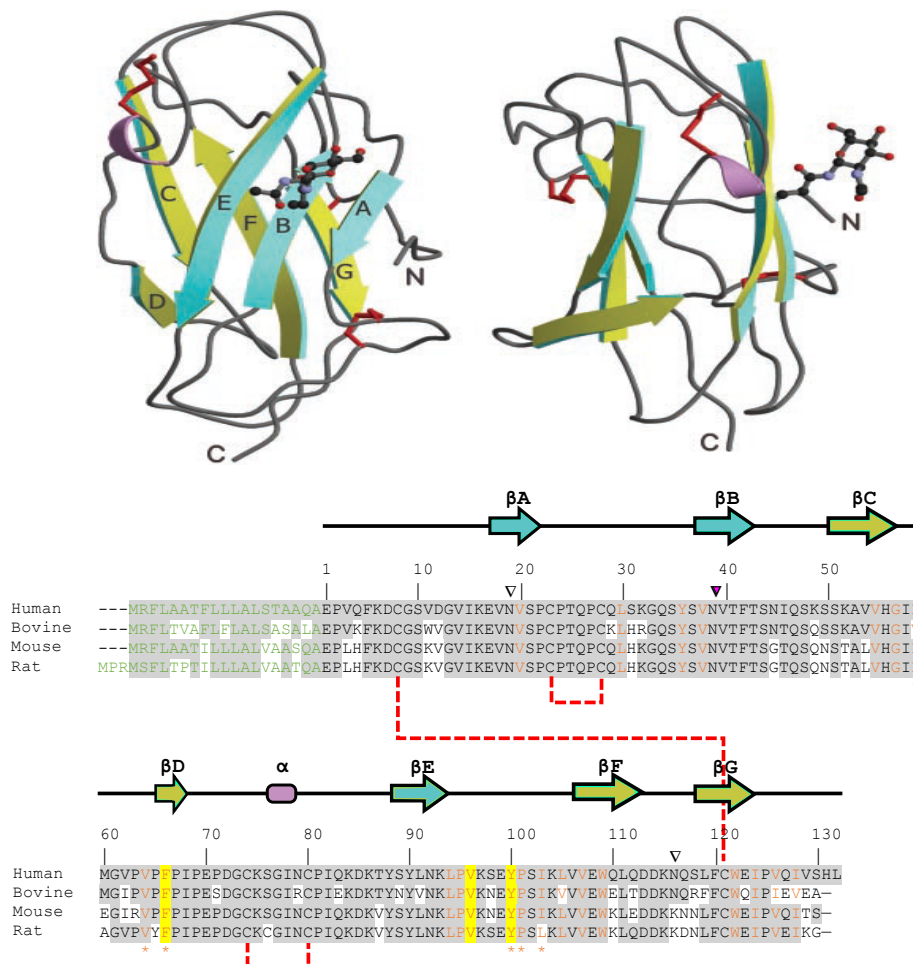


Figure 4. Structure of NPC2 protein. The two beta-sheets constituting the structural basis for the cholesterol binding pocket are marked in cyan and yellow. The alpha-helix is marked in purple. Disulphide bridges formed by cysteine residues are shown in red. **Top:** 3D structure of bovine NPC2 shown with 90 degree rotation and functionally important glycosylation site shown in ball-and-stick representation. Adapted from (92). **Bottom:** Sequence alignment of human, bovine, mouse, and rat NPC2 shown with identical residues marked in grey and residues differing from the human NPC2 sequence marked in white. Numbering starts with the first residue after the signalling peptide, which is shown in green letters. Glycosylation sites are marked with a triangle of which the functionally important site at Asn-39 is marked in magenta (70). Hydrophobic residues forming the cholesterol-binding pocket are marked with orange letters of which those forming the outer rim of the binding pocket are marked with a star and the cholesterol-binding residues are marked in bright yellow (72,76,77,93). NPC2 protein sequences were obtained from NCBI reference sequences NP_006423.1 (human), NP_776343.1 (bovine) NP_075898.1 (mouse) and NP_775141.2 (rat).

2 Hypothesis

As mentioned above, genetically modifying BCECs may represent a new potential route for drug delivery to the CNS. However further investigations of this approach are still needed to evaluate its full potential. Niemann-Picks disease type C2 comprises an obvious candidate for such further investigations, as it is caused by the deficiency of a small secretory protein, which can be taken up by the CI-M6PR to correct cellular dysfunctions in deficient cells. However, without being able to cross the BBB. Furthermore, a viral vector currently seems like the most promising approach due to a higher efficiency and thus higher gene expression, compared to non-viral vectors, as well as a potential long-term expression of genes.

Based on this, the hypothesis in this study was that BCECs could be genetically modified without compromising the BBB integrity in an *in vitro* BBB model using a viral vector to induce secretion of recombinant NPC2 protein towards both the CNS and the circulation, which could reverse cholesterol accumulations in NPC2 mutant fibroblasts.

The hypothesis was tested using primary rat brain endothelial cells (RBECs) in mono- and co-cultures, of which the co-cultures would allow for examination of both the RBEC barrier integrity as well as the secretion towards the CNS (abluminal) and circulation (luminal). In addition, HeLa cells were included as a positive control as they are easily genetically modified (94).

Gene modifications were done using a lentiviral vector, as it seemed to be the most favourable approach for correction of the NPC2 deficiency, due to its previously described abilities to infect non-dividing cells and induce a long-term expression resulting from integration into the host genome. Non-viral gene modifications were included for comparison. These were based on the commercially available Lipofectamine™ 3000, as this had previously been shown to result in a relative high transfection efficiency without compromising the BBB integrity when compared to other non-viral vectors (10). Gene modification efficiencies were estimated using flow cytometry, while the RBEC barrier integrity was examined based on immunocytochemistry (ICC) and measurements of the TEER.

Wildtype and NPC2 mutant fibroblasts were initially categorized and used to examine the therapeutic effect of recombinant NPC2 protein secreted from genetically modified cells. Filipin III staining of cholesterol was used to examine cholesterol accumulations, as an indicator of the therapeutic effect and bovine NPC2 (bNPC2) protein was included as a positive control, since it had previously been shown to be able to reverse the cholesterol accumulation (91). Finally, the potential of using the relative expression of the lysosomal genes Lamp1 and MCOLN1 as an indication of the therapeutic effect of NPC2 replacement was examined by quantitative gene expression analysis.

3 Materials

The following reagents were purchased from Life Technology (Nærum, Denmark, DK): Blasticidin (Cat. No. R21001), dNTP Mix (Cat. No. R0191), DreamTaq Green PCR Master Mix (Cat. No. K1081), Dulbecco's Modified Eagle Medium (DMEM) (Cat. No. 21885), Dulbecco's Modified Eagle Medium/Nutrient Mixture F12 (DMEM/F12) (Cat. No. 11320033), FastDigest BamHI (Cat. No. FD0054), FastDigest XhoI (Cat. No. FD0694), FastDigest Green Buffer 10X (Cat. No. B72), Fetal Bovine Serum (FBS) (Cat. No. 10500064), GeneJet Gel Extraction Kit (Cat. No. K0691), GeneRuler 1kb DNA ladder (Cat. No. SM0310), GeneJET Plasmid Miniprep Kit (Cat. No. K0502), GeneJet RNA purification kit (Cat. No. K0731), HEK 293FT Cells (Cat. No. R700-07), Lipofectamine™ 3000 (Cat. No. L3000), Maxima H Minus First-strand cDNA Synthesis Kit (Cat. No. K1651), Maxima SYBR Green/ROX qPCR Master Mix (2X) (Cat. No. K0223), Non-Essential Amino Acid (NEAA) solution 100X (Cat. No. 11140050), Opti-MEM™ Reduced Serum Medium (Cat. No. 31985070), Phosphate-buffered Saline (PBS) 10X (SH3025802), Phusion GC buffer 5X (Cat. No. F-519), Phusion High-Fidelity DNA Polymerase (Cat. No. F-530S), RPMI 1640 Medium, GlutaMAX™ (Cat. No. 61870-010), RNase-free DNase I (Cat. No. EN0525), Trypsin (Cat. No. 15090-46), pLenti6/V5 Directional TOPO Cloning Kit (#K4955-10), One Shot Stbl3 chemically competent E.coli (#K4955-10), ViraPower™ Lentiviral Directional TOPO™ Expression Kit (#K4950-00), Virapower Packaging Mix (#K497500), Penicillin-streptomycin (10,000 U/ml) (Cat. No. 15140122), Rabbit-anti-zona occidens (ZO-1) (#61-7300), Alexa 488 conjugated Goat-anti-rabbit-IgG (Cat. No. A11034), Alexa 594 conjugated Goat-anti-mouse-IgG (Cat. No. A11037). The following reagents were purchased from Sigma-Aldrich (Brøndby, Denmark, DK): Collagen type IV (Cat. No. C5533), Collagenase/Dispase (Cat. No. COLLDISP-RO), Crystal Violet (Cat. No. C0775), CTP- cAMP (Cat.No. C3912), Dimethyl Sulfoxide (Cat. No. D2650), Dulbecco's Modified Eagle medium – High glucose (Cat. No. D5796), Fibronectin (Cat. No. F1141), Filipin III from *Streptomyces filipinensis* (Cat No. F4767), Geneticin, G 418 disulfate salt (Cat. No. A1720), Heparin (Cat. No. H3149), Hydrocortisone (Cat. No. H4001), Insulin-transferrin sodium selenite (Cat. No. 110745470001), L-glutamine (Cat. No. G8540), Paraformaldehyde (Cat. No. 441244), Poly(ethylene) glycol (PEG) (Cat. No. 81260), Percoll® (Cat No. P1644), Poly-L-lysine (Cat. No. P6282), Puromycin (Cat. No. P8833), Gentamicin Sulphate (Cat. No. G1264), Triton™ X-100 (Cat. No. X100), Whatman® cellulose chromatography paper, 3 mm (Cat. No. Z270849), 2-(4-amidinophenyl)-1H-indole-6-carboximidine (DAPI) (Cat. No. D9542), 4-(3-Butoxy-4-methoxybenzyl)-2-imidazolidinone (RO-201724) (Cat. No. B8279), Mouse-anti-human α -SMA (Cat. No. A5228-2). Rabbit-anti-human NPC2 (Cat. No. TA332678) was purchased from BioNordika Denmark A/S, Herlev, Denmark, DK. Basic fibroblast growth factor (bFGF) (Cat. No. 100-18B) was purchased from PreproTech Nordic (Stockholm, Sweden, SE). Bovine Serum Albumin (Cat No. EQBAH62) was purchased from Europa Bioproducts (Cambridge, United Kingdom, UK). plasma derived bovine serum (Cat. No. 60-00-810) was from First Link Ltd., Wolverhampton, United Kingdom, UK. Gentamicin Sulphate (Cat. No. 17-518Z) was from Lonza Copenhagen, (Vallensbæk Strand, Denmark, DK). CytoFLEX Daily QC Fluorospheres (Cat. No. B53230) were from Beckman Coulter (Copenhagen, Denmark, DK). Fluorescence mounting media (Cat. No. S3023) and Mouse-anti-human vimentin (Cat. Nr. Mo725) were purchased from DAKO (Glostrup, Denmark, DK). Mouse NPC2 gene cDNA plasmid pCMV3-mNPC2-OFPSpark was from Sino Biological Inc. (Cat. No. MG52313-ACR). Macherey–Nagel NucleoBond Xtra Midi EF plasmid DNA purification kit (#740420.50) was purchased from AH Diagnostics (Aarhus, Denmark, DK). GelRed™ Nucleic Acid Stain, 10,000X (Cat. No. 41003) was from Bio Trend (Köln, Germany, D).

4 Methods

4.1 Cell growth

Cell cultures were maintained at 37°C and 5% CO₂ in different culture medium according to the cell type. All culture medium was sterile filtered through a 0.22 µm polyethersulfone vacuum filter. The cells were successively passaged in T75 and 175 flasks by trypsinization at 37°C with trypsin diluted 1:10 in 1X PBS until cells detached, after which trypsin was inhibited by addition of culture medium, diluting the trypsin at least 4 times. Details regarding the different cell types used are described in the following sections.

4.1.1.1 Growth of 293FT HEK cells

HEK 293FT cells were used for the production of NPC2 expression vira. HEK 293FT cells are favorable for virus production, as they express the adenovirus gene E1A as a result of transformation with human adenovirus type 5, which stimulate DNA replication, and stably express the SV40 large T antigen which causes promotion of DNA replication by inactivation of tumor suppressor genes (95,96). Furthermore, the HEK 293FT cells stably express the neomycin resistance gene, which is controlled by the SV40 promoter and is used to maintain the expression of the SV40 large T antigen by geneticin selection (97). HEK 293FT cells were grown in HEK culture medium consisting of DMEM– High glucose supplemented with 10 % FBS, 1X MEM Non-Essential Amino Acids (NEAA) Solution, and 0.025 mg/mL gentamicin sulphate. Upon thawing, the HEK 293FT cells were initially seeded in T75 flasks and maintained at 37° C and 5% CO₂ for 24 hours after which, the medium was replaced with fresh HEK culture medium supplemented with 500ug/mL Geneticin for selection.

4.1.1.2 Growth of primary rat astrocytes

Primary rat brain astrocytes were kindly provided by Annette Burkhart Larsen, Laboratory of Neurobiology at Aalborg University (30). The cells were grown in astrocyte culture medium consisting of DMEM – Low glucose, supplemented with 10% FBS and 1.25 mg/ml gentamicin sulphate. Primary astrocytes were seeded onto poly-l-lysine coated 12 well culture plates at a cell density of 3 x 10⁴ cells/cm² for a minimum of two weeks before being used in co-cultures. The primary astrocytes were kept in culture for up to three months, during which they were used in several co-cultures, however with at least one week in between each co-culture.

4.1.1.3 Isolation of Primary Rat Brain Endothelial Cells

2-3 weeks old Sprague-Dawley rats were used for isolation of Rat Brain Endothelial Cells (RBECS). Initially, the animals were anesthetized with isoflurane and the heads were rinsed in 96 % ethanol after which the rats were decapitated. Forebrains were taken out with dissecting forceps and put into a dish containing 1X PBS on ice. The forebrains were cut in half and meninges were removed by gently spreading half of a brain on sterile 3 mm chromatography paper. The tissue was then transferred to a dish containing DMEM/F12 and cut into small pieces using sterile scalpels. The tissue was enzymatically digested at 37°C and 280 rpm for 75 minutes by collagenase II and DNase I diluted in DMEM/F12. The digestion was terminated by further dilution of enzymes in DMEM/F12, followed by centrifugation at 1000 x g for 8 minutes to pellet the digested tissue. Microvessels were then separated by resuspension of the pellet in 20% bovine serum albumin in DMEM/F12 and centrifugation at 1000 x g for 20 minutes, by which microvessels were pelleted while a thick myelin layer containing neurons and glial cells, was located on top of the supernatant. The supernatant including myelin layer was discarded and microvessels were further digested in DMEM/F12 containing 1 mg/mL collagenase/dispase and 6.67 µg/mL DNase I in DMEM/F12 at 37°C and 250

rpm for 50 min. Again, digestion was terminated by addition of DMEM/F12 followed by centrifugation at 1000 x g for 7 minutes. Double digested microvessel fragments were then resuspended in DMEM/F12 and separated on a 33 % Percoll[®] gradient by centrifugation at 1000 x g for 10 minutes. The microvessel fragments were collected with a syringe from a whitish layer observed at the bottom of the tube, located just above a red layer, containing the red blood cells and pericytes. Collected microvessel fragments were then washed twice in DMEM/F12 by centrifugation at 1000 x g for 10 minutes and 700 x g for 7 minutes. Isolated microvessels were then either frozen in Fetal Bovine Serum (FBS) with 10 % dimethyl sulfoxide (DMSO) and stored at -140°C or used directly for construction of BBB models by resuspending the pellet in RBEC culture medium consisting of DMEM/F12 supplemented with 10 % plasma-derived bovine serum, 0.2 µg/ml heparin, 0.1 mg/ml insulin-transferrin-selenium, 1.25 mg/ml gentamicin sulfate and 1 ng/ml freshly added bFGF. Isolated microvessels in RBEC culture medium were seeded onto collagen IV and fibronectin precoated T-75 flasks. 4 µg/ml puromycin was added to the RBEC culture media for the first 3 days to ensure a pure culture of RBECs by exploiting their ability to thrive under the presence of puromycin due to their high expression of efflux pumps, which is not the case for pericytes (98).

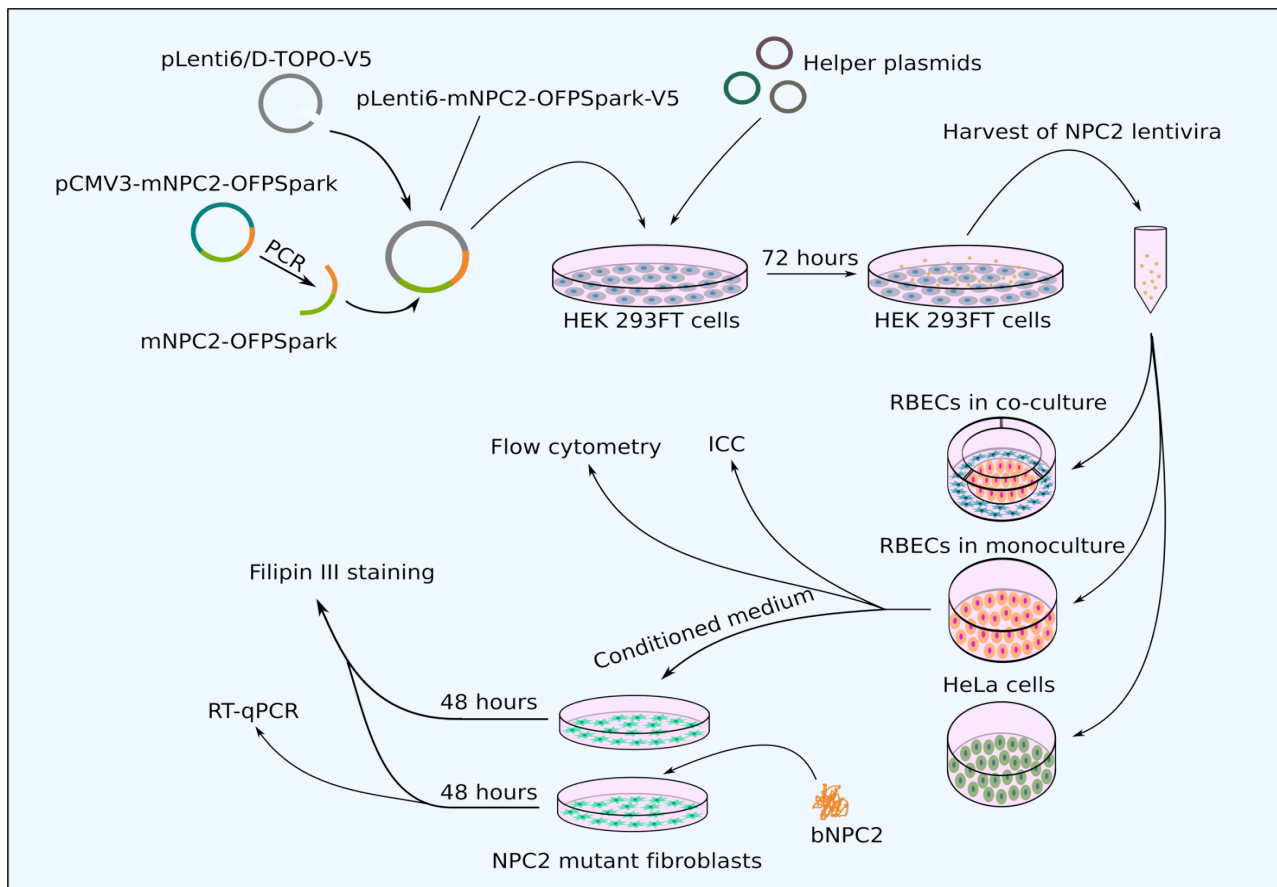


Figure 5. Overview of the processes involved in this study. The mouse NPC2 gene linked to an orange fluorescent protein tag (mNPC2-OFPSpark) was amplified by PCR and cloned into a lentiviral expression vector (pLenti6/D-TOPO-V5) to construct the NPC2 lentiviral expression vector pLenti6-mNPC2-OFPSpark-V5. This was used for co-transfection of HEK293FT cells with helper plasmids, to induce production of NPC2 expression lentiviral. These were harvested from the supernatant after 72 hours and used to genetically modify rat brain endothelial cells (RBECs) in co- and monocultures as well as HeLa cell, as positive controls. Genetically modified cells were examined by flow cytometry and ICC and the conditioned medium from these cells was collected and used to treat NPC2 mutant fibroblasts. Furthermore, purified bovine NPC2 (bNPC2) was used to treat NPC2 mutant fibroblasts by addition to the cell medium. Fibroblast were subsequently examined by Filipin III staining and those treated with bNPC2 was additionally analysed by RT-qPCR. All steps are described in detail in the following sections.

4.1.1.4 Construction of *in vitro* Blood-Brain-Barrier Models

Primary RBECs were used in two types of BBB models, comprising monocultures of RBECs or non-contact co-cultures of RBECs and astrocytes, see Figure 6. After 3 days of puromycin selection, RBECs were passaged onto collagen type IV and fibronectin precoated 24 well culture plates or 1.0 μm hanging filter inserts in 12 well culture plates for mono- or cocultures, respectively at a cell density of 1×10^5 cells/cm². Co-cultures were constructed on the following day by moving the filter inserts containing RBECs to another 12 well culture plate containing confluent primary astrocytes. To induce BBB properties, RBECs were treated with 250 μM cAMP, 17.5 μM RO and 550 nM HC, added to the RBEC culture medium in the upper chamber, while the medium in the lower chamber consisted of equal parts of RBEC culture medium and astrocyte conditioned medium, supplemented with 550 nM HC.

24 hours after construction of co-cultures, barrier integrity was measured as the TEER. The electrical resistance was measured using a Millicell ERS-2 Epithelial Volt-Ohm Meter and STX01 chopstick electrodes (Millipore). TEER was calculated by subtracting the electrical resistance of a coated filter insert without cells from the electrical resistance measured in co-cultures and multiplying the difference with the area of the filter insert. Only co-cultures with TEER values above 130 $\Omega \cdot \text{cm}^2$ were used for further experiments as it has previously been established that *in vitro* BBB models based on rat endothelial cells are inadequately tight below this point, based on the 4kDa FITC-labeled dextran (FD4) and 376 Da sodium fluorescein (FLU) permeability (99). Barrier integrity was evaluated every 24 hours during experiments based on a 150 $\Omega \cdot \text{cm}^2$ threshold, as this had previously been observed to be the limit for permeability to even smaller molecules like 182 Da mannitol (30).

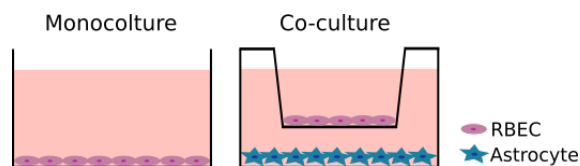


Figure 6: Schematic presentation of the *in vitro* BBB models included in this study.

4.1.1.5 Growth of HeLa cells

Immortalized cervical cancer cells, HeLa cells, were maintained in HeLa culture medium consisting of RPMI 1640 Medium, GlutaMAX™ supplemented with 10 % FBS and 0.025 mg/mL gentamicin sulfate. HeLa cells were frozen in cryoprotectant medium consisting of HeLa culture medium, supplemented with FBS to 30% and 7.5% DMSO and stored at -140° C.

4.1.1.6 Growth of Human Skin Fibroblasts

One normal human skin fibroblast cell line (GM08680) and two different NPC2 mutant human skin fibroblast cell lines (GM18445 and GM18455) were kindly provided by Christian Heegaard, Department of Molecular Biology, Aarhus University. The GM18445 NPC2 mutant human skin fibroblast cell line contains a missense mutation on both alleles changing residue Val-20 (see Figure 4) to Met, while the GM18455 NPC2 mutant human skin fibroblast cell line contains a missense mutation on one allele changing residue Cys-28 (see Figure 4) to Phe and a nonsense mutation on the other allele changing residue Glu-1 to a stop codon. In addition to that, the GM18445 NPC2 mutant fibroblast cell line contains four different mutations at the NPC1 gene. All fibroblasts were seeded at a density of 6,000 cells/cm² in fibroblast culture medium consisting of RPMI 1640 Medium, GlutaMAX™ supplemented with 10% FBS, 100 U/mL Penicillin-Streptomycin solution and 2 mM L-glutamine.

4.2 Production of NPC2 Lentiviral Vectors

NPC2 lentiviral vectors were produced using a ViraPower™ Lentiviral Directional TOPO™ Expression Kit. In general, the principle of this system is to clone the gene of interest into a lentiviral expression vector, which is then used for co-transfection of HEK 293FT Cells with three packaging plasmids encoding structural and replication proteins essential for the production of lentivirus in HEK 293FT cells. Subsequently, virus is harvested from the culture medium and used to induce gene expression in any mammalian cell line. The steps involved in the process is described in detail in the following sections.

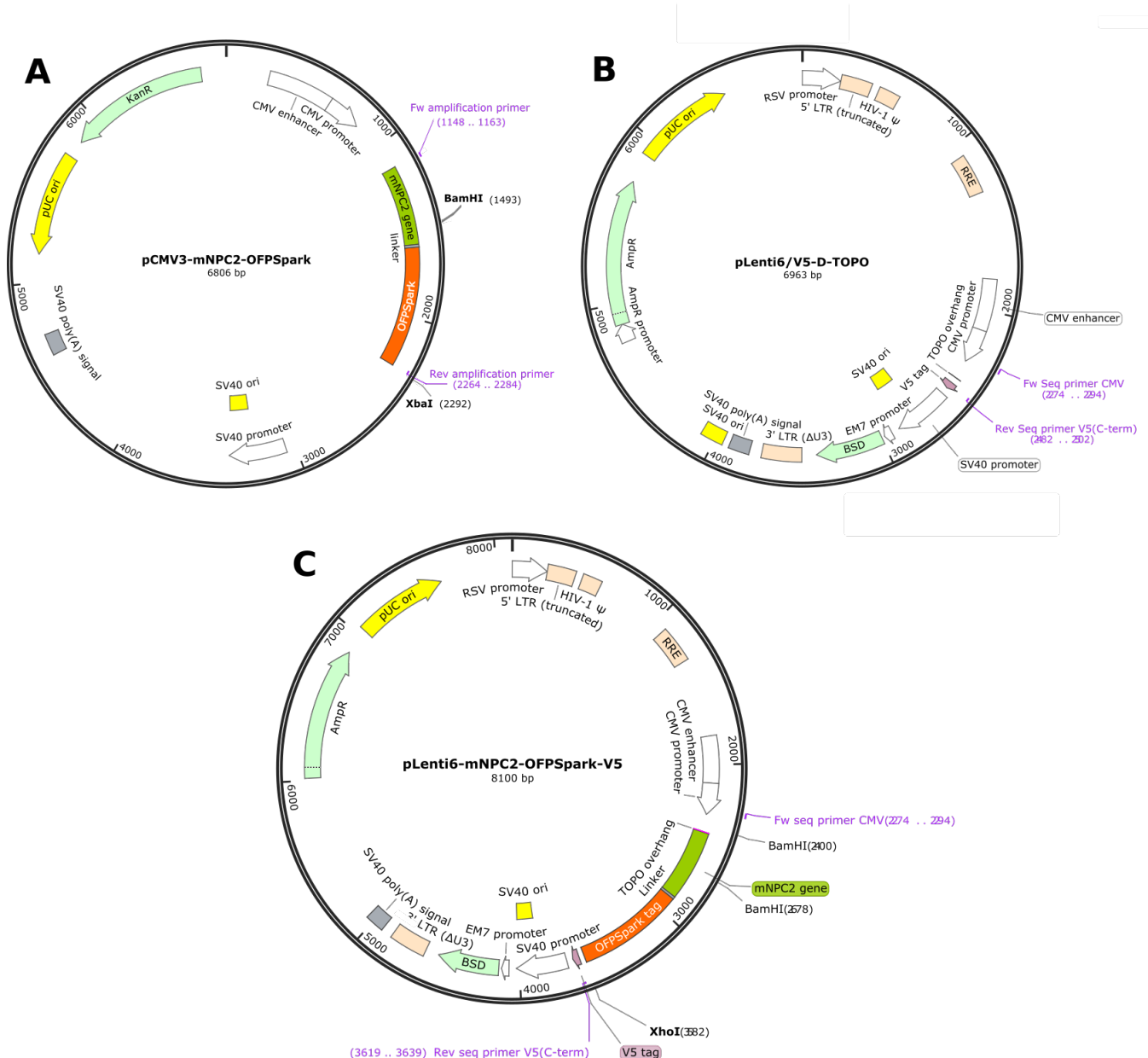


Figure 7. Plasmids involved in the cloning procedure. **A:** *pCMV3-mNPC2-OFPSpark*, containing the mouse *NPC2* gene (green) fused to an *OFPSpark* tag (orange), with *BamHI* and *XbaI* restriction sites and forward and reverse amplification primer binding sites. **B:** *pLenti6/V5-D-TOPO* lentiviral expression vector, containing a *TOPO* overhang, with forward and reverse sequencing primer binding sites. *AmpR* and *BSD* sequenced represents ampicillin and blasticidin resistance genes, respectively. **C:** *pLenti6-mNPC2-OFPSpark-V5* theoretical product of amplified *mNPC2-OFPSpark* sequence (green/orange) cloned into *pLenti6/V5-D-TOPO* with *BamHI* and *XhoI* restriction sites and with forward and reverse sequencing primer binding sites.

4.2.1 Construction of NPC2-OFPSpark lentiviral expression plasmid

Directional Topoisomerase 1 (TOPO) cloning was used to construct a lentiviral expression plasmid containing the mouse NPC2 gene linked to an OFPSpark tag, based on a pLenti6/V5 Directional TOPO Cloning Kit. The lentiviral expression vector used, pLenti6/V5-D-TOPO, was designed to contain a 5' four nucleotide single-stranded overhang (GTGG) for directional cloning and supplied linearized with Topoisomerase I attached to each end.

4.2.1.1 Amplification of mouse NPC2 gene

The mouse NPC2 gene, linked to an OFPSpark tag, was initially amplified from pCMV3-mNPC2-OFPSpark by polymerase chain reaction (PCR), with primers designed for following insertion into the lentiviral expression plasmid. The forward primer was designed to add four nucleotides complementary to the 5' overhang on pLenti6/V5-D-TOPO at the 3' of the mNPC2-OFPSpark sequence, whereas the reverse primer was designed to terminate the PCR reaction at the 5' end of the mNPC2-OFPSpark sequence. The optimized PCR reaction used to amplify the mNPC2-OFPSpark sequence was based on a Phusion High-Fidelity DNA Polymerase. 5 ng pCMV3-mNPC2-OFPSpark was used as template in a PCR reaction containing 0.5 μ M of each primer, 80 μ M dNTP Mix, 0.02 U/ μ L of Phusion DNA Polymerase and 33,3 % DMSO in 5X Phusion GC buffer. The PCR reaction was performed in a Veriti™ 96-Well Thermal Cycler (Applied Biosystems) with an initial denaturation at 98°C for 30 seconds, followed by 35 cycles of 98°C for 30 sec., 52°C for 30 sec. and 72°C for 50 sec. as well as a final extension of 72°C for 10 min. Resulting PCR products were analyzed by gel electrophoresis with a 1 kb DNA ladder in a 1 % agarose Tris-acetate-EDTA (TAE) gel, containing 1X GelRed™ and visualized on an Odyssey Fc Infrared Imaging System (Li-Cor). The mass concentration of the amplified mNPC2-OFPSpark sequence was estimated based on the intensity of the gel band representing DNA fragments with a length corresponding to the theoretic length of the mNPC2-OFPSpark sequence with added nucleotides, using the 1000bp band in the DNA ladder as reference. Intensities were estimated using ImageJ (version 2.0.0-rc-54/1.51g).

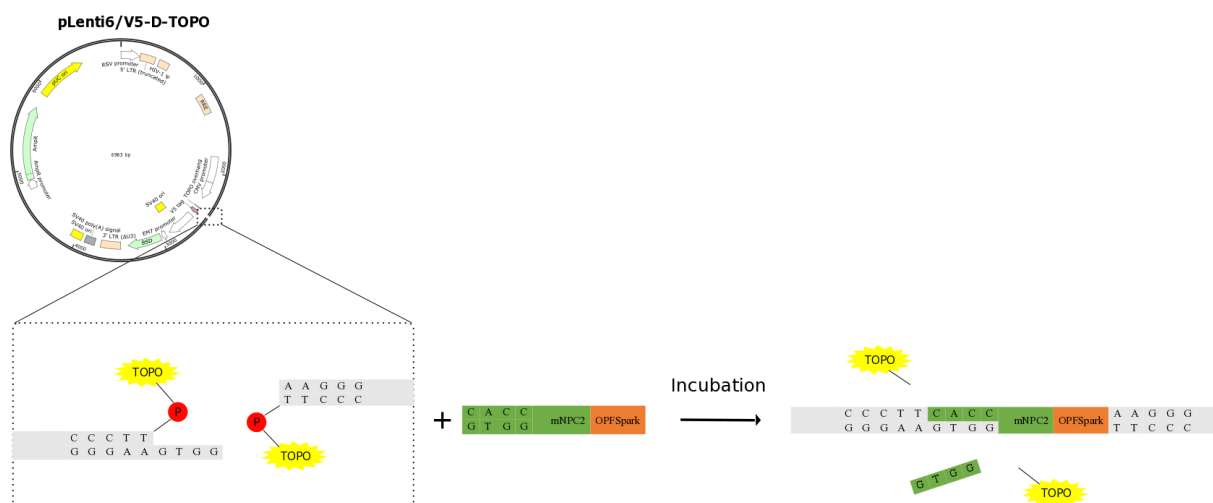


Figure 8. Topoisomerase I (TOPO) directional cloning reaction. Linearized TOPO lentiviral expression vector, pLenti6/V5-D-TOPO, with TOPO attached to each 3' phosphate (P) is incubated with amplified mNPC2-OFPSpark gene sequence containing a TOPO overhang (CACC). During incubation TOPO ligates the gene sequence into the lentiviral expression vector, directed by the TOPO overhang, after which TOPO is released.

4.2.1.2 Gel extraction of amplified NPC2 gene

The amplified mNPC2-OFPSpark sequence was purified following the PCR reaction by gel extraction, using a GeneJet Gel Extraction Kit. All remaining PCR product, as well as a GeneRuler 1kb DNA ladder, was loaded in a 1 % low-melting agarose Tris-acetate-EDTA (TAE) gel, containing 1X GelRed™ in which DNA fragments were separated by gel electrophoresis. Gel bands were briefly visualized on a TF-20M, 6 x 15 W UV transilluminator (Vilber Lourmat) and bands representing DNA fragment with a length corresponding to the theoretic length of the mNPC2-OFPSpark sequence with added nucleotides, were excised using a scalpel and transferred to a previously weighed Eppendorf tube. 1:1 (w/v) DNA Binding Buffer was added after which, the Eppendorf tube was incubated in a heating block at 60°C until the agarose was completely melted, resulting in a homogeneous solution. The homogeneous solution was transferred to a GeneJET purification column and purified by centrifugation, according to the manufacturer's protocol. Briefly, the method is based on silica-membrane purification, in which DNA bind to the silica-membrane within the purification column, which is then centrifuged for 1 minute at 12000 x g to remove agarose and buffers. A low-melting agarose gel was used to ensure complete removal of agarose in this step. Subsequently, the purification column was washed twice with the provided Washing Buffer followed by centrifugation of the empty purification column to remove excess Washing Buffer. Lastly, the DNA was eluted with the provided Elution Buffer.

4.2.1.3 Cloning of mouse NPC2 gene into lentiviral expression vector

The purified mNPC2-OFPSpark sequence was cloned into the lentiviral expression vector, pLenti6/V5-D-TOPO, included in the pLenti6/V5 Directional TOPO Cloning Kit, as illustrated in Figure 8. The cloning reaction was a 1:1 molar relationship between PCR product and lentiviral expression TOPO vector. Molar concentration of both PCR product and lentiviral expression TOPO vector was estimated from mass concentration, based on the following equation:

$$\text{Molecular weight (g/mol) for double stranded DNA} = (\text{number of bp} \times 660)$$

The TOPO cloning reaction was performed by mixing the lentiviral expression TOPO vector with the purified PCR product, diluted to a similar molar concentration, in 6X Salt Solution buffer followed by 15 minutes of incubation at room temperature. After incubating, the reaction was placed on ice. The products of the cloning reaction were then used for heat-shock transformation of One Shot Stbl3 chemically competent E.coli, included in the pLenti6/V5 Directional TOPO Cloning Kit. The transformation was done by gently mixing 3 µL cloning reaction product with 50 µL bacteria and placing the bacterial suspension on ice for 30 minutes. The bacterial suspension was then incubated for 30 seconds in a 42°C water bath followed by incubation on ice for 2 minutes. Next, the bacterial suspension was diluted in 250 µL sterile Super Optimal broth with Catabolite repression (SOC) medium also included in the pLenti6/V5 Directional TOPO Cloning Kit and incubated at 37°C and 230 rpm for 1 hour. After incubation, the bacterial solution was streaked onto LB agar plates containing 100µg/mL ampicillin for selection, closed with parafilm and incubated overnight at 37°C.

4.2.1.4 Screening of colonies by colony PCR

Bacterial colonies generated by transformation, with products of the cloning reaction, were subsequently screened by colony PCR. The 20 smallest, most sharply outlined colonies were picked for analysis. Each colony was picked with a pipette tip, which was then briefly touched onto a labeled square on a previously prepared LB agar plate containing 100µg/mL ampicillin and then transferred to a PCR tube containing 20 µL nuclease-free water. 5 µL of each bacterial colony solution was then

transferred to a new PCR tube and heated at 99°C for 7 minutes on the Veriti™ 96-Well Thermal Cycler to lyse the cells. The remaining 15 µL bacterial colony solution were incubated at 37°C overnight for amplification in LB broth medium with 100µg/mL ampicillin. Bacterial colony lysates were subsequently placed on ice and used as templates in PCR reactions using the set of sequencing primers provided with the pLenti6/V5 Directional TOPO Cloning Kit. The sequencing primers are designed to bind just before and after the TOPO insertion site creating different sized PCR products depending on the length of the DNA sequence inserted into the lentiviral expression vector, see Figure 7. One reaction was run for each clone as well a no-template control (NTC) containing all reagents except bacterial lysate. The PCR reactions were based on 2X DreamTaq Green PCR Master Mix in which 0.4 µM of each primer were mixed with 1 µL bacterial lysate for each 25 µL reaction. The colony PCR was run on the Veriti™ 96-Well Thermal Cycler with an initial denaturation at 95 °C for 5 minutes followed by 40 cycles of denaturation at 95° C for 30 seconds, annealing at 55° C for 30 seconds, and extension at 72° C for 30 seconds. A final extension was run at 72° C for 5 minutes. Resulting PCR products were analyzed by gel electrophoresis in 1% TAE agarose gels containing 1X GelRed™ and the gels were visualized on the Odyssey Fc Infrared Imaging System. Positive clones were selected based on the PCR products. Plasmids from the selected clones were then purified from the incubated bacterial solutions using a GeneJET Plasmid Miniprep Kit, according to the manufacturer's protocol. Briefly, bacteria were initially pelleted by centrifugation, resuspended in the Resuspension Solution, lysed with Lysis Solution and neutralized in Neutralization Solution to finally pellet chromosomal DNA by centrifugation at 12000 x g. The supernatant was then transferred to a GeneJET spin column, containing a DNA binding silica membrane, washed twice with a supplemented Wash Buffer, and finally purified plasmids was eluted in the supplemented Elution Buffer. Mass concentrations of the eluted plasmids were subsequently measured on a NanoDrop 1000 spectrophotometer (Fisher Scientific).

4.2.1.5 Verification of positive clones

Purified plasmids from positive clones, according to the colony PCR, were further verified by restriction enzyme (RE) digestion. RE digestion was performed by mixing 0.2-0.45 µg purified plasmid for each clone with 1:20 FastDigest BamHI and 1:20 FastDigest XhoI in 10X FastDigest Green Buffer and incubating at 37 °C for 15 minutes. Results from the RE-digestions were analyzed by gel electrophoresis in 1% TAE agarose gels containing 1X GelRed™ and the gels were visualized on the Odyssey Fc Infrared Imaging System. Based on the RE digestion, four positive and one negative clone was selected for sequence verification. Sequencing results were obtained by ordering the SUPREMERun service from GATC Biotech (Constance, Germany). The service is based on Sanger sequencing and supports sequencing runs up to 1000bp. Sequencing was done with the set of sequencing primers provided with the pLenti6/V5 Directional TOPO Cloning Kit and the results were analyzed using CLC Genomics Workbench 9. DNA sequences received from the sequencing of plasmids were initially trimmed to remove final parts of the sequence with signal intensities too low to distinguish one nucleotide from another. Then, the sequences were analyzed by alignment to the theoretical sequence of the cloned plasmid, pLenti6-mNPC2-OFPSpark-V5, see Figure 7.

4.2.1.6 Plasmid amplification and purification

Plasmids from positive clones, according to the sequencing results, were amplified by transforming One Shot Stbl3 chemically competent E.coli, using the same method as described for the screening of colonies by colony PCR, and subsequently purified using a Macherey–Nagel NucleoBond Xtra Midi EF plasmid DNA purification kit, according to the manufacturer's protocol. Briefly, one colony of transformed bacteria were inoculated in LB medium containing 100µg/mL ampicillin for amplification after which bacteria were pelleted by centrifugation and subsequently resuspended in

Resuspension Buffer containing RNase A and lysed by adding a Lysis Buffer. The lysate was then loaded into an equilibrated NucleoBond® Xtra Column Filter, inserted in a NucleoBond® Xtra Column, by gravity flow by which the lysate was filtrated and binding of plasmid DNA to a silica membrane at the bottom of the NucleoBond® Xtra Column. The NucleoBond® Xtra Column Filter was then washed once and removed, after which the NucleoBond® Xtra Column was washed twice to remove endotoxins. Finally, the plasmid DNA was eluted with elution buffer, precipitated using isopropanol, pelleted by centrifugation, washed with 70 % ethanol and reconstituted in TE-buffer. Lastly, plasmids from the positive clones were further purified by polyethylene-glycol (PEG) precipitation. A PEG solution, containing 20 % PEG6000 and 10% NaCl in H₂O, was added to plasmid DNA in a 0.6:1 (v/v) relationship and incubated on ice for 30 minutes. After incubation, plasmid DNA was pelleted by centrifugation at 20000 x g for 15 minutes, washed with 70% ethanol and resuspended in TE buffer. Plasmid mass concentrations were measured on a NanoDrop 1000 spectrophotometer (Thermo Scientific) and a RE double digestion with BamHI and XhoI was done, as previously described, as a quality control.

4.2.2 Production of NPC2 Lentiviral Vectors in HEK 293FT cells

HEK 293FT cells were used for the production of NPC2 lentiviral vectors two passages after initiation of geneticin selection. For the production of NPC2 lentiviral vectors, HEK 293FT cells were trypsinized and seeded onto 6 well cell culture plates in HEK culture medium without Geneticin at a density of 1.1×10^5 cells/cm².

4.2.2.1 Transfection of 293FT HEK cells

One day after being seeded onto 6 Well Cell Culture Plates, HEK 293FT cells were transfected to induce virus production. For each 6-well plate, five wells were used for transfection, while one well was used as a negative control. Prior to transfection the medium in all wells was aspirated and replaced with fresh HEK culture medium without Geneticin. Liposome-mediated transfection was used to deliver the previously constructed pLenti6-mNPC2-OFPSpark-V5 lentiviral expression plasmid and packaging plasmids into the HEK 293FT cells. Lipofectamine™ 2000, included in the ViraPower™ Lentiviral Directional TOPO™ Expression Kit, was used for transfection, according to the protocol included in the kit. In brief, DNA-Lipofectamine™ 2000 complexes are prepared by diluting DNA and Lipofectamine™ 2000 in sterile Opti-MEM™ Reduced Serum Medium, incubating the dilutions separately for 5 minutes at room temperature, after which the DNA dilution is transferred to the Lipofectamine™ 2000 dilution followed by 20 minutes of incubation at room temperature. To ensure equal amount of the different plasmids used for co-transfection, the DNA dilution was prepared with 1:4 lentiviral expression plasmid and 3:4 Virapower Packaging Mix containing three different packaging plasmids. The DNA-Lipofectamine™ 2000 complexes are then added to the HEK 293FT cells, which are subsequently incubated at 37° C and 5% CO₂. After 24 hours of incubation the medium is aspirated and replaced with fresh HEK culture medium without Geneticin, to remove the DNA-Lipofectamine™ 2000 complexes.

4.2.2.2 Harvest and Titration of Produced NPC2 Lentiviral Vectors

NPC2 lentiviral vectors were harvested from the conditioned HEK 293FT cell medium 72 hours post-transfection. The medium in all wells containing transfected HEK 293FT cells was aspirated and transferred to a 15 mL or 50 mL centrifuge tube and centrifuged at 3000 rpm and 4°C for 15 minutes to pellet debris. Subsequently, the virus containing supernatant was further purified by filtration through a 0.45 µm Millex-HV Syringe Filter and stored at -80°C in 1.5 mL lentiviral stocks. NPC2 lentiviral vectors were subsequently titrated to estimate the lentiviral concentration as the number of transducing units (TU)/mL. For titration of lentiviral stocks, HeLa cells were seeded onto 6 Well Cell

Culture Plates at a density of 5000 cells/cm² to reach 30-50 % confluence for transduction the following day. On the day of transduction, one lentiviral stock was thawed at room temperature and 10-fold serial dilutions of lentiviral stock ranging from 10⁻¹ to 10⁻⁵ were prepared in HeLa culture medium. The HeLa cells were then transduced by aspirating the HeLa culture medium and adding 1 mL of diluted lentiviral stock to each well as illustrated in Figure 9, leaving one well as a negative non-transduction control. 24 hours after transduction, the medium was aspirated from the HeLa cells and replaced with fresh HeLa culture medium, to remove virus particles. On the following day, 48 hours post-transduction, selection for positively transduced cells was initiated by aspirating the medium and replacing it with fresh HeLa culture medium supplemented with 4 µg/mL blasticidin, as the NPC2 expression vira would contain the blasticidin resistance gene from the constructed pLenti6-mNPC2-OFPSpark-V5 lentiviral expression plasmid, see Figure 7. The transduced HeLa cells were then kept under blasticidin selection for 12 days until no living cells were seen in the negative control well. On the 12th day of selection, the cells were fixed by washing the wells twice with 1X PBS, adding 1 mL methanol to each well and incubating 10 minutes on ice. Subsequently, the methanol was aspirated from the wells and the cells were dyed by adding 1 mL crystal violet solution, consisting of 0,5 % Crystal Violet and 25 % methanol, to each well. The cells were incubated for 10 minutes at room temperature before the crystal violet solution was removed and the cells were washed with 1X PBS until excess crystal violet solution was removed. The number of cell colonies was counted for each well, and the titer of the lentiviral stock was calculated as the average of the count in each well multiplied by its dilution factor. An additional titration without blasticidin selection was made to investigate the relationship between the lentiviral stock concentration and transduction efficiency. For this titration, HeLa cells were seeded and transduced with serial dilutions of lentiviral stock, as described above, and transduction efficiency was then analyzed by flow cytometry 48 hours post-transduction.

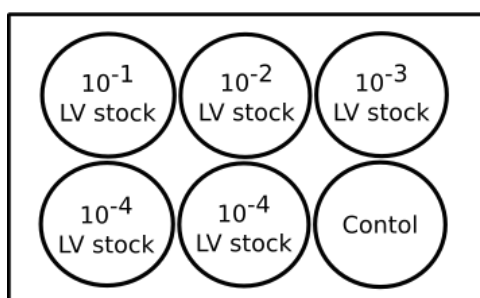


Figure 9. Illustration of the experimental setup for titration of NPC2 expression vira on HeLa cells.

4.3 Gene modification of *in vitro* Blood Brain Barrier Models

Gene modification was analyzed in both monoculture and non-contact co-culture BBB models as well as in monocultures of HeLa cells, constituting a positive control. All cells used for gene modification were seeded onto filter inserts or 24 well plates 2 days before gene modification and the medium was changed to fresh culture medium just prior to gene modification of cells in wells. Both lentiviral and non-viral gene modification was analyzed to allow for comparison between the two approaches. Lentiviral transduction was done by aspirating 400 µL medium from each well or filter insert and replacing it with 400 µL lentiviral stock. For transduction of RBECs on filter inserts, the lentiviral stock was supplemented with 250 µM cAMP, 17.5 µM RO and 550 nM HC to keep the concentration of these tight junction inducing factors constant. The cells were then incubated with virus for 24 hours, after which the media was changed to fresh culture medium to remove virus particles. Again, cAMP, RO and hydrocortisone were added to the medium for RBECs on filter inserts. Non-viral transfection was carried out using liposome-mediated transfection. Both the constructed pLenti6-mNPC2-OFPSpark-V5 lentiviral expression plasmid and the pCMV3-mNPC2-

OFPSpark, from which the NPC2 gene was initially amplified, were used for non-viral transfection. Lipofectamine™ 3000 was used for the transfections according to manufacturer's protocol with 0.5 µg DNA and 0.75 or 1.5 µL Lipofectamine™ 3000 per well or filter insert for RBECs and HeLa cells, respectively. DNA-Lipofectamine™ 3000 complexes were prepared by diluting DNA and Lipofectamine™ 3000 in sterile Opti-MEM™ Reduced Serum Medium separately. Subsequently, P3000 Reagent enhancer was added to the DNA dilution after which, the DNA dilution with P3000 Reagent was transferred to the Lipofectamine™ 3000 dilution. The solution was then incubated for 15 minutes at room temperature to allow DNA- Lipofectamine™ 3000 complexes to form. After incubation, 50 µL of the DNA- Lipofectamine™ 3000 complexes were transferred to the medium in each well or filter insert to induce transfection. Gene expression and genetic modification efficiency of both lentiviral and non-viral gene modifications were evaluated 48 hours post modifications for all setups. In addition to that, a smaller setup with RBECs in monoculture and HeLa cells were used to evaluate the duration of gene expression following lentiviral and non-viral gene expression. For this setup the cells were only genetically modified using NPC2 lentiviral vectors or pCMV3-mNPC2-OFPSpark and the percentage of genetically modified cells was evaluated 48, 96 and 144 hours post modification.

4.4 Flow Cytometry

Flow cytometry was used to estimate the efficiency of genetic modification as the percentage of genetically modified cells based on protein expression. Cells were prepared for flow cytometry by initially washing the cells twice in 1X PBS and detaching the cells by trypsinization, which was terminated by addition of culture medium. Detached cells from 3 wells or filter inserts were then transferred to a 1.5 mL Eppendorf tube and pelleted by centrifugation at 300 x g and 4°C for 5 minutes. Culture medium was then removed by aspirating the supernatant and washing the cells once with 1X PBS by centrifugation at 300 x g and 4°C for five minutes. Finally, the cells were resuspended in 1X PBS and placed on ice. Cells were then analyzed on a CytoFLEX S Flow Cytometer (Beckman Coulter) using the 561nm laser and 585/42 BP filter to enable detection of the OFPSpark tag through the PE channel. A quality control using CytoFLEX Daily QC Fluorospheres was run prior to analysis of any samples. Forward Scatter (FSC), Side Scatter (SSC) and PE acquisition gain was set to 88, 93 and 45 for RBECs and 61, 37 and 132 for HeLa cells. Up to 50000 events were recorded for each sample and single cell events were manually gated from SSC-Height by FSC-Height and FSC-Height by FSC-Width dot plots to eliminate debris and duplicates, respectively. Non-modified cells were included as negative controls and used to correct for auto fluorescence, allowing a false positive event rate at 0.5 %. Data analysis was carried out using CytExpert version 1.2.11.0.

4.5 Immunocytochemistry

Immunocytochemistry (ICC) was used to further evaluate on BBB integrity of RBECs in co-culture, in correlation with TEER measurements, as well as genetic modification efficiencies in correlation with flow cytometric results. Furthermore, ICC was used for characterization of human skin fibroblasts. Cells for ICC were initially fixed by washing the cells twice in 1X PBS, fixing for 5-10 minutes with 4 % paraformaldehyde and washing the cells twice in 1X PBS. All genetically modified cells, including non-modified controls, were stained with antibodies against NPC2 (rabbit-anti-human NPC2) and genetically modified RBECs from co-cultures were additionally used for staining with antibodies against the tight junction protein ZO-1 (rabbit-anti ZO-1). Fibroblasts were stained with antibodies against vimentin (mouse-anti-human vimentin) and α-SMA (mouse-anti-human α-SMA) for characterization. Prior to antibody staining, fixed cells were incubated in an incubation buffer consisting of 1X PBS supplemented with 3% Bovine Serum Albumin and 0.2% Triton X-100 for 30 minutes, to block non-specific binding sites and to permeabilize the cells, respectively. The

cells were then incubated with primary antibody diluted 1:250 in the incubation buffer for 1 hour, and subsequently washed two times for 5 minutes in a wash buffer consisting of the incubation buffer diluted 1:50 in 1X PBS. After that, secondary antibodies directed against the species of the primary antibody were diluted 1:250 in the incubation buffer and added to cells, which were then incubated for 1 hour under protection from light. The secondary antibodies included Alexa 488 conjugated Goat-anti-rabbit IgG and Alexa 594 conjugated Goat-anti-mouse IgG. A secondary control, without incubation with primary antibody, was included for all cell types, to assess unspecific binding of the secondary antibody. Following the incubation with secondary antibodies, cells were washed once in 1X PBS for five minutes. Subsequently, all cell nuclei were stained by incubation for 4 minutes with 2-(4-amidinophenyl)-1H-indole-6-carboxamide (DAPI) diluted 1:500 in 1X PBS, followed by two washing steps with 1X PBS for 5 minutes. Finally, coverslips and filters containing the stained cells were mounted on object slides using DAKO fluorescent mounting media. All incubation steps involved in ICC was done at room temperature on a belly dancer. Antibody staining as well as OFPSpark expression in genetically modified cells was subsequently examined on a AxioObserver Z1 fluorescence microscope equipped with ApoTome and AxioCam MR camera under a Plan-Apochromat 40x/1.3 Oil DIC objective. Alexa 488 was visualized using the GFP channel with 488 nm excitation and 509 nm emission while Alexa 594 and the OFPSpark tag was visualized with 280 nm excitation and 618 nm emission. DAPI was visualized through the DAPI channel with 353 nm excitation and 465 nm emission. Image processing was subsequently done using ImageJ (version 2.0.0-rc-54/1.51g).

4.6 NPC2 Replacement Assay

NPC2 mutant human skin fibroblast were treated with conditioned medium from genetically modified RBECs and HeLa cells, including their non-modified controls. Conditioned medium was collected from genetically modified cells 48 hours post modification. In addition to that, NPC2 mutant fibroblasts were treated with fibroblast culture medium supplemented with 10 μ g/mL bovine NPC2 protein (bNPC2), as a positive control, and basic fibroblast culture medium as negative controls. bNPC2 was purified from bovine milk and kindly provided by Christian Heegaard, Department of Molecular Biology, Aarhus University (91). NPC2 mutant human skin fibroblasts were seeded in 24 well plates 24 hours prior to treatment. On the day of treatment, the medium was aspirated and replaced with either 600 μ L conditioned medium supplemented with 100 μ L fibroblast culture medium per well or 600 μ L fibroblast culture medium with or without 10 μ g/mL bNPC2. Normal human skin fibroblasts were included for comparison and incubated in fibroblast culture medium. Fibroblast were examined by either Filipin III staining of cholesterol or reverse transcriptase quantitative polymerase chain reaction (RT-qPCR) 48 hours after treatment initiation. For Filipin III staining of cholesterol, fibroblasts were seeded onto coverslips in 24 well plates. After treatment, the cells were fixed by washing twice in 1X PBS, fixing for 5-10 minutes with 4 % paraformaldehyde and lastly washing the cells twice in 1X PBS, as previously described for ICC. The cells were then Filipin III stained by incubating for one hour with 0.5 mg/ml Filipin III in DMSO diluted 1:50 in 1X PBS to a final Filipin III concentration of 10 μ g/mL. Subsequently, the cells were washed three times in 1X PBS for 5 minutes and coverslips containing the stained cells were mounted on object slides using DAKO fluorescent mounting media. Filipin III stained cholesterol depositions were then visualized using 353 nm excitation and 465 nm emission filters on an AxioObserver Z1 fluorescence microscope equipped with AxioCam MR R3 camera under a Plan-Apochromat 20x/0.8 M27 objective (Carl Zeiss, Germany). Successive image processing was done in ImageJ (version 2.0.0-rc-54/1.51g).

4.7 Reverse Transcriptase Quantitative Polymerase Chain Reaction

RT-qPCR was used to examine the possibility of evaluating the effect of the treatment of NPC2 mutant fibroblasts based on gene expression as well as to characterize the fibroblast cell lines used in the study. RNA was therefore purified from normal and NPC2 mutant fibroblast as well as NPC2 mutant fibroblast treated with bNPC2 as described in the previous paragraph.

4.7.1.1 RNA purification

RNA purification was done using a GeneJET RNA Purification Kit. In brief, cells are initially detached and lysed with Lysis Buffer, supplemented with 286 mM β -mercaptoethanol, after which the lysates are mixed with ethanol and transferred to a GeneJET RNA Purification Column, containing a silica membrane to which RNA molecules will bind under the presence of ethanol and guanidine thiocyanate, included in the Lysis Buffer. The RNA binding silica membrane is then washed three times by centrifugation with different wash buffers and purified RNA can finally be eluted in nuclease-free water. Mass concentrations of the purified RNA were subsequently measured on a NanoDrop 1000 spectrophotometer. Cells from six to eight wells in a 24 well plate were collected as one sample during RNA purification and three to four replicates were made of each sample.

4.7.1.2 DNase treatment

Purified RNA was then DNase treated to remove genomic DNA from the samples. This was done using RNase-free DNase I. 0.3 – 1 μ g RNA, depending on the RNA concentrations, were incubated at 37°C for 30 minutes with 1 U DNase I and 10X Reaction Buffer with $MgCl_2$ in DPEC treated water. EDTA was subsequently added to a final concentration of 4.55 mM, followed by incubation at 65 C for 10 minutes to inactivate the DNase.

4.7.1.3 cDNA synthesis

DNase treated RNA was then used as templates for cDNA synthesis based on the Thermo Scientific Maxima H Minus First-strand cDNA Synthesis Kit. For cDNA synthesis, 200 ng DNase treated RNA was mixed with 25 pmol oligo (dT)₁₈ and random hexamer primer, 0.5 mM dNTP Mix and Maxima H Minus Enzyme Mix in 5X RT Buffer. The synthesis was then performed in the Veriti™ 96-Well Thermal Cycler with an initial incubation at 25°C for 10 minutes, followed by 30 minutes of incubation at 50°C and 5 minutes at 85°C.

Table 1. Gene-specific primer pairs used for investigation of gene expression in human skin fibroblasts. All primer pairs are designed for the human gene.

Gene	Reference sequence	Forward primer	Reverse primer
Actin-β	NM_001101.3	CCGCCGCCAGCTCACCAT	GCCCCACGATGGAGGGGAAG
HPRT1	NM_000194.2	GCCCTGGCGTCGTGATTAGT	TGGCTCCCATCTCCTTCATCA
GOLGA1	NM_002077.3	CTTTGCTGGCTTCCCAGAGAGA	ATGTGGGCCAAGGGCTTATGG
PRPF31	NM_015629.3	GCAGCCCGTGTGGACAGTTT	CCTCGCTTCTCCGCTGTCC
ZNF5	NM_001145347.1	AGCACCATGGAGGACCCGAA	GGGTGCTCCCGCTTCATGTG
CBFA2T2	NM_001032999.2	GCAGCCCGTGTGGACAGTTT	CCTCGCTTCTCCGCTGTCC
CI-M6PR	NM_000876.3	GGGACTCGTTCACACGCAGA	CAGGTCTGCCACCGTCTTT
NPC2	NM_006432.3	GCGTCCCAGTTCCTTTCCC	GTTGCCACTCCACCACCAGT
LAMP1	NM_005561.3	GATGCCACCATCCAGGCGTA	GGTGCCGCTCACGTTGTACT
MCOLN1	NM_020533.2	CTGCGACAAGTTTCGAGCCAAG	GTCGGAAGGCGATGGTGTCT

4.7.1.4 RT-qPCR

For investigation of the treatment effect at the gene level, the expression of the lysosomal genes, LAMP1 and MCOLN1 was examined, as the expression of these has previously been found to be altered in lysosomal storage diseases (84). Furthermore, the expression of CI-M6PR and NPC2 was examined for characterization of the human skin fibroblasts. In addition to that, reference genes (RGs) were included for normalization of gene expression. The expression of six different RGs was examined across all samples and the most stably expressed genes were used for normalization. Actin- β and hypoxanthine Phosphoribosyltransferase 1 (HPRT1) were included as RGs, since these are traditionally used as reference genes in the Laboratory of Neurobiology at Aalborg University. Furthermore, golgin A1 (GOLGA1), pre-mRNA processing factor 3 (PRPF31), zinc finger protein 5 (ZNF5) and core binding factor, alpha subunit 2, translocation partner 2 (CBFA2T2) were included as RGs, as these were found to be the most suitable for the specific experiment using the web-based gene expression analysis tool, Genevestigator (NEBION / ETH, Zurich). The gene-specific primers are listed in Table 1. The qPCR reactions were performed with 2.5 ng cDNA, 1 μ mol of each primer and Maxima 2X SYBR Green/ROX qPCR Master Mix in a Stratagene Mx 3000P QPCR System (Agilent Technologies). The reaction was run with an initial denaturation at 95°C for 10 minutes, followed by 40 cycles of denaturation at 95°C for 30 seconds, annealing at 60°C for 30 seconds and extension at 72°C for 30 seconds as well as a final melting curve analyses which included denaturation at 95°C for one minute, annealing at 55°C for 30 seconds and denaturation at 95°C for 30 seconds. To be able to identify contamination, no template controls (NTCs) containing all reagents except for cDNA and no reverse transcriptase controls (RT-) containing DNase treated RNA instead of cDNA were included. All samples were run in triplicates and outliers differing more than 0.5 from other triplicates in threshold cycle (Ct) values were excluded. Relative gene expression was calculated by the Pfaffl method, based on the formula below, and primer efficiencies were determined based on a standard curve of 2-fold serial dilutions cDNA pooled from all samples.

$$\text{Relative gene expression} = \frac{E_{\text{Gene of interest}}^{-Ct}}{\sqrt[n]{E_{RG1}^{-Ct} + E_{RG2}^{-Ct} + \dots + E_{RGn}^{-Ct}}}$$

4.8 Statistics

All statistical analysis was done using GraphPad Prism (version 6.0c) with 0.05 significance level. D'Agostino and Pearson omnibus normality test was used to investigate the distribution of data. However, as most data sets were obtained from cell cultures with relatively low sample numbers, tests for normality were often impossible to make. Results are shown as median with interquartile range to account for possible skewness in data sets that did not pass the normality test, while normally distributed data sets are presented with mean and standard deviation. Differences in TEER value changes, relative gene expression, and transfection efficiencies were analyzed by the Kruskal-Wallis test with Dunn's multiple comparison test and a 0.05 significance level.

5 Results

NPC2 expression lentivira were produced and used to genetically modified RBECs to secrete recombinant mNPC2-OFPSpark protein. Conditioned medium from genetically modified cells, containing the secreted recombinant protein was subsequently used in a NPC2 replacement assay to investigate the effect on cholesterol accumulation in NPC2 mutant human skin fibroblast. In the following sections, results from the production of NPC2 expression lentivirus, gene modifications of RBECs and HeLa cells, characterization of human skin fibroblasts and NPC2 replacement assays are presented.

5.1 Production of NPC2 expression virus

NPC2 expression vira were constructed using the ViraPower™ Lentiviral Directional TOPO™ Expression Kit, in which the gene of interest is cloned into a lentiviral expression vector plasmid, which is then used for co-transfection of HEK 293FT Cells with three packaging plasmids encoding structural and replication proteins essential for the production of lentivirus. Cloning of the NPC2 lentiviral expression plasmid, pLenti6-mNPC2-OFPSpark-V5, yielded several clones of which the 20 most defined clones were screened by colony PCR using bacterial lysates as templates. The primers used for colony PCR were designed to amplify across the inserted mNPC2-OFPSpark sequence (see Figure 7) creating a 1,366 bp long PCR product in case of successful cloning of the mNPC2-OFPSpark sequence into the pLenti6/V5-D-TOPO vector. Ligation of an empty vector would produce a 229 bp long PCR product. PCR products from seven clones (C3, C4, C5, C7, C9, C11 and C14) showed gel bands with a size corresponding to the theoretical size of the product produced by amplification from successfully cloned pLenti6-mNPC2-OFPSpark-V5, while PCR products from 12 clones (C1, C2, C6, C10, C12, C13, C15-19) showed gel bands with a size corresponding to the product of amplification from an empty vector, see Figure 10. Furthermore, a gel band with a size corresponding to a DNA sequence of approximately 500 bp was seen in all lanes containing PCR products from positive clones as well as one lane containing only this band (C8), indicating unspecific binding of the primers within the mNPC2-OFPSpark sequence. The lane only containing the 500 bp PCR product can thus be explained by amplification from the mNPC2-OFPSpark-V5 sequence alone.

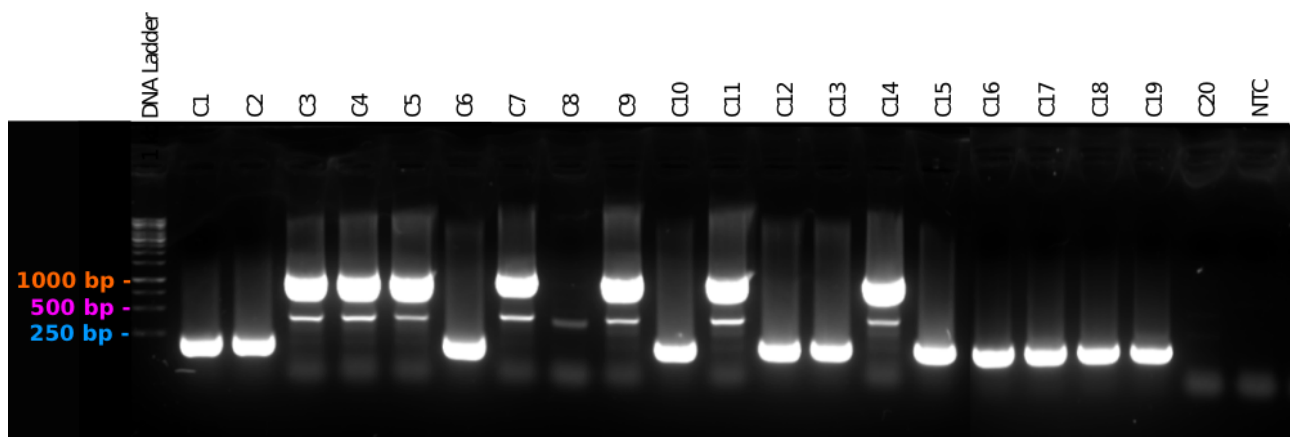


Figure 10. Screening of clones resulting from the cloning of NPC2 lentiviral expression plasmid, pLenti6-mNPC2-OFPSpark-V5. Products of a colony PCR using bacterial lysates from 20 clones (C1-C20), including a no-template control (NTC) is shown. Primers designed to amplify across the inserted mNPC2-OFPSaprk sequence resulting in theoretical products of 1366 bp and 229 bp from amplification of successfully cloned pLenti6-mNPC2-OFPSpark-V5 and ligation of the empty pLenti6/V5-D-TOPO vector, respectively.

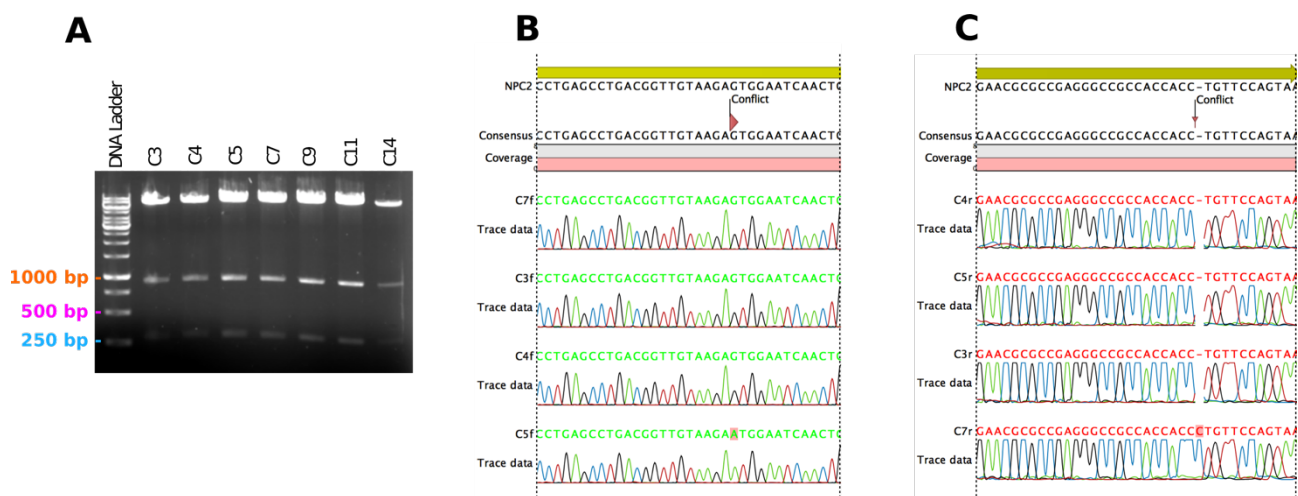


Figure 11. Clone verifications. *A*: BamHI and XhoI double digested plasmids purified from positive clones. *B*: Sequencing results from forward sequencing of plasmid purified from four positive clones (C3, C4, C5 and C7). *C*: Sequencing results from reverse sequencing of plasmid purified from four positive clones (C3, C4, C5 and C7). Both forward and reverse sequencing results are aligned to the theoretic sequence of cloned pLenti6-mNPC2-OFPSpark-V5 (NPC2). Only the aligned sections containing inconsistencies from the theoretic sequence of pLenti6-mNPC2-OFPSpark-V5 are shown, with inconsistencies marked as conflicts.

Plasmids were amplified and purified from the seven positive clones and further verified by double RE digestion with BamHI and XhoI and sequencing. Results of the RE digestion and sequencing is shown in Figure 11. The pLenti6-mNPC2-OFPSpark-V5 has two BamHI restriction sites and one XhoI restriction site, see Figure 7. The double digestion with these two enzymes would create one large DNA fragment with the theoretic size of 6918 bp and two smaller DNA fragments with the theoretic size of 904 bp and 278 bp. As seen in Figure 11, digestion of plasmids from all seven clones showed exactly three DNA bands with sizes corresponding to the size of the theoretic fragments resulting from BamHI and XhoI digestion of pLenti6-mNPC2-OFPSpark-V5, indicating the presence of successfully cloned pLenti6-mNPC2-OFPSpark-V5 in these clones, in agreement with the results of the colony PCR. Plasmids from four positive clones were subsequently sequenced using the previously mentioned forward and reverse sequencing primers. The resulting sequencing products were between 750-800 bp with an overlap between products produced by the forward and reverse primer for all clones, eliminating the possibility of non-verified gaps in the investigated sequence. As shown in Figure 11, sequencing products of plasmids from two clones (C3 and C4) were perfectly aligned to the theoretic sequence of pLenti6-NPC2-OFPSpark-V5, while one alignment inconsistency was found in the forward sequencing product of one clone (C5) and in the reverse sequencing product of another clone (C7). The sequencing results thus confirmed the presence of successfully cloned pLenti6-mNPC2-OFPSpark-V5 lentiviral expression plasmid in DNA from two clones (C3 and C4), which was subsequently used for lentiviral production in HEK cells.

NPC2 expression lentivira were produced by co-transfection of HEK 293FT cells with sequence-verified pLenti6-mNPC2-OFPSpark-V5 lentiviral expression plasmid and three packaging plasmids encoding structural and replication proteins essential for the production of lentivirus in HEK 293FT cells. Harvested lentivira were subsequently titrated by transduction of HeLa cells followed by blasticidin selection for 12 days, to determine the lentiviral concentration as the number of TU/mL, and by flow cytometry with transduced HeLa cells 48 hours post-transfection, to determine the correlation between lentiviral stock concentration and transduction efficiency. Results of the titrations are shown in Figure 12. The results of the flow cytometry revealed transduction efficiencies below the non-transfected controls when using 10^{-4} and 10^{-3} lentiviral stock dilutions, corresponding to no transduced cells. Transduction with 10^{-2} and 10^{-1} lentiviral stock dilution resulted in transduction

efficiencies of 0.88% and 3.49%, respectively, which is above the level of non-transfected controls, but still very low considering that HeLa cells, which are normally easily transduced, were used for the titration. Transduction with undiluted lentiviral stock resulted in markedly higher transduction efficiencies than any of the lentiviral stock dilutions investigated, with a median transduction efficiency of 23.41%. Based on these results it was therefore decided to use undiluted lentiviral stock for the following transductions, as the transduction non-dividing RBECs was expected to be less efficient than transduction of HeLa cells.

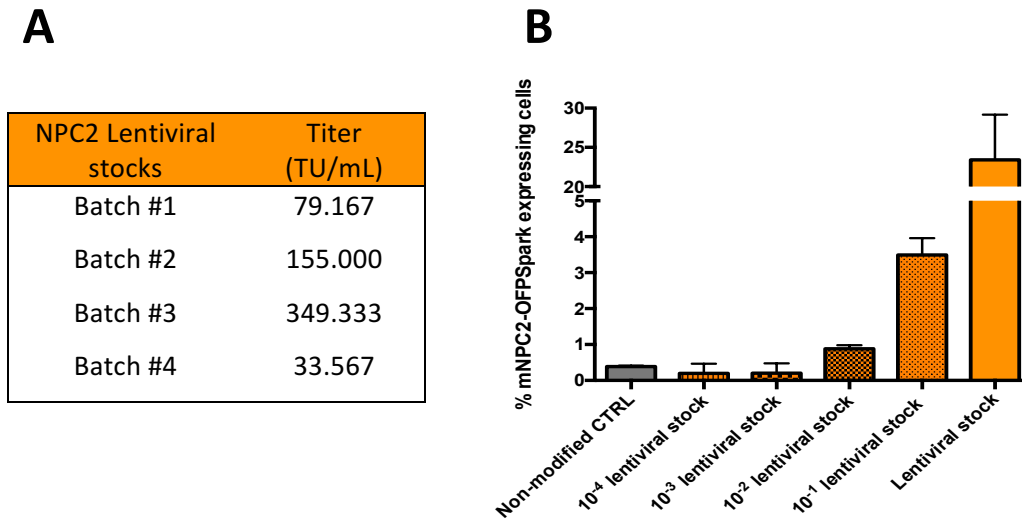


Figure 12. Viral titrations of produced NPC2 lentivirus. **A:** Viral titers of produced NPC2 lentiviral stocks, presented as the number of transducing units (TU) per mL. **B:** Transduction efficiencies of different viral stock dilutions, presented as the percentage mNPC2-OFPSpark positive cells measured by flow cytometry. Data are presented as median with interquartile range (n=4).

5.2 Gene Modification of Primary Rat Brain Endothelial Cells

RBECs in mono- and co-cultures were genetically modified to express and secrete recombinant NPC2-OFPSpark protein, along with HeLa cells comprising positive controls. Both lentiviral and non-viral gene modification approaches were used and the genetically modified cells were analyzed by flow cytometry and immunocytochemistry.

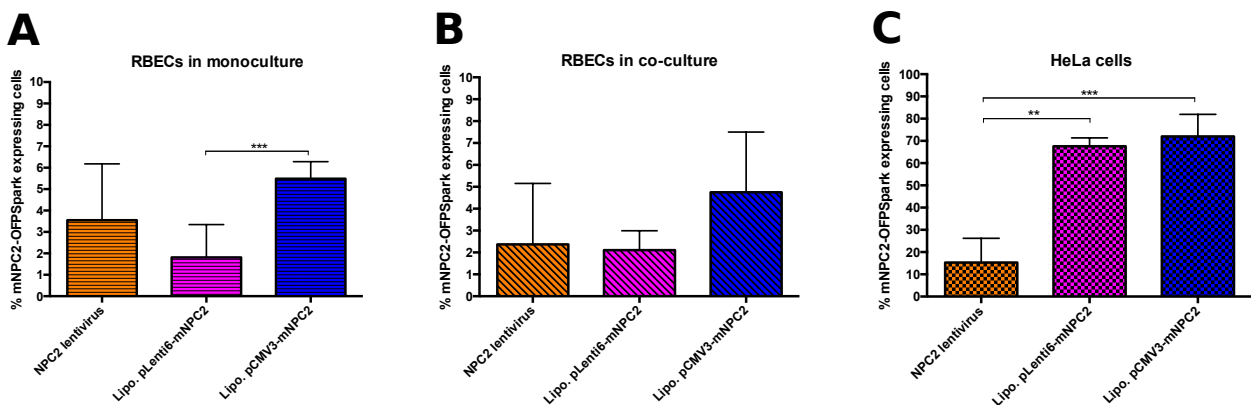


Figure 13. Gene modification efficiencies of genetically modified RBECs presented as the percentage mNPC2-OFPSpark expressing cells measured by flow cytometry. **A:** RBECs in monoculture (n=7-13). **B:** RBECs in co-culture (n=5-7). **C:** HeLa cells (n=7-12). Gene modifications included viral gene modification with the produced NPC2 lentivirus, non-viral gene modification with pLenti6-mNPC2-OFPSpark-V5 and non-viral gene modification with pCMV3-mNPC2-OFPSpark. Data are presented as median with interquartile range. Differences between the three different approaches were examined by Kruskal-Wallis test with Dunn's multiple comparison tests (**P-value<0.01, ***P-value<0.001).

Results of the flow cytometry of genetically modified RBECs in monoculture revealed a median lentiviral gene modification efficiency of 3.55 % while the efficiency of non-viral gene modification with pLenti6-mNPC2-OFPSpark-V5 was statistical significantly lower than the efficiency of non-viral gene modification with pCMV3-mNPC2-OFPSpark, with median efficiencies of 1.81 % and 5.49% respectively. No statistical significant difference was observed between the lentiviral gene modification efficiency and the non-viral gene modification efficiency with pLenti6-mNPC2-OFPSpark-V5 or pCMV3-NPC2-OFPSpark, possibly because of a large variation in lentiviral gene modification efficiencies. However, the median efficiency of lentiviral gene modifications seemed to be higher than the efficiency of non-viral gene modification with pLenti6-mNPC2-OFPSpark-V5 and lower than the efficiency of non-viral gene modification with pCMV3-mNPC2-OFPSpark.

Results of flow cytometry of genetically modified RBECs in co-cultures showed a lentiviral gene modification efficiency of 2.37% while the efficiency of non-viral gene modification with pLenti6-mNPC2-OFPSpark-V5 and pCMV3-mNPC2-OFPSpark was 2.11 % and 4.75%, respectively. The gene modification efficiencies of RBECs in co-culture were hence generally lower than those observed for RBECs in monoculture, but with a similar pattern of the different gene modification approaches. As observed for the RBECs in monoculture, a large variation in lentiviral gene modification efficiencies was seen. In addition to that, a large variation in gene modification efficiency was seen for the non-viral modifications with pCMV3-mNPC2-OFPSpark, probably because of a lower number of replicates, compared to the RBECs in monoculture. Again, the efficiency of non-viral gene modification with pLenti6-mNPC2-OFPSpark-V5 seemed to be lower than the efficiency of non-viral gene modification with pCMV3-mNPC2-OFPSpark. However, no statistically significant differences between the lentiviral and non-viral approaches were observed for this setup, possibly due to large variations and a smaller sample size.

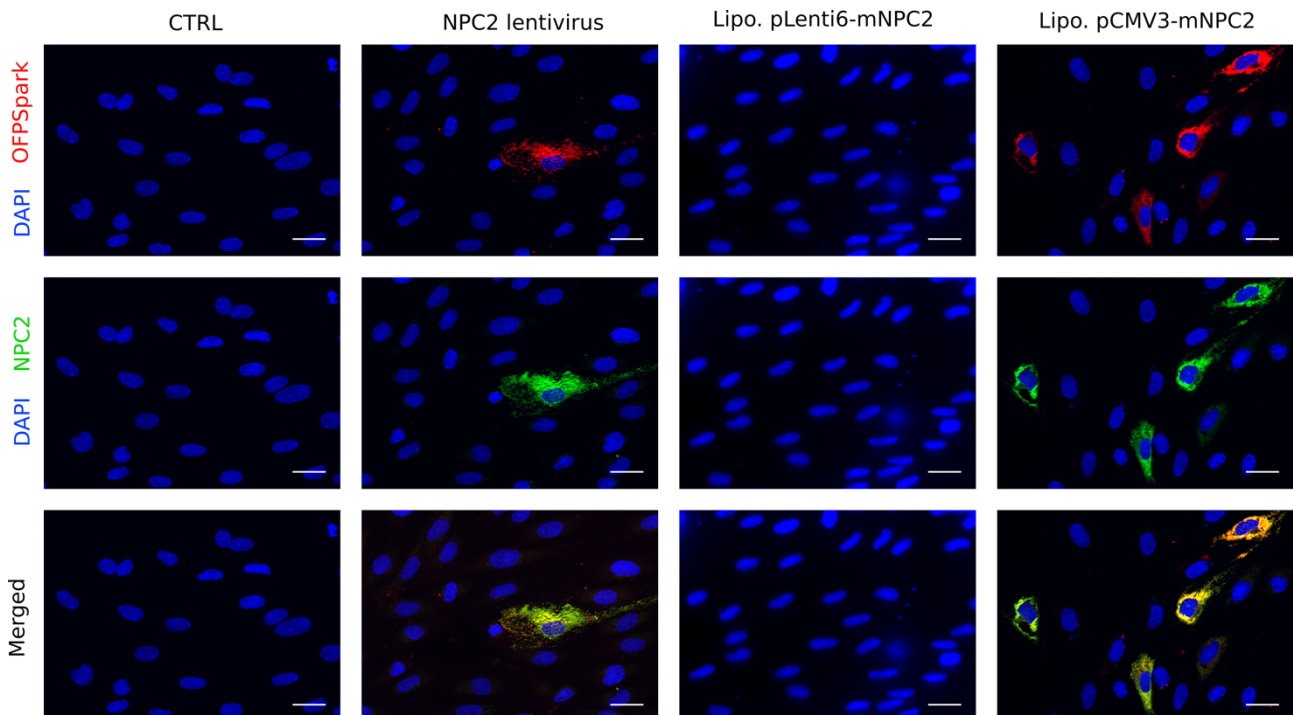


Figure 14. Genetically modified RBECs in monoculture. In the top row the fluorescence caused by **OFPSpark** expression (red) with DAPI (blue) staining of cell nuclei is shown, while immunocytochemical staining of **NPC2** (green) is shown in the middle row with DAPI (blue) staining of cell nuclei. The bottom row shows **merged** OFPSpark and NPC2 with DAPI. **CTRL** represents non-modified RBEC monoculture controls. **NPC2 lentivirus** represents RBECs in monoculture, genetically modified with NPC2 lentivirus, while **Lipo.pLenti6-mNPC2** and **Lipo.pCMV3-mNPC2** represents RBECs in monoculture genetically modified with pLenti6-mNPC2-OFPSpark-V5 and pCMV3-mNPC2-OFPSpark, respectively. Scale bar represents 25µm.

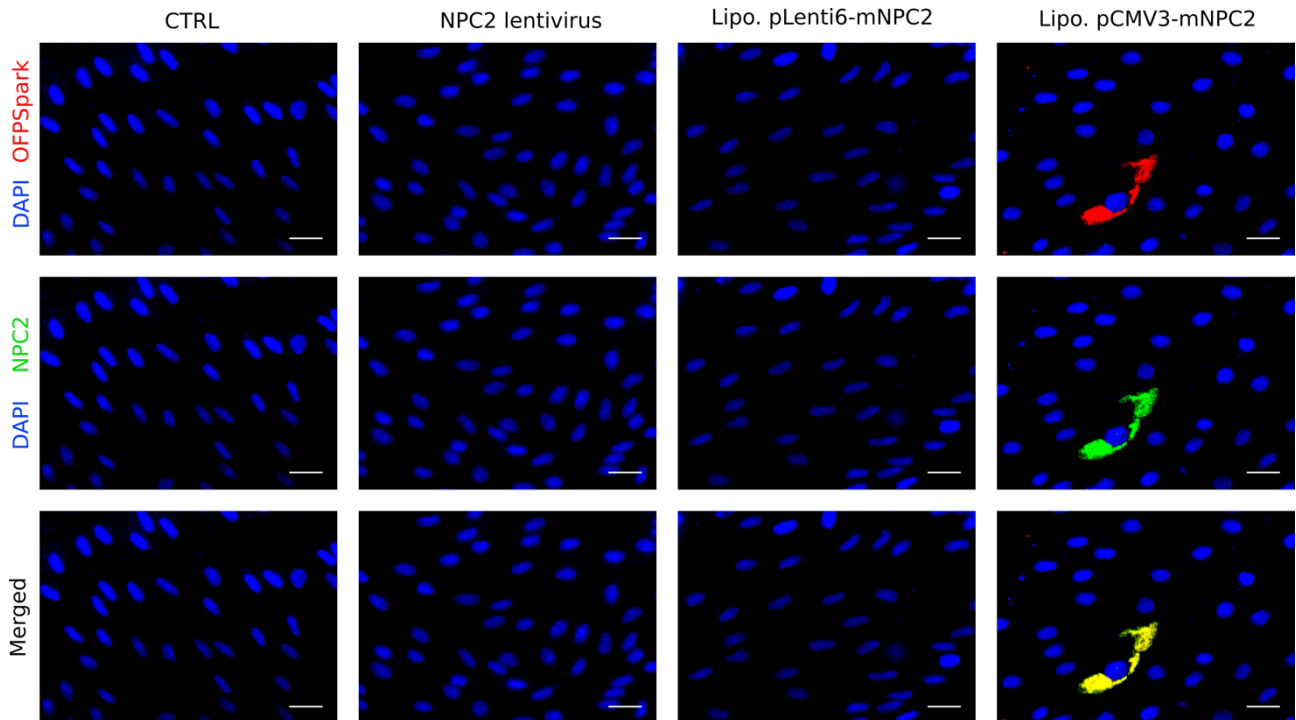


Figure 15. Genetically modified RBECs in co-culture. In the top row the fluorescence caused by **OFPSpark** expression (red) with DAPI (blue) staining of cell nuclei is shown, while immunocytochemical staining of **NPC2** (green) is shown in the middle row with DAPI (blue) staining of cell nuclei. The bottom row shows **merged** OFPSpark and NPC2 with DAPI. **CTRL** represents non-modified RBEC co-culture controls. **NPC2 lentivirus** represents RBECs in co-culture, genetically modified with NPC2 lentivirus, while **Lipo.pLenti6-mNPC2** and **Lipo.pCMV3-mNPC2** represents RBECs in co-culture genetically modified with pLenti6-mNPC2-OFPSpark-V5 and pCMV3-mNPC2-OFPSpark, respectively. Scale bar represents 25 μ m.

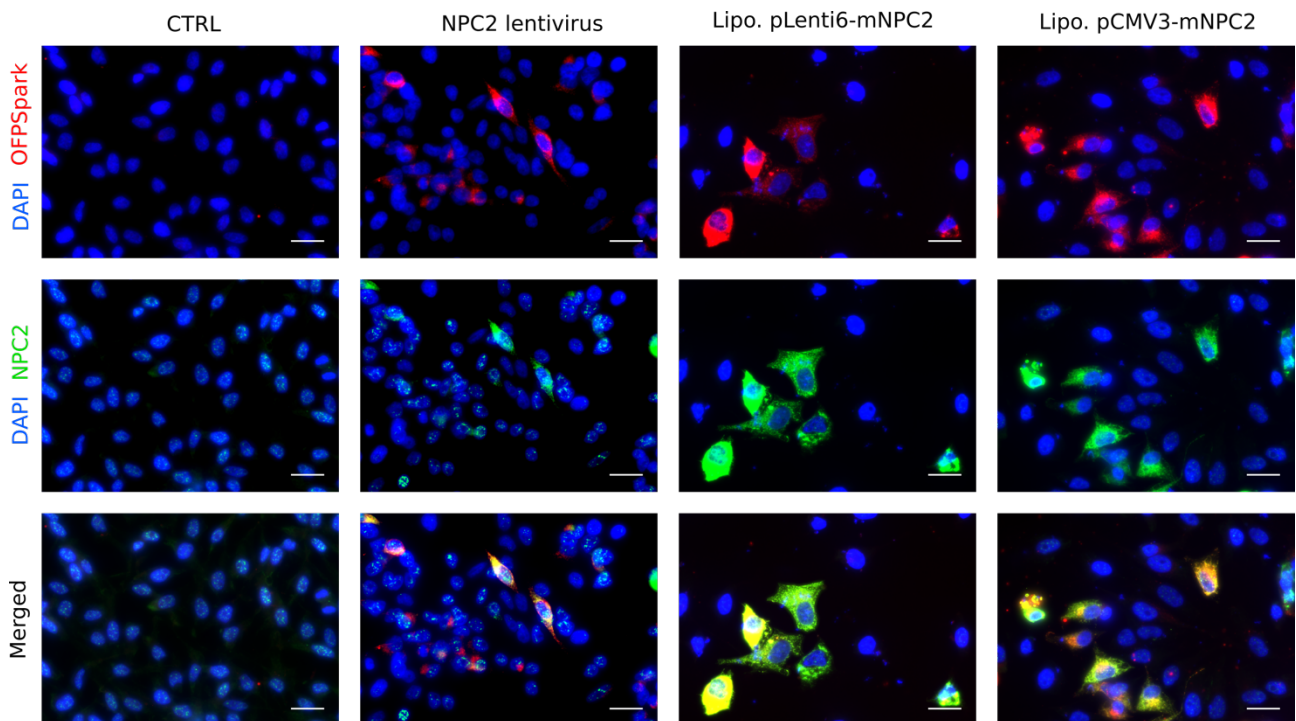


Figure 16. Genetically modified HeLa cells. In the top row the fluorescence caused by **OFPSpark** expression (red) with DAPI (blue) staining of cell nuclei is shown, while immunocytochemical staining of **NPC2** (green) is shown in the middle row with DAPI (blue) staining of cell nuclei. The bottom row shows **merged** OFPSpark and NPC2 with DAPI. **CTRL** represents non-modified HeLa cell controls. **NPC2 lentivirus** represents HeLa cells, genetically modified with NPC2 lentivirus, while **Lipo.pLenti6-mNPC2** and **Lipo.pCMV3-mNPC2** represents HeLa cells genetically modified with pLenti6-mNPC2-OFPSpark-V5 and pCMV3-mNPC2-OFPSpark, respectively. Scale bar represents 25 μ m.

The results of flow cytometry with genetically modified HeLa cells, included as positive controls, showed a lentiviral gene modification efficiency of 15.33% while the efficiency of non-viral gene modification with pLenti6-mNPC2-OFPSpark-V5 and pCMV3-mNPC2-OFPSpark was 67.56 % and 72.0%, respectively. Hence, the efficiencies of all approaches were markedly higher in HeLa cells compared to RBECs, but while the lentiviral gene modification efficiencies were 4-6-fold higher, the non-viral gene modification efficiencies were 13-37-fold higher in HeLa cells compared to RBECs. In HeLa cells the efficiency of lentiviral gene modification was hence statistical significantly lower than the efficiencies of both non-viral gene modifications efficiency, in contrast to the observed efficiencies from RBECs. Furthermore, the difference between efficiencies of non-viral gene modification with pLenti6-mNPC2-OFPSpark-V5 and pCMV3-mNPC2-OFPSpark was much less pronounced in HeLa cells than in RBECs as the efficiency of both non-viral approaches was very high.

Immunocytochemistry of genetically modified RBECs in monocultures is shown in Figure 14. Immunocytochemical staining of NPC2 showed a complete co-localization with the fluorescent OFPSpark, supporting the use of fluorescent OFPSpark as a marker for recombinant NPC2-OFPSpark protein in flow cytometry. A varying intensity was observed between the OFPSpark fluorescence, corresponding to a varying gene expression among the cells. The same variation was however not observed from the immunocytochemical staining of NPC2, as the signal is amplified several times in this case. More OFPSpark positive cells were found among the RBECs genetically modified with pCMV3-mNPC2-OFPSpark compared to RBECs genetically modified with NPC2 lentivirus, corresponding to the difference in gene modification efficiency observed with flow cytometry. As expected, no positive cells were found among the non-modified RBEC monoculture controls. However, this was also the case for RBECs in monoculture genetically modified with pLenti6-mNPC2-OFPSpark-V5, which can probably be explained by the very low gene modification efficiency observed in the flow cytometric analysis, see Figure 14.

Immunocytochemical staining of genetically modified RBECs in co-culture is shown in Figure 15. The immunocytochemical staining only showed OFPSpark and NPC2 positive cells among those genetically modified with pCMV3-mNPC2-OFPSpark, which was probably due to the very low gene modification efficiencies observed with flow cytometry of these cells. Again, a complete co-localization was observed between fluorescent OFPSpark and immunocytochemical staining of NPC2.

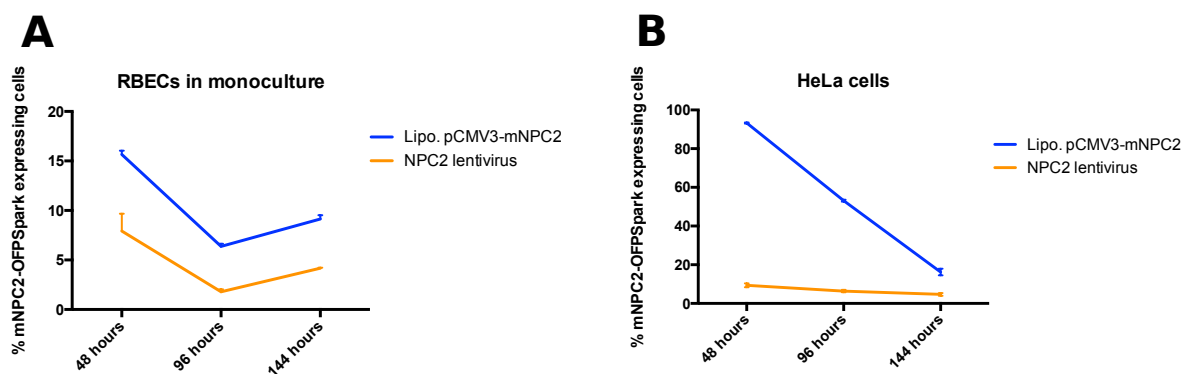


Figure 17. Duration of gene expression presented as the percentage mNPC2-OFPSpark expressing cells measured by flow cytometry (median +ICR). A: Gene expression RBECs in monoculture 48, 96 and 144 hours post gene modifications (n=2). B: Gene expression in HeLa cells 48, 96 and 144 hours post gene modifications (n=2). Two different gene modification approaches were investigated, including viral gene modification with the produced NPC2 lentivirus and non-viral gene modification with pCMV3-mNPC2-OFPSpark.

Immunocytochemical staining of genetically modified HeLa cells also showed a complete co-localization between OFPSpark and NPC2 consistent with what was observed for genetically modified RBECs in mono- and co-culture, see Figure 16. More OFPSpark and NPC2 positive cells were generally seen in the genetically modified HeLa cells, in agreement with the generally higher gene modification efficiencies of HeLa cells observed by flow cytometry. No OFPSpark positive cells were seen between the non-modified HeLa controls. Yet, the immunocytochemical NPC2 staining of these revealed an unspecific staining of the nuclei of HeLa cells. This was however mostly evident on the non-modified HeLa controls, where no specific NPC2 binding was seen.

For evaluation of the duration of the gene expression, RBECs in monoculture and HeLa cells were genetically modified with virus or pCMV3-mNPC2-OFPSpark. The percentage of mNPC2-OFPSpark expressing cells was estimated 48, 96 and 144 hours post modification by flow cytometry. As seen in Figure 17, the non-viral gene modification with pCMV3-mNPC2-OFPSpark generally results in a higher percentage of mNPC2-OFPSpark expressing cells compared to gene modification with NPC2 lentivirus, consistent with the results described above.

When looking at the RBECs in monoculture, the change in the percentage of mNPC2-OFPSpark expressing cells was approximately similar between the two approaches. However, when looking at the HeLa cells, a huge drop in the percentage of mNPC2-OFPSpark expressing cells was observed for cells genetically modified with the non-viral approach, while the percentage of mNPC2-OFPSpark expressing cells were more stable for cells genetically modified with the virus. No statistical testing was applied to these results, as the number of samples was very low. Therefore, it is not possible to make any conclusion based on these results alone. However, the distinct difference in the change of the percentage of mNPC2-OFPSpark expressing cells over time observed in HeLa cells might be an indicator of a higher long-term gene expression as a result of lentiviral gene modification, compared to non-viral gene modification.

5.3 Integrity of *in-vitro* Blood-Brain-Barrier Model During Gene Modification

The barrier integrity of RBECs in co-culture was evaluated throughout the experiments based on TEER as well as 48 hours post gene modifications based on the ZO-1 expression. The ZO-1 expression was examined by immunocytochemistry, which revealed a continuous ZO-1 expression at the cell to cell borders of both non-modified RBEC controls and lentiviral and non-viral genetically modified RBECs, see Figure 18 (A-D). The ZO-1 expression in non-modified RBEC controls did seem a little more continuous when compared to the genetically modified RBECs. Again, NPC2-OFPSpark expressing RBECs could only be observed among those genetically modified with pCMV3-mNPC2-OFPSpark, corresponding to the very low gene modification efficiencies observed with flow cytometry of the RBECs in co-culture.

TEER measurements revealed reduction in TEER for all RBECs in co-cultures, including the non-modified controls, however never below the $150 \Omega \cdot \text{cm}^2$ threshold, see Figure 18E. When comparing the TEER reductions as the percentage of the TEER measured before gene modifications, RBECs genetically modified with lentivirus showed a statistically significantly larger reduction in TEER 24 hours post gene modification, when compared to non-modified control RBECs, see Figure 18F. However, no statistical significant differences in the TEER reduction was seen 48 hours post modification indicating that none of the gene modification approaches examined resulted in disruption of the barrier integrity consistent with the results of the ZO-1 staining.

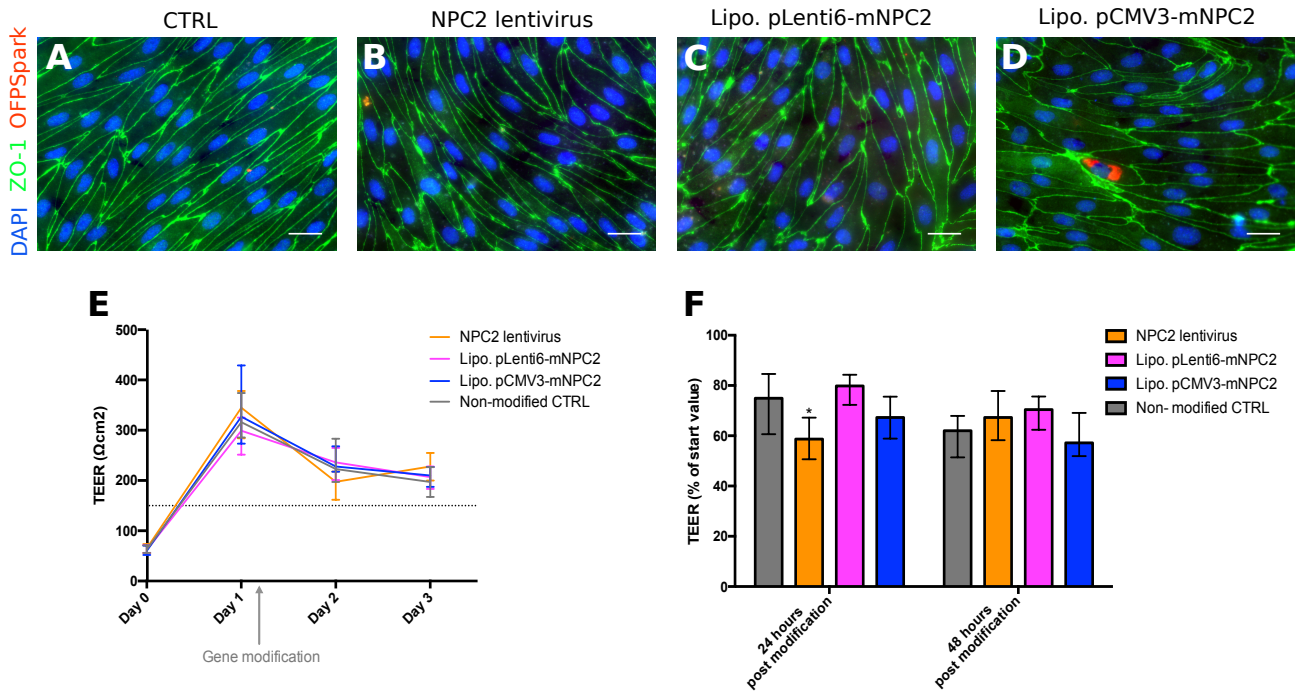


Figure 18. ZO-expression and TEER in genetically modified RBECs in co-culture. **A:** ZO-1 expression in non-modified RBEC co-culture controls. **B:** ZO-1 expression in RBECs in co-culture genetically modified with NPC2 lentivirus. **C:** ZO-1 expression in RBECs in co-culture genetically modified with pLenti-mNPC2-OFPSpark-V5. **D:** ZO-1 expression in RBECs in co-culture genetically modified with pCMV3-mNPC2-OFPSpark. Scale bars represent 25 μm . **E:** TEER measurements of RBECs in co-culture after cell seeding (day 0), after tight junction induction (day 1) and after gene modifications (day 2 + 3) presented as median with interquartile range. The dotted line indicates the 150 $\Omega\cdot\text{cm}^2$ threshold for a tight barrier. **F:** Change in TEER values 24 and 48 hours post gene modification expressed as percentage of the start value before gene modifications (median+ICR). Differences between genetically modified and non-modified RBEC co-culture controls were examined with Kruskal-Wallis test with Dunn's multiple comparison test (*P-value < 0.05).

5.4 Characterization of Human Skin Fibroblasts

Human skin fibroblasts included in this study were initially characterized by Filipin III staining of cholesterol as well as immunocytochemical staining of vimentin and α -SMA expression, see Figure 19. The immunocytochemical staining showed a clear expression of the fibroblast marker vimentin in all the included cell lines, see Figure 19D-F. The α -SMA staining of all cell lines, showed a mixture of cells with a clear expression of α -SMA fibers and cells with no expression or a diffuse expression throughout the cytoplasm, indicating a mixture of fibroblasts and myofibroblasts, see Figure 19G-I. Hence, the three different fibroblast cell lines showed similar expression of both vimentin and α -SMA allowing for a comparison between the cells. The Filipin III staining of wildtype fibroblasts showed small single sporadic staining of cholesterol localized around the cell nuclei, but no clear staining of cholesterol, see Figure 19A. However, when examining the Filipin III staining of GM 18455 NPC2 mutant fibroblasts a massive cholesterol accumulation was seen around the cell nuclei, corresponding to the localization of lysosomes, see Figure 19B. The Filipin III staining of GM 18445 NPC2 mutant fibroblasts showed fairly low cholesterol accumulation, localized around the cell nuclei, making the distinction between these cells and the wildtype fibroblasts difficult for some of the cells, see Figure 19C. To ensure possible evaluation of the effect, of treatment with extracellular NPC2 protein, on cholesterol accumulations, only wildtype (GM08680) and GM18455 NPC2 mutant fibroblasts were therefore included in following experiments.

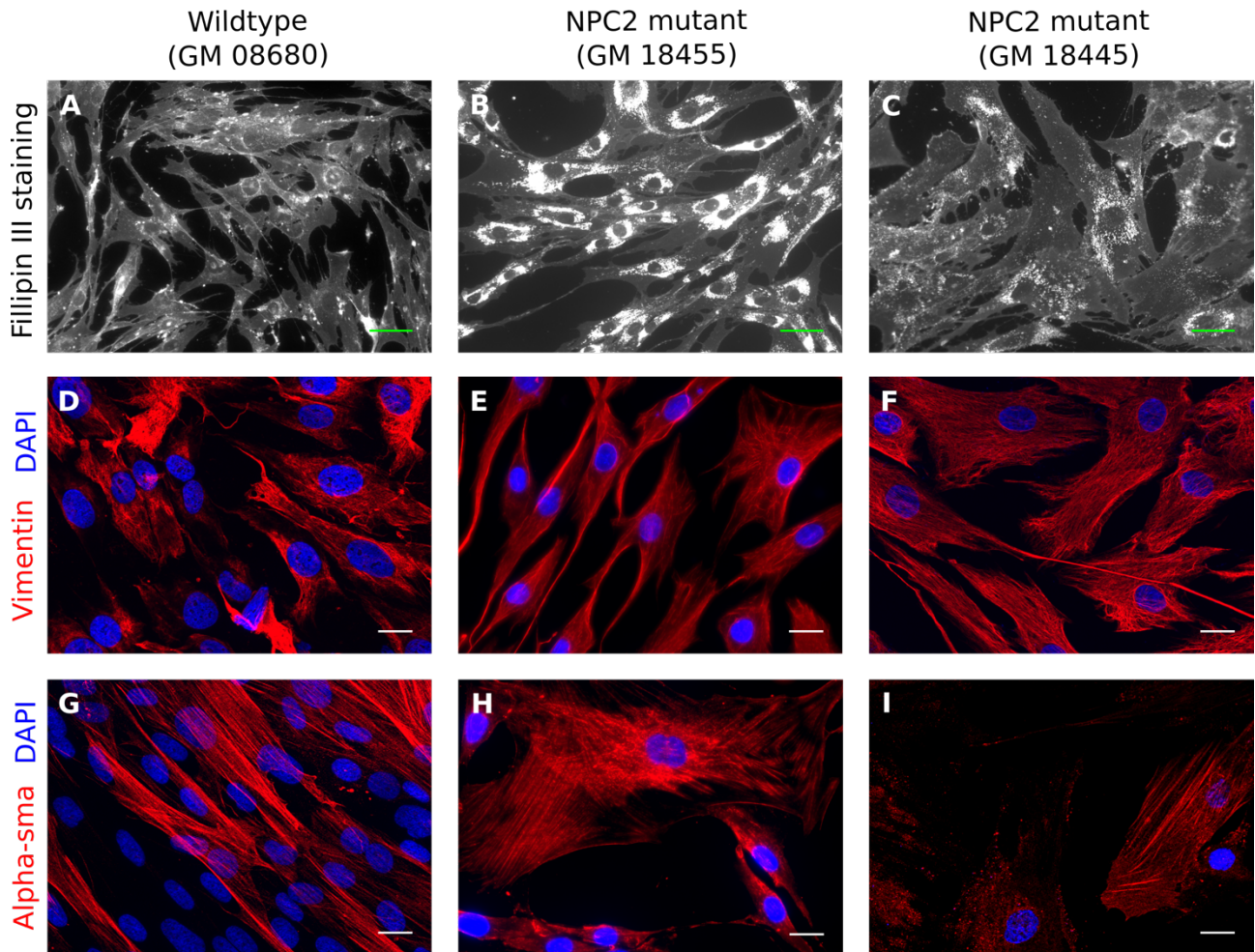


Figure 19. Characterization of wildtype (GM08680) and NPC2 mutant (GM18455 and GM18445) human skin fibroblasts. **A-C:** Filipin III staining of cholesterol, with cholesterol shown in white. Green scale bar 50 μ m. **D-F:** Immunocytochemical staining of vimentin with DAPI nucleostaining. **G-I:** Immunocytochemical staining of alpha-SMA with DAPI nuclei staining. White scale bar 25 μ m.

5.5 NPC2 Replacement Assays

The included GM18455 NPC2 mutant fibroblasts were initially treated with extracellular bNPC2 as a positive control. Filipin III staining of cholesterol in these, compared to wildtype and untreated NPC2 mutant fibroblasts is shown in Figure 20. Addition of extracellular bNPC2 resulted in a markedly reduced cholesterol accumulation similar to the level seen in healthy wildtype fibroblasts, see Figure 20. These results demonstrate that the cholesterol accumulations observed in untreated NPC2 mutant fibroblasts can be reversed by the addition of extracellular NPC2 protein.

As mentioned previously, extracellular NPC2 protein is transported into the cells via the CI-M6PR pathway, making CI-M6PR expression essential for successful extracellular NPC2 replacement. To confirm the capability of the included fibroblast cell lines to conduct extracellular NPC2 uptake, relative CI-M6PR gene expression was examined by RT-qPCR. For estimation of relative gene expression, the stability of six different potential reference genes was initially examined across all fibroblast cDNA samples prepared for RT-qPCR. As equal concentrations of cDNA were used in all RT-qPCR reactions, Ct values were compared directly for evaluation of the reference gene stability. As seen in Figure 21A, the Ct values obtained from RT-qPCR reactions with ZNF5 and GOLGA1 displayed the least variation across all samples, based on the standard deviation. Thus, these two genes were used as reference genes for calculation of relative gene expression in the included fibroblasts. The relative gene expression of CI-M6PR was examined for both wildtype fibroblasts,

untreated GM18455 NPC2 mutant fibroblasts and GM18455 NPC2 mutant fibroblasts treated with extracellular bNPC2 protein. As seen in Figure 21B, CI-M6PR is expressed in all examined conditions. The relative CI-M6PR gene expression in untreated NPC2 mutant fibroblasts seemed to be slightly increased compared to the relative CI-M6PR gene expression in wildtype fibroblasts, however no statistical significant difference was observed between the two included cell types supporting a possible comparison between these. The relative CI-M6PR gene expression in bNPC2 treated mutant fibroblasts showed to be statistical significantly increased when compared to the relative CI-M6PR expression in wildtype fibroblasts, which could be caused by some positive feedback mechanism. However, such conclusions cannot be made from the experiments included in this thesis.

NPC2 mutant fibroblasts were treated with conditioned medium from RBECs and HeLa cells genetically modified to secrete mNPC2-OFPSpark. Filipin III staining of NPC2 mutant fibroblasts treated with conditioned medium from genetically modified HeLa cells, including a non-modified HeLa control, is seen in Figure 22. The Filipin III staining revealed a markedly reduced cholesterol accumulation in nearly all cells as a result of treatment with conditioned medium from both genetically modified HeLa cells and non-modified HeLa controls. It is therefore impossible to evaluate the effect of recombinant mNPC2-OFPSpark protein, present in the conditioned medium from genetically modified cells as a result of the gene modifications, based on these results. The lowest proportion of NPC2 mutant fibroblasts with clear cholesterol accumulations was immediately seen in NPC2 mutant fibroblasts treated with conditioned medium from virally transduced HeLa cells. However, the Filipin III staining does not allow for any quantitative comparisons.

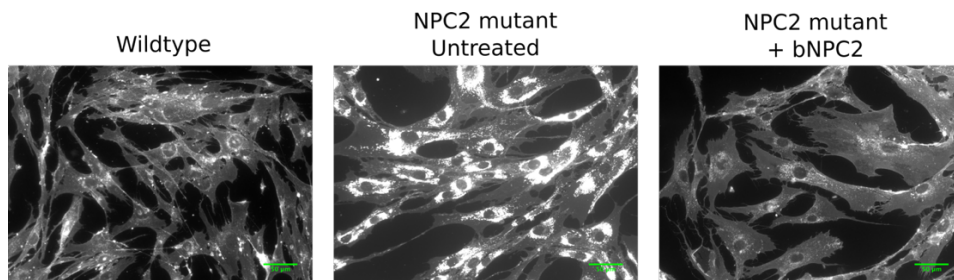


Figure 20. Filipin III staining of cholesterol in wildtype (GM08680) and NPC2 mutant (GM18455) human skin fibroblasts untreated and treated with 10µg/mL bNPC2 added to the medium for 48 hours.

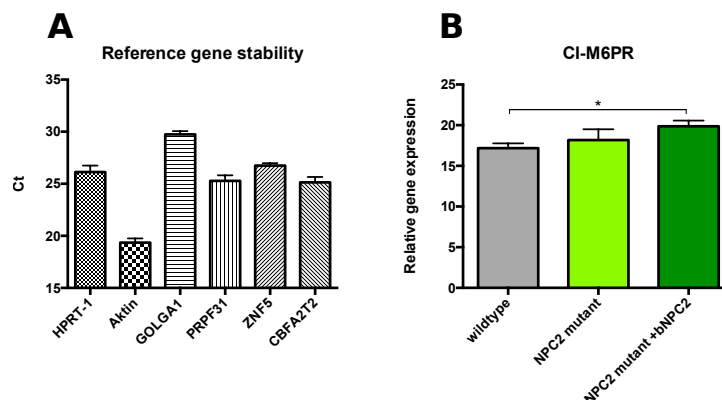


Figure 21. A: Reference gene stability in human skin fibroblast samples expressed as cycle threshold (Ct) values from qPCR (mean±SD). The smallest variation was seen for ZNF5 (26,75±0,23) and GOLGA1 (29,75±0,31) B: Relative CI-M6PR expression in wildtype (GM08680) and GM18455 NPC2 mutant fibroblasts with or without 10µg/mL bNPC2 added to the medium. Differences between the relative gene expression in wildtype, NPC2 mutant and NPC2 mutant +bNPC2 was examined with Kruskal Wallis test with Dunn's multiple comparison test (*P-value <0.05).

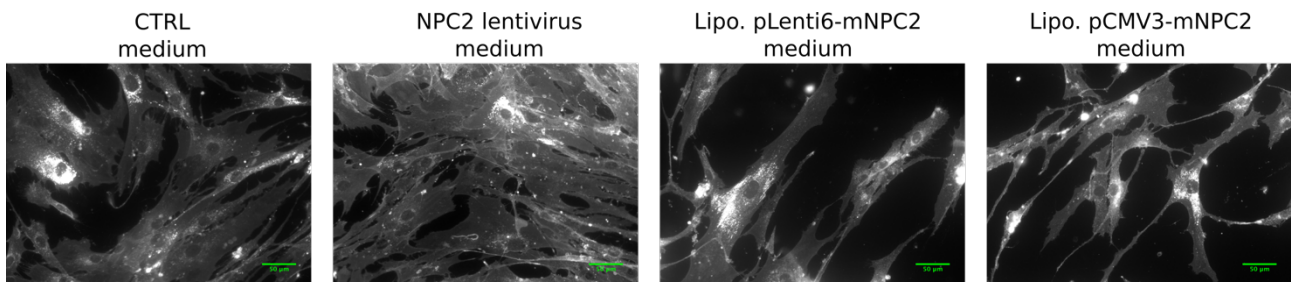


Figure 22. Filipin III staining of NPC2 mutant (GM18455) human skin fibroblasts treated with conditioned medium from genetically modified HeLa cells. CTRL medium is conditioned medium from non-modified HeLa cell controls. NPC2 lentivirus medium represents conditioned medium from HeLa cells genetically modified with NPC2 lentivirus, while Lipo.pLenti6-mNPC2 medium and Lipo.pCMV3-mNPC2 medium represents conditioned medium from HeLa cells genetically modified with pLenti6-mNPC2-OFPSpark-V5 and pCMV3-mNPC2-OFPSpark, respectively.

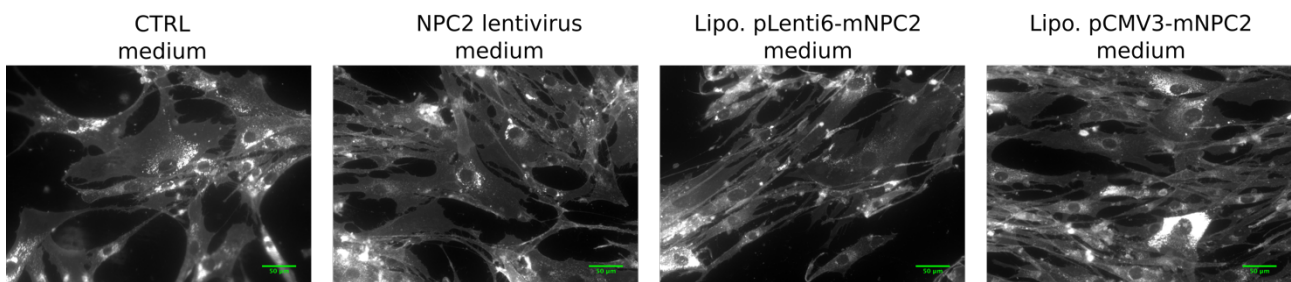


Figure 23. Filipin III staining of NPC2 mutant (GM18455) human skin fibroblasts treated with conditioned medium from genetically modified RBECs in monoculture. CTRL medium is conditioned medium from non-modified RBEC monoculture controls. NPC2 lentivirus medium represents conditioned medium from RBECs in monoculture, genetically modified with NPC2 lentivirus, while Lipo.pLenti6-mNPC2 medium and Lipo.pCMV3-mNPC2 medium represents conditioned medium from RBECs in monoculture genetically modified with pLenti6-mNPC2-OFPSpark-V5 and pCMV3-mNPC2-OFPSpark, respectively.

Filipin III staining of NPC2 mutant fibroblasts treated with conditioned medium from genetically modified RBECs in monocultures revealed similar tendencies as those seen for NPC2 mutant fibroblasts treated with conditioned medium from genetically modified HeLa cells, see Figure 23. Again, a reduced cholesterol accumulation was observed in all cases, including the treatment with conditioned medium from non-modified RBEC monoculture controls, making an evaluation of the effect of recombinant mNPC2-OFPSpark, secreted as a result of the gene modifications, difficult. Treatment with conditioned medium from genetically modified RBECs in monoculture appears to result in complete reversal of the cholesterol accumulations in some cells, while no cells with complete reversal of the cholesterol accumulation were observed among NPC2 mutant fibroblasts treated with conditioned medium from non-modified RBECs in monoculture. However, a quantitative comparison based on the Filipin III staining is practically impossible, as mentioned previously.

Filipin III staining of NPC2 mutant fibroblasts treated with conditioned medium from genetically modified RBECs in co-culture is shown in Figure 24. Again, a clear reduction in cholesterol accumulation is seen in all NPC2 mutant fibroblasts treated with conditioned medium from the bottom chamber of the co-cultures, representing the brain side of the BBB, including the non-modified RBEC controls. However, the Filipin III staining of NPC2 mutant fibroblasts treated with conditioned RBEC medium from the upper chamber of the co-cultures, representing the blood side of the BBB, revealed a difference between the NPC2 mutant fibroblasts treated with conditioned medium from genetically modified and non-modified RBECs in co-culture. While a complete reversal of cholesterol accumulation was observed in almost all NPC2 mutant fibroblasts treated with conditioned medium from the top chamber of genetically modified RBECs in co-culture, regardless of the gene modification approach, a reduced but still visible cholesterol accumulation was observed in all NPC2 mutant fibroblasts treated with conditioned medium from the top chamber of non-

modified RBECs in co-culture. Hence, the recombinant mNPC2-OFPSpark protein secreted as a result of gene modification of RBECs in co-culture does seem to induce a further reduction of cholesterol accumulation in NPC2 mutant fibroblasts. However, no clear conclusions can be made regarding the direction of mNPC2-OFPSpark secretion due to the missing difference between the Filipin III staining of NPC2 mutant fibroblasts treated with conditioned medium from the bottom chamber of genetically modified and non-modified RBECs in co-culture.

In addition to the Filipin III staining of cholesterol, the effect on gene regulation in NPC2 mutant fibroblasts, treated with extracellular NPC2, was examined. The main purpose of this was to investigate the possibility of using a more quantitative measure of the effect of NPC2 replacement. As some lysosomal genes have previously been found to be up-regulated in lysosomal storage diseases, the relative gene expression of Lamp1 and MCOLN1 was investigated by RT-qPCR in wildtype human skin fibroblasts, untreated NPC2 mutant fibroblasts and NPC2 mutant fibroblasts treated with bNPC2 protein added to the medium. As seen in Figure 25A, no statistical differences were found between the relative Lamp1 expression in the included fibroblasts even though the relative gene expression seemed to be increased in NPC2 mutant fibroblasts compared to wildtype fibroblasts. However, the relative gene expression of MCOLN1 was found to be statistical significantly increased in untreated NPC2 mutant fibroblasts compared to wildtype fibroblasts, see Figure 25B. In addition to that, the relative gene expression of MCOLN1 seems to decrease as a result of 48 hours of treatment with extracellular bNPC2, however not statistical significant.

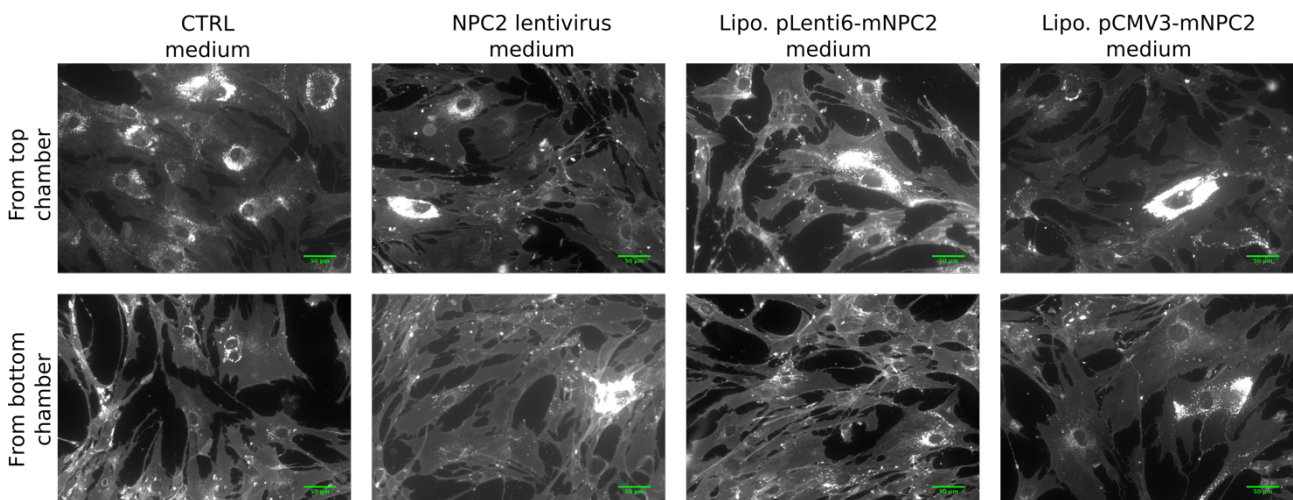


Figure 24. Filipin III staining of NPC2 mutant (GM18455) human skin fibroblasts treated with conditioned medium from the top and bottom chamber of genetically modified RBECs in co-culture. CTRL medium is conditioned medium from non-modified RBEC co-culture controls. NPC2 lentivirus medium represents conditioned medium from RBECs in co-culture, genetically modified with NPC2 lentivirus, while Lipo. pLenti6-mNPC2 medium and Lipo.pCMV3-mNPC2 medium represents conditioned medium from RBECs in co-culture genetically modified with pLenti6-mNPC2-OFPSpark-V5 and pCMV3-mNPC2-OFPSpark, respectively.

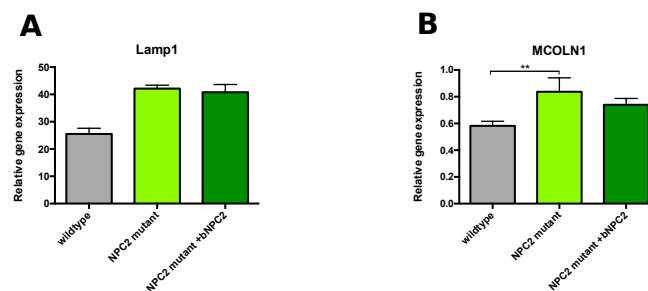


Figure 25. Relative gene expression of Lamp1 and MCOLN1 in wildtype (GM08680) and NPC2 mutant (GM18455) human skin fibroblasts. Data are presented as median with interquartile range and differences between wildtype, NPC2 mutant and NPC2 mutant treated with bNPC2 was tested with Kruskal-Wallis test with Dunn's multiple comparison test (**P-value<0.01).

6 Discussion

In the following section, results from this study will be discussed and compared to results of other studies. Furthermore, future perspectives will be discussed in relation to other relevant studies.

6.1 Production of NPC2 Lentiviral vectors

The NPC2 expression vira were generally produced with relatively low titers. According to the manufacturer's protocol, the Lentiviral expression kit should yield viral titers ranging from 100.000 TU/mL to 500.000 TU/mL (100). Furthermore, reviews on viral gene therapy report that lentiviral vectors can be produced with titers of 10^6 and even 10^9 (42,56). This could be caused by a number of different reasons. First of all, unsuccessful cloning could have affected the yield of NPC2 lentivira. However, the sequencing used for verification of cloned plasmids showed complete alignment to the theoretical sequence of the cloned plasmids used for NPC2 lentivirus production, indicating that the relatively low titers were due to other factors.

The size of the gene inserted into the viral vector also might affect the production of vira as the titer has previously been found to decrease with increasing insert size (41). The NPC2-OFPSpark sequence inserted in the viral vector in this study was 1137 bp which is far from the maximum loading capacity of 5.6 kb specified in the manufacturer's protocol (100). However, previous unpublished experiences with the Lentiviral expression kit from Laboratory of Immunology and Laboratory of Neurobiology at Aalborg University have shown similar titers with a different insert of approximately the same size and higher titers with a different insert of approximately half the size of the insert used in this study. The size of the insert used in this study hence might have decreased the titers of produced NPC2 expression lentivirus, even though it is far from the maximum loading capacity specified in the manufacturer's protocol (100).

In addition, the efficiency of co-transfection of HEK-293 FT cells with cloned NPC2 lentiviral expression plasmid and supplied mix of packaging plasmids could have affected the production of NPC2 lentivira and the following titrations of these. Production of NPC2 lentivirus would only take place in HEK-293 FT cells which were successfully co-transfected with all plasmids, including the constructed NPC2 expression plasmid and three different packaging plasmids. However, the Packaging Mix, containing the three different packaging plasmids had been used several times before this study. Hence, several freeze-thaw cycles might have caused some degree of degradation, resulting in a lower concentration of the plasmids needed for the production of lentivirus (101). Furthermore, a large variation was observed between the titers of different NPC2 lentivirus batches. This could be explained by variations in the viability of the HEK 293 FT cells prior to the production of NPC2 lentivirus, which can affect the transfection efficiency. All HEK-293 FT cells were thawed from vials of the same cell stock, cultured under geneticin selection for an equally long time, and seeded at the same density prior to production of NPC2 lentivira, which served to increase the reproducibility. However, small variations might still have affected the viability of the HEK 293FT cells, which would, in turn, affect the production of NPC2 lentivirus.

Another reason for the variation between titers of the different virus batches could be variation in the efficiency of the transduction of HeLa cells with produced NPC2 lentivirus. HeLa cells used for titration of NPC2 lentiviruses were seeded at the same density prior to viral titrations, but contrary to the HEK 293 FT cells used for production of NPC2 lentivira, the HeLa cells were not necessarily cultured for an equally long time or taken from the same cell stock, which might have caused differences in the viability and thus transduction efficiencies. Standardising the culturing of HeLa cells prior to titrations might thus be a way to improve the reproducibility of the titration of viruses. Another approach could be to base the titration on the presence of lentiviral DNA in transduced cells 96 hours post-transduction measured by qPCR, as suggested by Barczak et al. (102). This way the number of transduced cells could be measured more directly than the estimation based on colony

formation under antibiotic selection. Furthermore, this would represent a less time-consuming method for titration. However, small variations between titers of different lentiviral stocks can never be completely eliminated, hence production of larger batches would be favourable for future studies.

6.2 Lentiviral Gene Modification of Rat Brain Endothelial Cells

A lentiviral vector was chosen for the gene modification of BCECs due to previously reported higher efficiency compared to non-viral approaches as well as the ability of lentivirus to infect non-dividing cells. However, both the immunocytochemical staining and flow cytometry analysis showed very low lentiviral modification efficiencies at the same level as those observed for non-viral modifications in RBECs. In HeLa cells the lentiviral gene modification efficiency was even lower than the non-viral gene modification efficiencies, indicating that the low lentiviral efficiency was not cell type specific. In addition to a generally low lentiviral gene modification efficiency in this study, a statistical significant difference was observed when comparing the efficiency of the two different non-viral gene modifications. These were carried out using either pLenti6-mNPC2-OFPSpark-V5, used for production of lentivirus, or pCMV3-mNPC2-OFPSpark, containing a different expression vector backbone. As the two plasmids used for non-viral gene modifications were both designed to induce expression of the exact same protein, the observed difference in transfection efficiency must be due to differences in the expression vector backbone containing the enhancer and promoter regions, which are some of the main features affecting the level of gene expression (41,42). Both plasmids contain the CMV promoter and enhancer, see Figure 7. However, the length of the CMV enhancer sequence differs between the two plasmids, with the pCMV3-mNPC2-OFPSpark containing the longest CMV enhancer sequence. Thus, the observed difference in non-viral gene modification efficiencies for RBECs in monoculture indicates that the pLenti6/V5-D-TOPO expression vector backbone is associated with a reduced gene expression, possibly caused by a shorter CMV enhancer sequence. As the lentiviral gene modifications are based on the same expression vector backbone, the lentiviral modification efficiencies observed in this study might hence not represent the full potential of the lentiviral approach. Previous unpublished experiences with lentiviral gene modifications, based on the pLenti6/V5-D-TOPO expression vector backbone, in different setups by the Laboratory of Immunology and Laboratory of Neurobiology at Aalborg university showed similar problems with reduced gene expression, ultimately resulting in terminating the use of this vector backbone in both cases, which further supports that this vector backbone is associated with a reduced gene expression. Neither the CMV enhancer or CMV promoter regions were fully sequenced during the sequence verification as the sequencing primers used for this was only designed to investigate the insertion of the mNPC2-OFPSpark sequence. Thus, it is not possible to confirm that the CMV promoter and enhancer sequences, of the pLenti6/V5-D-TOPO expression vector backbone, are in fact identical to the theoretical sequence provided with the kit.

Furthermore, while the CMV promoter is one of the most commonly used as it is considered as one of the most powerful promoters in many cell types, it might not always be the most optimal choice for efficient gene expression (41,103–105). Variations in CMV directed gene expression has been observed in multiple studies including a possible silencing of the CMV promoter following transduction, especially with lentiviral vectors (41,103,106). Hence, reduced CMV promoter activity might also be an explanation of the low lentiviral gene modification efficiency observed in this study. Nevertheless, non-viral gene modification with the pLenti6-mNPC2-OFPSpark-V5 did induce gene expression to a similar level as the non-viral gene modification with pCMV3-mNPC2-OFPSpark in HeLa cells, indicating that the low lentiviral gene modification efficiency was associated with the viral approach rather than the promoter activity, in this case. Either because of a cell-specific reduction in promoter activity that did not apply to HeLa cells or because of lentiviral gene modification specific features affecting the efficiency. While the pseudotyping of lentiviral vector

with the VSV-G capsid allows for production with high titers, the VSV-G protein has been shown to excite transient cytotoxicity in mammalian cells lines, which could have affected the lentiviral gene modification efficiencies in general in this study (67,107). Another factor which might have reduced the lentiviral gene modification efficiency was the use of undiluted lentiviral stock for transductions as a result of the low lentiviral titers. The lentiviral stock was consisting of HEK 293-FT culture medium which had already been used in HEK 293-FT cultures for 72 hours during virus production leading to a decreased concentration of nutrients, while the concentration of cell waste products would have increased. This might have resulted in compromised cell culture conditions which could decrease the transgene expression.

Furthermore, the use of undiluted lentiviral stock could probably explain the large variation observed for the lentiviral gene modification efficiency due to the large variation in lentiviral titers, as the number of lentiviral vector particles per cell, often referred to as the Multiplicity of Infection (MOI), differed depending on the lentiviral batch used for transduction. The MOI is obviously affecting the gene modification efficiency and a varying MOI was probably the main reason for the observed variation in lentiviral gene modification efficiency in this study. The use of undiluted viral stock in this study corresponded to a MOI between 0.1 and 0.7 for RBECs and 0.4 and 3.7 for HeLa cells (see Appendix I), which might, in addition to varying gene modification efficiencies, have contributed to the low lentiviral gene modification efficiencies observed in this study (100,108). These complications could have been avoided by concentrating the produced lentiviral using ultracentrifugation (109). However, this was not possible at the beginning of this study as no ultracentrifuge was available from the biosafety class 2 certified areas, required for lentiviral work. Yet, purification and concentration of produced lentiviral vectors are considered as a necessary optimization step for future experiments to ensure removal of potentially limitations factors of the used medium as well the possibility of increasing and standardizing the MOI.

Few other studies have been focusing on transduction of BCECs, instead of attempting to cross them (9). Furthermore, the efficiency of transduction is not always measured or might be assessed differently in different studies, which compromises a comparison between studies. While a number of studies have investigated the efficiency of lentiviral transduction of vascular endothelial cells from different tissues, many of these focus on the development of endothelial cells targeted lentiviral vectors rather than the unspecific VSV-G pseudotyped lentiviral vector used in this study (110–113). In one study, focusing on the development of a primary human endothelial cell dual-targeted lentiviral vector, Pariente et al. used an unspecific VSV-G pseudotyped lentiviral vector for comparison of different endothelial specific promoters and showed a 40-60% efficiency when transducing human umbilical vein endothelial cells (HUVECs) at a MOI at 1-5 (110). Another study, also focusing on the development of cell specific lentiviral vectors, observed a 68% efficiency when transducing HUVECs with an unspecific VSV-G pseudotyped lentiviral vector at a MOI at 1 (113). In a third study, VSV-G pseudotyped lentiviral vectors are reported to induce transgene expression in 63% of primary liver endothelial cells at a MOI at 3 (111). All of these studies demonstrate a markedly higher lentiviral transduction efficiency when transducing endothelial cells than what was observed in this study. However, in all of these studies the transductions were done at a 3 to 15-fold higher MOI than what was the case in this study. Sakoda et al. examined the correlation between MOI and transduction efficiency in a study comparing the efficiency of lentiviral vectors to adenoviral and retroviral vectors for transduction of primary bovine aortic endothelial cells (112). They observed an exponentially increasing lentiviral transduction efficiency with increased MOI from approximately 5% at a MOI at 1 to almost 100 % at a MOI at 50 (112). These results are actually corresponding to the efficiencies of lentiviral transduction of RBECs in this study, which were done at MOIs below 1 and resulted in efficiencies of 3.55% and 2.37% for RBECs in mono- and co-cultures, respectively.

In addition to that, none of these studies examined the mitotic activity at the time of transduction, which have previously been found to affect the lentiviral transduction efficiency (108). Naldini et al. demonstrated a decrease in transfection efficiency when inducing cell cycle arrest in G0 phase, which is consistent with the observed difference in lentiviral transduction efficiency of RBECs and HeLa cells observed in this study (108). The RBEC co-culture model used in this study, have previously been demonstrated to exhibit no or very little mitotic activity at the time during which gene modifications took place (10). Thus, the higher lentiviral transductions efficiencies reported in the other studies could also be partially caused by a higher mitotic activity.

The non-viral transfection efficiency observed in this study from modification of RBECs with pCMV3-mNPC2-OFPSpark was lower than what was previously observed from transfection of RBECs with a similar non-viral vector (10). Larsen et al. demonstrated non-viral transfection efficiencies of 27.74% and 8.41 % for RBECs in mono- and co-cultures, respectively (30). However, the experimental setups differed slightly from this study, which could be the reason for these differences. In the study by Larsen et al. transgene expression was assessed 24 hours post modifications and presented as mean efficiencies, while the transgene expression was assessed 48 hours post modifications in this study and presented as median efficiencies. Furthermore, small variations in RBEC viability and mitotic activity could have affected the transfection efficiencies, as the non-viral transfection efficiencies are strongly associated with the rate of cell division, which was demonstrated by the pronounced difference between the transfection efficiency in RBECs and HeLa observed in both this study and the study by Larsen et al. (10). The non-viral transfection efficiencies observed in HeLa cells in this study did, on the other hand, approximately correspond to those observed from non-viral transfection of HeLa cells by Larsen et al. (10).

6.3 Possibly Stable Long-term Expression Following Lentiviral Gene Modification

In addition to the investigated gene modification efficiencies based on the gene expression 48 hours post modification, a smaller setup was used to investigate the potential long-term transgene expression. Even though it is not possible to make any general conclusions based on this small setup, the clear difference between the change in transgene expression, following lentiviral and non-viral gene modification of HeLa cells, does point towards a higher long-term gene expression as a result of lentiviral gene modification, compared to non-viral gene modification. The observed drop in transgene expression following non-viral gene modification can be explained by the loss of delivered genetic material during the nuclear disassembly at cell division, which can further explain why the difference is most evident in the HeLa cells, which are rapidly dividing due to their malignancy (114). However, this is prevented by the integration into the host cell genome following lentiviral gene modifications, which explains the more stable transgene expression observed in HeLa cell genetically modified with lentivirus. These preliminary results thus point towards a possibly stable long-term transgene expression following lentiviral gene modification which would be both interesting and highly relevant to investigate further in a larger setup. In a previous study, Mao et al. found a stable transgene expression for up to 9 weeks following *in vitro* lentiviral transfection of HEK 293FT cells (115). Moreover, Sakoda et al. observed a slight initial decrease in transgene expression following *in vitro* lentiviral transduction of primary bovine aortic endothelial cells, which stabilised after 10 passages and stayed higher than transgene expression following both retroviral and adenoviral transduction (112). In addition to that, Blömer et al. were able to show stable transgene expression for more than 6 months following injections of lentiviral vectors into the striatum and hippocampus in rats and Biffi et al. were able to demonstrate lentiviral mediated transgene expression in Metachromatic leukodystrophy patients 2 years after transplantation with transduced hematopoietic stem cells (116,117). Thus, the stable long-term transgene expression following lentiviral

transduction, indicated by the results of this study would be in agreement with previous findings from both *in vitro* and *in vivo* studies (112,115–117).

6.4 Intact *in vitro* Blood-Brain-Barrier Integrity Following Lentiviral Gene Modification

Neither ZO-1 expression nor TEER measurements 48 hours post gene modifications showed signs of *in vitro* BBB disruption following gene modifications. When comparing the TEER reductions 24 hours post gene modifications, as the percentage of the TEER measured before gene modifications, RBECs genetically modified with lentivirus did, however, show a statistically significantly larger TEER reduction than the non-modified RBECs. As described previously, the medium was changed on cells, genetically modified with lentivirus, 24 hours post modification to remove lentivirus particles. The larger TEER reduction observed 24 hours post modification for these cells could, therefore, be caused by the medium change. However, the influence of the medium change was initially examined on non-modified RBECs during which no difference in TEER was observed as a result of medium change 48 hours post barrier induction, compared to cells with no medium change, see Appendix II. Instead, the reduction in TEER might be due to the fact that more than 50 % of the RBEC medium was replaced with lentiviral stock during the 24 hours of lentiviral gene modification of these cells. As described previously, the lentiviral stock consisted of used medium which might have compromised the cell culture conditions during these 24 hours due to decreased nutrient concentrations and increased concentrations of cell waste products. Furthermore, the lentiviral stock was based on culture medium prepared for HEK 293-FT cells, which lacks several reagents important for optimal RBEC culturing. These different medium compositions hence could have either influenced the TEER measurement directly or indirectly as a result of compromised RBEC culture conditions, which also explains why no difference is observed between the TEER measurements 48 hours post modifications. Furthermore, the TEER measurements stayed above the $150 \Omega \cdot \text{cm}^2$ threshold throughout the entire experiment in all situations, which is in agreement with previous results from transfection of a similar *in vitro* BBB model based on RBECs (10).

No permeability analyses were included in this study, even though it would have improved the evaluation of the *in vitro* BBB integrity. However, the *in vitro* BBB model used in this study had previously been characterized by passive permeability to radiolabeled D-Mannitol (182 Da) which showed that the low apparent permeability was seen at $150 \Omega \cdot \text{cm}^2$ after which higher TEER did not result in a further decrease in permeability (30). A similar correlation between TEER measurements and passive permeability was therefore assumed to take place in this study. The passive permeability was highly relevant in this study in order to exclude that both lentiviral and non-viral gene modification vectors and secreted recombinant NPC2 could not cross the barrier passively. However, passive permeability to NPC2 (16,6 kDa) was not expected as the TEER stayed above $150 \Omega \cdot \text{cm}^2$ throughout the entire experiment. Permeability to the lentiviral and non-viral gene modification vectors could have caused the gene modification vectors to cross the endothelial cell layer and induce gene modification of the astrocytes seeded in the bottom chamber rather than the RBECs. This could have been examined by a immunocytochemical staining and flow cytometric analysis of the astrocytes, similar to those applied to genetically modified RBECs and HeLa cells. However, this was not expected at TEER values above $150 \Omega \cdot \text{cm}^2$.

Furthermore, it could have been relevant to analyse whether the recombinant NPC2 secreted from genetically modified cells could cross the BBB via transcytosis, as this would be very important for the evaluation of the direction of recombinant NPC2 secretion, essential for the evaluation of the proposed strategy of protein delivery to the CNS through BCEC gene modification. This could have been tested by adding a known concentration of NPC2 to either the top or bottom chamber followed by a quantification of the NPC2 concentration in the opposite chamber. The NPC2 concentration

could have been quantified by an enzyme-linked immunosorbent assay (ELISA), however, acquisition of a NPC2 specific ELISA-kit was not possible within the limits of this study. Nevertheless, NPC2 have previously been observed not to be able to cross the BBB in an *in vivo* study (91). Therefore, NPC2 transcytosis was not expected to take place in this study.

6.5 Reversed Cholesterol Accumulation in NPC2 Mutant Fibroblasts Following Addition of Conditioned Medium from both Genetically Modified and Non-Modified Cells

Filipin III staining of cholesterol was used to assess the therapeutic effect of NPC2 replacement in NPC2 mutant fibroblast based on mNPC2-OFPSpark secreted from genetically modified RBECs and HeLa cells, as positive controls. However, a marked reduction in cholesterol accumulations was observed as a result of treatment with conditioned medium from non-modified cells, which makes the evaluation of the therapeutic effect of mNPC2-OFPSpark secreted as a result of the gene therapy more or less impossible. The reduction in cholesterol accumulations observed as a result of treatment with conditioned medium from non-modified cells could be caused by an endogenous NPC2 protein secretion from these cells, as both the RBECs and HeLa cells possess the normal NPC2 gene. This could have been further investigated by measuring the NPC2 concentrations in conditioned medium from both genetically modified and non-modified cells with an ELISA, but as mentioned previously this was not possible within the limits of this study.

In a previous study, Naureckiene et al. examined the treatment of NPC2 mutant fibroblasts with conditioned medium from Chinese hamster ovary (CHO) cells genetically modified to express recombinant NPC2 (69). Contrary to the observations in this study, they did not observe any therapeutic effect from treatment with conditioned medium from non-modified CHO cells. However, in the study by Naureckiene et al. only 0.3 % conditioned medium was added to the fibroblast culture medium, which was enough to see a therapeutic effect of the conditioned medium from genetically modified CHO cells. Dilution of the conditioned medium thus may have reduced the concentration of endogenous NPC2 secreted by non-modified CHO cells to a level below the minimal NPC2 concentration required for a therapeutic effect, allowing for an evaluation of the effect of recombinant NPC2. They also tried to increase the percentage of conditioned medium to 10 %, which resulted in a partial reversal of the cholesterol accumulation in NPC2 mutant fibroblasts treated with conditioned medium from non-modified CHO cells. The results from Naureckiene et al. therefore indicates a relatively high natural secretion of endogenous NPC2.

In a different study, Larsen et al. examined the recombinant protein secretion from RBECs in co-cultures, following transfection with a non-viral vector similar to the one used for transfection with pCMV3-mNPC2-OFPSpark in this study, with a slightly higher transfections efficiency (10). They measured a secretion from transfected RBECs corresponding to recombinant proteins concentrations of 1.5ng/mL and 0.13ng/mL in the medium from top and bottom chambers, respectively, which is far below the 10 µg/mL of bNPC2 used for reversal of cholesterol accumulation in the present study. With a relatively high natural secretion of endogenous NPC2, it would therefore be very difficult to estimate the effect of recombinant NPC2 secreted by a small proportion of genetically modified RBECs, compared to non-modified RBEC controls. It is therefore most likely that the reversed cholesterol accumulations observed in this study are caused by an endogenous NPC2 secretion from the RBECs. Nevertheless, it is uncertain whether a lower concentration than the 10 µg/mL could induce a similar effect, as the minimal NPC2 concentration required for a therapeutic effect was not investigated in this study.

A modest difference between the therapeutic effect of treatment with conditioned medium from genetically modified and non-modified cells could only be observed in NPC2 mutant fibroblasts treated with conditioned medium from the top chamber of RBECs in co-culture, representing the

blood side of the in vitro BBB model. Although it is practically impossible to make any quantitative conclusions based on the Filipin III staining of cholesterol, this difference does indicate that the recombinant mNPC2-OFPRSpark protein secreted as a result of the gene modification is functional. Furthermore, this could indicate a relatively lower secretion of endogenous NPC2 from RBECs with induced BBB properties, which would only be visible in the medium from the top chamber, as the medium from the bottom chamber would also contain endogenous NPC2 secreted from astrocytes. However, this needs to be further investigated to be able to make any clear conclusions, and one way to do this could be by simply genetically modifying the NPC2 mutant fibroblasts, as a reversed cholesterol accumulation, in this case, could only be a result of the expression of the recombinant NPC2 protein.

No conclusions could be made regarding the direction of secretion from RBECs in co-culture based, which is considered as a crucial point of evaluation for the proposed strategy of protein delivery to the CNS through BCEC gene modification. Thus, further studies of the direction of secretion of recombinant protein are still needed. This could have been examined in this setup by measuring the concentration of secreted mNPC2-OFPSpark protein in the top and bottom chambers with an ELISA.

6.6 Potential Quantitative Evaluation of the Therapeutic Effect of NPC2 Replacement Based on Relative Lysosomal Gene Expression

The relative expression of lysosomal genes was examined by RT-qPCR in NPC2 mutant fibroblasts with or without NPC2 replacement therapy in order to investigate the possibility of evaluating the effect of NPC2 replacement therapy quantitatively at the gene level. Yet, this only revealed a statistically significantly increased expression of MCOLN1 in untreated NPC2 mutant fibroblasts compared to wildtype. However, the relative expression of Lamp1 also seemed to be increased in untreated NPC2 mutant fibroblasts compared to wildtype fibroblasts and moreover, the relative gene expression of MCOLN1 seems to decrease as a result of 48 hours of treatment with extracellular bNPC2 but not to a statistically significant level in this study. The lack of statistical significance might be a result of a very small sample size in this experiment. However, the results of the relative gene expression of especially MCOLN1 indicates an up-regulation of lysosomal genes in NPC2, which might be normalized by treatment with extracellular NPC2 protein, indicating a possibility of using this as a quantitative measure of the effect of NPC2 replacement enabling a more systematic comparison of therapeutic effects. It could, therefore, be interesting to investigate this further, by including more lysosomal genes in a larger setup with more biologic samples. Furthermore, the duration of the NPC2 replacement therapy could be varied as it is uncertain how fast a possible downregulation of the lysosomal gene expression could be measured by RT-qPCR. Sardiello et al. examined the regulation of biogenesis and found that the expression of a lysosomal genes was regulated by TFEB as TFEB overexpression resulted in varying degrees of overexpression of 23 different lysosomal genes, including Lamp1 and MCOLN1 (84). Furthermore, they were able to demonstrate an activation of TFEB in response to induced lysosomal storage by translocation of TFEB from the cytoplasm to the cell nucleus. A similar tendency could be observed in embryonic fibroblasts from three different LSD mouse models, in which TFEB was primarily located within the nucleus, while a cytoplasmic localization was observed in wildtype mouse fibroblasts, indicating a constant activation of TFEB in LSDs. They also examined the direct effect on lysosomal gene expression following induced lysosomal storage and found the MCOLN was markedly increased, consistent with the observed increase in MCOLN1 expression in untreated NPC2 mutant fibroblasts in this study, while Lamp1 was not included in that analysis. Furthermore, they observed a continuously increase in MCOLN1 expression up to 100 hours following induced lysosomal storage (84). They did not observe whether the increase could be reversed by reversing the lysosomal storage, but the continuous increase for 100 hours following lysosomal storage could indicate that reversal of

the MCOLN1 expression to a normal level would take more than the 48 hours investigated in this study. Thus, the reduction in MCOLN1 gene expression observed 48 hours post NPC2 replacement in this study could probably have been even increased to a significant level with a prolonged incubation following NPC2 replacement.

6.7 Future Perspectives – From *in vitro* to *in vivo*

In this study, the possibility of genetically modifying BCECs to secrete protein, in order to circumvent the CNS drug delivery limitations caused by the BBB, was investigated in an *in vitro* model. However, the findings in this study cannot be directly translated to the *in vivo* situation for which reason *in vivo* studies are undoubtedly needed for further evaluation of this strategy. Nevertheless, there are still several variables which could preferably be clarified in the *in vitro* situation before moving to *in vivo* studies.

First of all, the secretion direction from genetically modified BCECs needs to be further investigated, as this is considered absolutely crucial for the proposed strategy. While secretion to the brain side of the BBB is obviously crucial to ensure delivery to the CNS, secretion to the blood side could represent potential side effects of the treatment depending on the protein secreted. In the case of Niemann-Picks disease type C2, a bidirectional secretion would be considered advantageous, as it would have the potential of treating both the CNS and visceral related symptoms. Even though *in vitro* studies of the direction of secretion might not fully represent the *in vivo* situation, it still offers the advantage of enabling a relatively simple quantification of the ratio of secretion of transgene to the blood and brain side of the BBB. Previous studies have shown some controversy regarding the main secretory direction, as mentioned in the introduction (10,13). In the study by Larsen et al. they used the *in vitro* BBB model mimicking the *in vivo* situation most closely and found a primary secretion to the blood side following non-viral transfection of BCECs (10). However, it is unsure whether this would also be the case, when using a viral vector to induce the secretion of a different protein.

Furthermore, an increased transduction efficiency would be preferred in order to ensure BCEC secretion throughout the entire CNS. It should therefore be investigated whether addition of a higher concentration of viral vectors, to increase the MOI and thereby transduction efficiency, would cause a different effect on the BBB integrity than what was observed in this study. This could also advantageously be investigated initially *in vitro* to limit the use of animals.

In addition to that, the choice of promoter should probably be reconsidered due to the possibility of silencing of the CMV promoter (41,103,106). As mentioned previously, the activity of different promoter might differ in different tissues and while several different promoters have been used for gene modification of endothelial cells, no systematic comparison regarding the efficiency of these has been made, which complicates the choice of an optimal promoter for long-term expression in BCECs (9). In a recent study by Körbelin et al. they saw transgene expression in the majority of genetically modified BCECs *in vivo* using the hybrid CMV/ β -actin (CAG) promoter (12). Yet, in this study, the delivery of genetic material was done using an AAV vector, which does not induce integration. It is therefore uncertain whether the same results could be achieved when using lentiviral vector which does induce integration. However, the results from Körbelin et al. and others have demonstrated promising long-term episomal transgene expressions following AAV mediated gene transfer, especially in slowly or non-dividing cells (12,58,118). It should therefore be considered whether the lentiviral approach is still the most preferable as the integration does include a risk of mutagenesis in addition to the potential long-term expression, which is not the case for AAV vectors (42).

When moving to *in vivo* studies it would additionally be very important to consider the biodistribution of the viral vector following systemic injections. Both lentiviral and AAV vectors

have been found to accumulate in especially liver tissue following systemic injection, with the potential to induce hepatocellular carcinomas (12,15,119–121). Therefore, different attempts have been made to alter the natural tropism of the viral surface, including the insertion of ligands or phage selected peptides or *in vivo* screening of random virus display peptide libraries (15,122,123). In the study by Körbelin et al. they examined the targeting specificity of an AAV2 vector developed from *in vivo* screening of a random AAV2 peptide library and found an efficient and brain endothelial cell specific transgene expression following intravenous administration in mice (12). They were able to demonstrate a 1,000-fold higher transgene expression in brain tissue than in liver tissue following intravenous administration of their AAV2 vector, with the transgene expression in liver being practically invisible with *in vivo* luminescence imaging, while the transgene expression in brain was clearly visible. Compared to a wildtype AAV2 vector, they could observe a 650-fold higher transgene expression in brain following intravenous administration of the brain endothelial specific AAV2 vector, which stayed at the same level throughout an observation period of more than 660 days. Furthermore, transgene expression induced by the specific AAV2 vector co-localised with the endothelial cell marker CD3, indicating that the targeting was BCEC specific (12). Combined with the preferable safety profile of AAV vectors, the BCEC specific AAV2 vector examined by Körbelin et al. thus may represent a promising gene therapy vector candidate for future *in vivo* studies of the NPC2 replacement therapy, based on secretion from genetically modified BCECs, which was investigated in the present study. However, Körbelin et al. did not examine the secretion from genetically modified BCECs following transduction with their BCEC specific AAV2 vector, which would be very interesting as it is considered crucial for the proposed strategy in the present study.

6.8 Other Relevant Applications of the Proposed Strategy

Even though further studies are still required to fully evaluate the proposed strategy of genetically modifying BCECs to secrete proteins to the CNS, the potential applications of this strategy are not restricted to the treatment of NPC2. While NPC2 is a very rare disease, it belongs to a large group of lysosomal storage diseases with a combined incidence of 1:6700 (124). Of these, 75% presents with CNS related symptoms, making the delivery of drugs to the CNS extremely relevant (124). Several of these, including Gaucher's disease, Mucopolysaccharidosis types I, II and VI, and Pompe disease, are caused by deficiency of a soluble protein similar to the situation in NPC2 (78,82). Genetically modifying BCECs to express and secrete soluble protein to the CNS, could therefore represent an effective treatment in several lysosomal storage diseases with slight modification to fit the different diseases (78).

Moreover, further studies of the intracellular mechanisms directing the secretion of recombinant proteins towards either the brain or blood side of the BBB, could be highly relevant with regards to assess the possibilities of manipulating these to a primary secretion towards the CNS. With the possibility of manipulating the direction of secretion, the applications of this strategy could potentially be extended to include several other CNS diseases.

7 Conclusion

The aim of this study was to test the hypothesis that, BCECs could be genetically modified using a viral vector to induce secretion of recombinant NPC2 protein towards both the CNS and the circulation, which could reverse cholesterol accumulations in NPC2 mutant fibroblasts without compromising the BBB integrity in an *in vitro* BBB model. Based on the results from the immunocytochemical staining and flow cytometric analysis of genetically modified cells, it can be concluded that RBECs can be genetically modified using a lentiviral vector to produce recombinant NPC2, however with a relatively low efficiency, which could probably be increased by increasing the MOI and reconsidering the choice of promoter. The lentiviral gene modification additionally seemed to induce a stable long-term expression, compared to non-viral gene modification, in agreement with previous findings. Moreover, it was concluded that the barrier integrity in and *in vitro* BBB model was not compromised by lentiviral gene modification, based on the continuous ZO-1 staining and TEER staying above the 150 $\Omega \cdot \text{cm}^2$ threshold. Based on the Filipin III staining of cholesterol in NPC2 mutant fibroblasts, it was not possible to make any clear conclusions regarding the bidirectional secretion and therapeutic effect of recombinant NPC2 secreted from genetically modified RBECs, probably due to a relatively high natural secretion of endogenous NPC2. However, the treatment of NPC2 mutant fibroblasts with conditioned medium from the top chamber of genetically modified RBECs in co-cultures did indicate a therapeutic effect of recombinant NPC2 secreted from genetically modified cells, in agreement with previous findings. Furthermore, the investigations of the relative expression of lysosomal genes in NPC2 mutant fibroblasts indicated a possible quantitative measure of therapeutic effects based on the relative expression of MCOLN1. However, this needs to be further investigated to be able to make any final conclusions.

8 References

1. Pardridge WM. The blood-brain barrier: bottleneck in brain drug development. *NeuroRx* [Internet]. Am. Soc. for Experimental NeuroTherapeutics; 2005 Jan [cited 2017 Nov 18];2(1):3–14. Available from: <http://www.ncbi.nlm.nih.gov/pubmed/15717053>
2. Daneman R, Zhou L, Kebede AA, Barres BA. Pericytes are required for blood–brain barrier integrity during embryogenesis. *Nature* [Internet]. Nature Publishing Group; 2010 Nov 25 [cited 2017 Nov 18];468(7323):562–6. Available from: <http://www.nature.com/doi/10.1038/nature09513>
3. Abbott NJ, Patabendige AAK, Dolman DEM, Yusof SR, Begley DJ. Structure and function of the blood–brain barrier. *Neurobiol Dis* [Internet]. 2009 [cited 2017 Nov 15];37:13–25. Available from: https://ac-els-cdn-com.zorac.aub.aau.dk/S0969996109002083/1-s2.0-S0969996109002083-main.pdf?_tid=0f3148b4-c9fb-11e7-81cc-00000aacb35d&acdnat=1510746759_1b4a38d614c08620802aec1760f84e87
4. Alvarez JI, Dodelet-Devillers A, Kebir H, Ifergan I, Fabre PJ, Terouz S, et al. The Hedgehog pathway promotes blood-brain barrier integrity and CNS immune quiescence. *Science* [Internet]. American Association for the Advancement of Science; 2011 Dec 23 [cited 2017 Nov 18];334(6063):1727–31. Available from: <http://www.ncbi.nlm.nih.gov/pubmed/22144466>
5. Misje Mathiisen T, Lehre KP, Christian Danbolt N, Petter Ottersen O. The Perivascular Astroglial Sheath Provides a Complete Covering of the Brain Microvessels: An Electron Microscopic 3D Reconstruction. [cited 2017 Nov 18]; Available from: <https://synapseweb.clm.utexas.edu/sites/default/files/synapseweb/files/2010gliamathiisenottesentheperivascastrostheath.pdf>
6. Armulik A, Genové G, Mäe M, Nisancioglu MH, Wallgard E, Niaudet C, et al. Pericytes

- regulate the blood–brain barrier. *Nature* [Internet]. Nature Publishing Group; 2010 Nov 25 [cited 2017 Nov 15];468(7323):557–61. Available from: <http://www.nature.com/doi/10.1038/nature09522>
7. Patel MM, Goyal BR, Bhadada S V, Bhatt JS, Amin AF. Getting into the Brain. *CNS Drugs* [Internet]. Springer International Publishing; 2009 [cited 2017 Nov 18];23(1):35–58. Available from: <http://link.springer.com/10.2165/0023210-200923010-00003>
 8. Pardridge WM. Drug Transport across the Blood–Brain Barrier. *J Cereb Blood Flow Metab* [Internet]. SAGE PublicationsSage UK: London, England; 2012 Nov 29 [cited 2017 Nov 18];32(11):1959–72. Available from: <http://journals.sagepub.com/doi/10.1038/jcbfm.2012.126>
 9. Assmann JC, Körbelin J, Schwaninger M. Genetic manipulation of brain endothelial cells in vivo. *Biochim Biophys Acta - Mol Basis Dis* [Internet]. Elsevier B.V.; 2016;1862(3):381–94. Available from: <http://linkinghub.elsevier.com/retrieve/pii/S0925443915003002>
 10. Larsen AB, Andresen TL, Aigner A, Thomsen LB, Moos T. Transfection of primary brain capillary endothelial cells for protein synthesis and secretion of recombinant erythropoietin: a strategy to enable protein delivery to the brain. *Cell Mol Life Sci* [Internet]. 2017 [cited 2017 Oct 19];74:2467–85. Available from: <https://link.springer.com/content/pdf/10.1007%2Fs00018-017-2501-5.pdf>
 11. Tajes M, Ramos-Fernández E, Weng-Jiang X, Bosch-Morató M, Guivernau B, Eraso-Pichot A, et al. The blood-brain barrier: Structure, function and therapeutic approaches to cross it. *Mol Membr Biol* [Internet]. 2014;31(5):152–67. Available from: <http://www.tandfonline.com/doi/full/10.3109/09687688.2014.937468>
 12. Körbelin J, Dogbevia G, Michelfelder S, Ridder DA, Hunger A, Wenzel J, et al. A brain microvasculature endothelial cell-specific viral vector with the potential to treat neurovascular and neurological diseases. *EMBO Mol Med* [Internet]. EMBO Press; 2016 Jun 1 [cited 2017 Nov 18];8(6):609–25. Available from: <http://www.ncbi.nlm.nih.gov/pubmed/27137490>
 13. Jiang C, Koyabu N, Yonemitsu Y, Shimazoe T, Watanabe S, Naito M, et al. In Vivo Delivery of Glial Cell-Derived Neurotrophic Factor Across the Blood–Brain Barrier by Gene Transfer into Brain Capillary Endothelial Cells. *Hum Gene Ther* [Internet]. 2003 [cited 2017 Nov 18];14:1181–91. Available from: <http://online.liebertpub.com.zorac.aub.aau.dk/doi/pdf/10.1089/104303403322168019>
 14. Thomsen LB, Lichota J, Kim KS, Moos T. Gene delivery by pullulan derivatives in brain capillary endothelial cells for protein secretion. *J Control Release* [Internet]. Elsevier; 2011 Apr 10 [cited 2017 Nov 18];151(1):45–50. Available from: <http://www.sciencedirect.com.zorac.aub.aau.dk/science/article/pii/S0168365911000058>
 15. Chen YH, Chang M, Davidson BL. Unique molecular signatures of disease brain endothelia provide - a novel site for CNS-directed enzyme therapy. 2011;15(10):1215–8.
 16. Abbott NJ, Rönnbäck L, Hansson E. Astrocyte–endothelial interactions at the blood–brain barrier. *Nat Rev Neurosci* [Internet]. Nature Publishing Group; 2006 Jan 1 [cited 2017 Nov 18];7(1):41–53. Available from: <http://www.nature.com/doi/10.1038/nrn1824>
 17. Butt AM, Jones HC, Abbott NJ. Electrical resistance across the blood-brain barrier in anaesthetized rats: a developmental study. *J Physiol* [Internet]. 1990 Oct 1 [cited 2017 Nov 18];429(1):47–62. Available from: <http://doi.wiley.com/10.1113/jphysiol.1990.sp018243>
 18. Liu W-Y, Wang Z-B, Zhang L-C, Wei X, Li L. Tight Junction in Blood-Brain Barrier: An Overview of Structure, Regulation, and Regulator Substances. *CNS Neurosci Ther* [Internet]. Blackwell Publishing Ltd; 2012 Aug 1 [cited 2017 Nov 15];18(8):609–15. Available from: <http://doi.wiley.com/10.1111/j.1755-5949.2012.00340.x>

19. Wolburga H, Lippoldt A. Tight junctions of the blood–brain barrier: development, composition and regulation. *Vascul Pharmacol* [Internet]. Elsevier; 2002 Jun 1 [cited 2017 Nov 18];38(6):323–37. Available from: <http://www.sciencedirect.com.zorac.aub.aau.dk/science/article/pii/S1537189102002008>
20. Lecrux C, Hamel E. The neurovascular unit in brain function and disease. *Acta Physiol* [Internet]. Blackwell Publishing Ltd; 2011 Sep 1 [cited 2017 Nov 18];203(1):47–59. Available from: <http://doi.wiley.com/10.1111/j.1748-1716.2011.02256.x>
21. Nakagawa S, Deli MA, Kawaguchi H, Shimizudani T, Shimono T, Kittel Á, et al. A new blood–brain barrier model using primary rat brain endothelial cells, pericytes and astrocytes. *Neurochem Int* [Internet]. Pergamon; 2009 Mar 1 [cited 2017 Nov 18];54(3–4):253–63. Available from: <http://www.sciencedirect.com.zorac.aub.aau.dk/science/article/pii/S0197018608001976>
22. Perrière N, Yousif S, Cazaubon S, Chaverot N, Bourasset F, Cisternino S, et al. A functional in vitro model of rat blood–brain barrier for molecular analysis of efflux transporters. *Brain Res* [Internet]. Elsevier; 2007 May 30 [cited 2017 Nov 18];1150:1–13. Available from: <http://www.sciencedirect.com.zorac.aub.aau.dk/science/article/pii/S0006899307004027>
23. Burek M, Salvador E, Förster CY. Generation of an immortalized murine brain microvascular endothelial cell line as an in vitro blood brain barrier model. *J Vis Exp* [Internet]. MyJoVE Corporation; 2012 Aug 29 [cited 2017 Nov 18];(66):e4022. Available from: <http://www.ncbi.nlm.nih.gov/pubmed/22951995>
24. Wuest DM, Lee KH. Optimization of endothelial cell growth in a murine in vitro blood-brain barrier model. *Biotechnol J* [Internet]. Wiley-Blackwell; 2012 Mar [cited 2017 Nov 18];7(3):409–17. Available from: <http://www.ncbi.nlm.nih.gov/pubmed/22095877>
25. Franke H, Galla H-J, Beuckmann CT. An improved low-permeability in vitro-model of the blood–brain barrier: transport studies on retinoids, sucrose, haloperidol, caffeine and mannitol. *Brain Res* [Internet]. Elsevier; 1999 Feb 6 [cited 2017 Nov 18];818(1):65–71. Available from: <http://www.sciencedirect.com.zorac.aub.aau.dk/science/article/pii/S0006899398012827>
26. Patabendige A, Skinner RA, Abbott NJ 2013. Establishment of a simplified in vitro porcine blood–brain barrier model with high transendothelial electrical resistance. *Brain Res* [Internet]. Elsevier; 2013 Jul 12 [cited 2017 Nov 18];1521:1–15. Available from: <http://www.sciencedirect.com.zorac.aub.aau.dk/science/article/pii/S0006899312011432>
27. Gaillard P, Voorwinden L, Nielsen J, Ivanov A, Atsumi R, Engman H, et al. Establishment and functional characterization of an in vitro model of the blood–brain barrier, comprising a co-culture of brain capillary endothelial cells and astrocytes. *Eur J Pharm Sci* [Internet]. Elsevier; 2001 Jan 1 [cited 2017 Nov 18];12(3):215–22. Available from: <http://www.sciencedirect.com.zorac.aub.aau.dk/science/article/pii/S0928098700001238>
28. Bernas MJ, Cardoso FL, Daley SK, Weinand ME, Campos AR, Ferreira AJG, et al. Establishment of primary cultures of human brain microvascular endothelial cells to provide an in vitro cellular model of the blood-brain barrier. *Nat Protoc* [Internet]. Nature Publishing Group; 2010 Jul 10 [cited 2017 Nov 18];5(7):1265–72. Available from: <http://www.nature.com/doi/10.1038/nprot.2010.76>
29. Helms HC, Abbott NJ, Burek M, Cecchelli R, Couraud P-O, Deli MA, et al. In vitro models of the blood–brain barrier: An overview of commonly used brain endothelial cell culture models and guidelines for their use. *J Cereb Blood Flow Metab* [Internet]. SAGE PublicationsSage UK: London, England; 2016 May 11 [cited 2017 Nov 18];36(5):862–90. Available from: <http://journals.sagepub.com/doi/10.1177/0271678X16630991>
30. Larsen AB, Thomsen LB, Thomsen MS, Lichota J, Fazakas C, Krizbai I, et al. Transfection

of brain capillary endothelial cells in primary culture with defined blood–brain barrier properties. *Fluids Barriers CNS* [Internet]. 2015 [cited 2017 Oct 19];12. Available from: <https://fluidsbarrierscns.biomedcentral.com/track/pdf/10.1186/s12987-015-0015-9?site=fluidsbarrierscns.biomedcentral.com>

31. Arthur F, Shivers R, Bowman P. Astrocyte-mediated induction of tight junctions in brain capillary endothelium: an efficient in vitro model. *Dev Brain Res* [Internet]. Elsevier; 1987 Nov 1 [cited 2017 Nov 18];36(1):155–9. Available from: <http://www.sciencedirect.com.zorac.aub.aau.dk/science/article/pii/0165380687900757?via%3Dihub>
32. Nakagawa S, Deli MA, Nakao S, Honda M, Hayashi K, Nakaoka R, et al. Pericytes from Brain Microvessels Strengthen the Barrier Integrity in Primary Cultures of Rat Brain Endothelial Cells. *Cell Mol Neurobiol* [Internet]. Springer US; 2007 Sep 20 [cited 2017 Nov 18];27(6):687–94. Available from: <http://link.springer.com/10.1007/s10571-007-9195-4>
33. Helms HC, Waagepetersen HS, Nielsen CU, Brodin B. Paracellular Tightness and Claudin-5 Expression is Increased in the BCEC/Astrocyte Blood–Brain Barrier Model by Increasing Media Buffer Capacity During Growth. *AAPS J* [Internet]. Springer US; 2010 Dec 22 [cited 2017 Nov 18];12(4):759–70. Available from: <http://www.springerlink.com/index/10.1208/s12248-010-9237-6>
34. Wilhelm I, Fazakas C, Krizbai IA. In vitro models of the blood-brain barrier. *Methods Mol Biol*. 2011;814:431–49.
35. Rubin LL, Hall DE, Porter S, Barbu K, Cannon C, Horner HC, et al. A cell culture model of the blood-brain barrier. *J Cell Biol* [Internet]. Rockefeller University Press; 1991 Dec 15 [cited 2017 Nov 18];115(6):1725–35. Available from: <http://www.ncbi.nlm.nih.gov/pubmed/1661734>
36. Bendfeldt K, Radojevic V, Kapfhammer J, Nitsch C. Basic Fibroblast Growth Factor Modulates Density of Blood Vessels and Preserves Tight Junctions in Organotypic Cortical Cultures of Mice: A New In Vitro Model of the Blood–Brain Barrier. *J Neurosci* [Internet]. Society for Neuroscience; 2007 Oct 8 [cited 2017 Nov 18];23(27):9254–62. Available from: <http://www.ncbi.nlm.nih.gov/pubmed/14534260>
37. Weidenfeller C, Schrot S, Zozulya A, Galla H. Murine brain capillary endothelial cells exhibit improved barrier properties under the influence of hydrocortisone. *Brain Res* [Internet]. Elsevier; 2005 Aug 16 [cited 2017 Nov 18];1053(1–2):162–74. Available from: <http://www.sciencedirect.com.zorac.aub.aau.dk/science/article/pii/S000689930500942X>
38. Förster C, Waschke J, Burek M, Leers J, Drenckhahn D. Glucocorticoid effects on mouse microvascular endothelial barrier permeability are brain specific. *J Physiol* [Internet]. Blackwell Publishing Ltd; 2006 Jun 1 [cited 2017 Nov 18];573(2):413–25. Available from: <http://doi.wiley.com/10.1113/jphysiol.2006.106385>
39. Hoheisel D, Nitz T, Franke H, Wegener J, Hakvoort A, Tilling T, et al. Hydrocortisone Reinforces the Blood–Brain Barrier Properties in a Serum Free Cell Culture System. *Biochem Biophys Res Commun* [Internet]. Academic Press; 1998 Mar 6 [cited 2017 Nov 18];244(1):312–6. Available from: <http://www.sciencedirect.com.zorac.aub.aau.dk/science/article/pii/S0006291X97980517>
40. Srinivasan B, Kolli AR, Esch MB, Abaci HE, Shuler ML, Hickman JJ. TEER Measurement Techniques for In Vitro Barrier Model Systems. *J Lab Autom*. 2015;
41. Gan Y, Zheng J, Stetler RA, Cao G. Gene delivery with viral vectors for cerebrovascular diseases. 2015;347(6224):882–6.
42. Choudhury SR, Hudry E, Maguire CA, Sena-Esteves M, Breakefield XO, Grandi P. Viral vectors for therapy of neurologic diseases. 2017 [cited 2017 Nov 15]; Available from:

https://ac-els-cdn-com.zorac.aub.aau.dk/S002839081630048X/1-s2.0-S002839081630048X-main.pdf?_tid=d642b890-ca4e-11e7-8dc8-00000aacb362&acdnat=1510782741_75185d982c866737b348a0ec93a00650

43. Pathak A, Patnaik S, Gupta KC. Recent trends in non-viral vector-mediated gene delivery. *Biotechnol J* [Internet]. WILEY-VCH Verlag; 2009 Nov 1 [cited 2017 Nov 18];4(11):1559–72. Available from: <http://doi.wiley.com/10.1002/biot.200900161>
44. Alvarez-Erviti L, Seow Y, Yin H, Betts C, Lakhani S, Wood MJA. Delivery of siRNA to the mouse brain by systemic injection of targeted exosomes. *Nat Biotechnol* [Internet]. Nature Research; 2011 Apr 20 [cited 2016 Jul 28];29(4):341–5. Available from: <http://www.nature.com/doi/10.1038/nbt.1807>
45. Saraiva J, Nobre RJ, Pereira de Almeida L. Gene therapy for the CNS using AAVs: The impact of systemic delivery by AAV9. *J Control Release*. 2016;241:94–109.
46. Davidson BL, Breakefield XO. Neurological diseases: Viral vectors for gene delivery to the nervous system. *Nat Rev Neurosci* [Internet]. Nature Publishing Group; 2003 May 1 [cited 2017 Nov 18];4(5):353–64. Available from: <http://www.nature.com/doi/10.1038/nrn1104>
47. Barcia C, Jimenez-Dalmaroni M, Kroeger KM, Puntel M, Rapaport AJ, Larocque D, et al. One-year Expression From High-capacity Adenoviral Vectors in the Brains of Animals With Pre-existing Anti-adenoviral Immunity: Clinical Implications. *YMTHE* [Internet]. 2007 [cited 2017 Nov 18];15:2154–63. Available from: https://ac-els-cdn.com/S1525001616327319/1-s2.0-S1525001616327319-main.pdf?_tid=bb7d8fe4-cc92-11e7-909d-00000aacb360&acdnat=1511031804_4a860d08c9e6c17006e9577ea711a6b1
48. Wood M, Charlton H, Wood K, Kajiwarra K, Byrnes A. Immune responses to adenovirus vectors in the nervous system. *Trends Neurosci* [Internet]. Elsevier Current Trends; 1996 Nov 1 [cited 2017 Nov 18];19(11):497–501. Available from: <http://www.sciencedirect.com.zorac.aub.aau.dk/science/article/pii/S0166223696100606>
49. Dubensky TW. (Re-)Engineering tumor cell-selective replicating adenoviruses: A step in the right direction toward systemic therapy for metastatic disease. *Cancer Cell* [Internet]. Cell Press; 2002 May 1 [cited 2017 Nov 18];1(4):307–9. Available from: <http://www.sciencedirect.com/science/article/pii/S1535610802000624>
50. Byrnes AP, MacLaren RE, Charlton HM. Immunological instability of persistent adenovirus vectors in the brain: peripheral exposure to vector leads to renewed inflammation, reduced gene expression, and demyelination. *J Neurosci* [Internet]. Society for Neuroscience; 1996 May 1 [cited 2017 Nov 18];16(9):3045–55. Available from: <http://www.ncbi.nlm.nih.gov/pubmed/8622134>
51. Wilson JM. Lessons learned from the gene therapy trial for ornithine transcarbamylase deficiency The Phase I Gene Therapy Clinical Trial for OTCD. *Mol Genet Metab* [Internet]. 2009 [cited 2017 Nov 16];96:151–7. Available from: [http://www.mgmjournal.com/article/S1096-7192\(08\)00499-X/pdf](http://www.mgmjournal.com/article/S1096-7192(08)00499-X/pdf)
52. Chioocca EA, Choi BB, Cai WZ, DeLuca NA, Schaffer PA, DiFiglia M, et al. Transfer and expression of the lacZ gene in rat brain neurons mediated by herpes simplex virus mutants. *New Biol* [Internet]. 1990 Aug [cited 2017 Nov 18];2(8):739–46. Available from: <http://www.ncbi.nlm.nih.gov/pubmed/2178004>
53. Diefenbach RJ, Miranda-Saksena M, Douglas MW, Cunningham AL. Transport and egress of herpes simplex virus in neurons. *Rev Med Virol* [Internet]. John Wiley & Sons, Ltd.; 2008 Jan 1 [cited 2017 Nov 18];18(1):35–51. Available from: <http://doi.wiley.com/10.1002/rmv.560>
54. Sena-Esteves M, Saeki Y, Fraefel C, Breakefield XO. HSV-1 amplicon vectors simplify

- and versatility. *Rev Mol Ther* [Internet]. 2000 [cited 2017 Nov 18];2(1). Available from: <http://www.idealibrary.com>
55. Spaete RR, Frenkel N. The herpes simplex virus amplicon: a new eucaryotic defective-virus cloning-amplifying vector. *Cell* [Internet]. Elsevier; 1982 Aug 1 [cited 2017 Nov 18];30(1):295–304. Available from: <http://www.ncbi.nlm.nih.gov/pubmed/6290080>
 56. Costantini LC, Bakowska JC, Breakefield XO, Isacson O. Gene therapy in the CNS. *Gene Ther* [Internet]. Nature Publishing Group; 2000 Jan 8 [cited 2017 Nov 18];7(2):93–109. Available from: <http://www.nature.com/articles/3301119>
 57. Bessis N, GarciaCozar FJ, Boissier M-C. Immune responses to gene therapy vectors: influence on vector function and effector mechanisms. *Gene Ther* [Internet]. Nature Publishing Group; 2004 Oct 29 [cited 2017 Nov 18];11(S1):S10–7. Available from: <http://www.nature.com/articles/3302364>
 58. Leone P, Shera D, McPhee SWJ, Francis JS, Kolodny EH, Bilaniuk LT, et al. Long-term follow-up after gene therapy for canavan disease. *Sci Transl Med* [Internet]. NIH Public Access; 2012 Dec 19 [cited 2017 Nov 18];4(165):165ra163. Available from: <http://www.ncbi.nlm.nih.gov/pubmed/23253610>
 59. Xiao W, Chirmule N, Berta SC, McCullough B, Gao G, Wilson JM. Gene therapy vectors based on adeno-associated virus type 1. *J Virol* [Internet]. American Society for Microbiology (ASM); 1999 May [cited 2017 Nov 18];73(5):3994–4003. Available from: <http://www.ncbi.nlm.nih.gov/pubmed/10196295>
 60. Urabe M, Ding C, Kotin RM. Insect Cells as a Factory to Produce Adeno-Associated Virus Type 2 Vectors. *Hum Gene Ther* [Internet]. 2002 [cited 2017 Nov 18];13:1935–43. Available from: <http://online.liebertpub.com.zorac.aub.aau.dk/doi/pdf/10.1089/10430340260355347>
 61. Calcedo R, Vandenberghe LH, Gao G, Lin J, Wilson JM. Worldwide Epidemiology of Neutralizing Antibodies to Adeno-Associated Viruses. *Source J Infect Dis* [Internet]. 2009 [cited 2017 Nov 23];199(3):381–90. Available from: <http://www.jstor.org/stable/40254430>
 62. Boutin S, Monteilhet V, Veron P, Leborgne C, Benveniste O, Franç Oise Montus M, et al. Prevalence of Serum IgG and Neutralizing Factors Against Adeno-Associated Virus (AAV) Types 1, 2, 5, 6, 8, and 9 in the Healthy Population: Implications for Gene Therapy Using AAV Vectors. [cited 2017 Nov 23]; Available from: <http://online.liebertpub.com.zorac.aub.aau.dk/doi/pdf/10.1089/hum.2009.182>
 63. Naldini L. Gene therapy returns to centre stage. *Nature* [Internet]. Nature Publishing Group; 2015 Oct 14 [cited 2017 Nov 18];526(7573):351–60. Available from: <http://www.nature.com/doi/finder/10.1038/nature15818>
 64. Hacein-Bey-Abina S, Kalle C Von, Schmidt M, McCormack MP, Wulffraat N, Leboulch P, et al. LMO2-Associated Clonal T Cell Proliferation in Two Patients after Gene Therapy for SCID. *Source Sci New Ser* [Internet]. 2003 [cited 2017 Nov 18];302(5644):415–9. Available from: <http://www.jstor.org/stable/3835321>
 65. Cattoglio C, Facchini G, Sartori D, Antonelli A, Miccio A, Cassani B, et al. Hot spots of retroviral integration in human CD34² hematopoietic cells. 2007 [cited 2017 Nov 18];110:1770–8. Available from: <http://www.bloodjournal.org.zorac.aub.aau.dk/content/bloodjournal/110/6/1770.full.pdf>
 66. Montini E, Cesana D, Schmidt M, Sanvito F, Ponzoni M, Bartholomae C, et al. Hematopoietic stem cell gene transfer in a tumor-prone mouse model uncovers low genotoxicity of lentiviral vector integration. *Nat Biotechnol* [Internet]. Nature Publishing Group; 2006 Jun 28 [cited 2017 Nov 18];24(6):687–96. Available from: <http://www.nature.com/doi/finder/10.1038/nbt1216>
 67. Burns JC, Friedmann T, Driever W, Burrascano M, Yee J-K, Driever W. Vesicular

- Stomatitis Virus G Glycoprotein Pseudotyped Retroviral Vectors: Concentration to Very High Titer and Efficient Gene Transfer into Mammalian and Nonmammalian Cells. *Source Proc Natl Acad Sci United States Am Genet* [Internet]. 1993 [cited 2017 Nov 20];90(90):8033–7. Available from: <http://www.jstor.org/stable/2362959>
68. Ashtari N, Jiao X, Rahimi-Balaei M, Amiri S, E. Mehr S, Yeganeh B, et al. Lysosomal Acid Phosphatase Biosynthesis and Dysfunction: A Mini Review Focused on Lysosomal Enzyme Dysfunction in Brain. *Curr Mol Med* [Internet]. 2016 Jun 20 [cited 2016 Sep 23];16(5):439–46. Available from: <http://www.eurekaselect.com/openurl/content.php?genre=article&issn=1566-5240&volume=16&issue=5&spage=439>
 69. Naureckiene S, Sleat DE, Lackland H, Fensom A, Vanier MT, Wattiaux R, et al. Identification of HE1 as the Second Gene of Niemann-Pick C Disease. *Source Sci New Ser* [Internet]. 2000 [cited 2017 Nov 18];290(5500):2298–301. Available from: <http://www.jstor.org/stable/3081713>
 70. Vanier MT, Millat G. Structure and function of the NPC2 protein. *Biochim Biophys Acta - Mol Cell Biol Lipids* [Internet]. 2004 [cited 2017 May 15];1685(1):14–21. Available from: <http://www.sciencedirect.com/science/article/pii/S1388198104001301>
 71. Storch J, Xu Z. Niemann-Pick C2 (NPC2) and intracellular cholesterol trafficking. *Biochim Biophys Acta* [Internet]. NIH Public Access; 2009 Jul [cited 2017 Nov 16];1791(7):671–8. Available from: <http://www.ncbi.nlm.nih.gov/pubmed/19232397>
 72. Vanier MT. Niemann-Pick disease type C Disease definition. *Vanier Orphanet J Rare Dis* [Internet]. 2010 [cited 2017 Nov 16];5. Available from: <http://www.ajrd.com/content/5/1/16>
 73. Vanier M, Millat G. Niemann-Pick disease type C. *Clin Genet* [Internet]. Munksgaard International Publishers; 2003 Sep 15 [cited 2017 Nov 18];64(4):269–81. Available from: <http://doi.wiley.com/10.1034/j.1399-0004.2003.00147.x>
 74. Sleat DE, Wiseman JA, El-Banna M, Price SM, Verot L, Shen MM, et al. Genetic evidence for nonredundant functional cooperativity between NPC1 and NPC2 in lipid transport. *Proc Natl Acad Sci U S A* [Internet]. National Academy of Sciences; 2004 Apr 20 [cited 2017 Nov 18];101(16):5886–91. Available from: <http://www.ncbi.nlm.nih.gov/pubmed/15071184>
 75. Vincent I, Bu B, Erickson RP. Understanding Niemann-Pick type C disease: a fat problem. *Curr Opin Neurol* [Internet]. 2003;16(2):155–61. Available from: http://www.ncbi.nlm.nih.gov/entrez/query.fcgi?cmd=Retrieve&db=PubMed&dopt=Citation&list_uids=12644742
 76. Xu S, Benoff B, Liou H-L, Lobel P, Stock AM. Structural basis of sterol binding by NPC2, a lysosomal protein deficient in Niemann-Pick type C2 disease. *J Biol Chem* [Internet]. NIH Public Access; 2007 Aug 10 [cited 2017 May 16];282(32):23525–31. Available from: <http://www.ncbi.nlm.nih.gov/pubmed/17573352>
 77. Ko DC, Binkley J, Sidow A, Scott MP. The integrity of a cholesterol-binding pocket in Niemann-Pick C2 protein is necessary to control lysosome cholesterol levels. *Proc Natl Acad Sci U S A* [Internet]. National Academy of Sciences; 2003 Mar 4 [cited 2017 May 16];100(5):2518–25. Available from: <http://www.ncbi.nlm.nih.gov/pubmed/12591949>
 78. Sands M, Davidson B. Gene therapy for lysosomal storage diseases. *Mol Ther* [Internet]. Nature Publishing Group; 2006 May [cited 2016 Sep 23];13(5):839–49. Available from: <http://www.nature.com/doifinder/10.1016/j.ymthe.2006.01.006>
 79. Infante RE, Wang ML, Radhakrishnan A, Kwon HJ, Brown MS, Goldstein JL, et al. NPC2 Facilitates Bidirectional Transfer of Cholesterol between NPC1 and Lipid Bilayers, a Step in Cholesterol Egress from Lysosomes. *Source Proc Natl Acad Sci United States Am* [Internet]. 2008 [cited 2017 Nov 18];105(40):15287–92. Available from:

<http://www.jstor.org/stable/25464404>

80. Wang ML, Motamed M, Infante RE, Abi-Mosleh L, Kwon HJ, Brown MS, et al. Identification of surface residues on Niemann-Pick C2 essential for hydrophobic handoff of cholesterol to NPC1 in lysosomes. *Cell Metab* [Internet]. NIH Public Access; 2010 Aug 4 [cited 2017 Jun 13];12(2):166–73. Available from: <http://www.ncbi.nlm.nih.gov/pubmed/20674861>
81. Wraith JE, Baumgartner MR, Bembi B, Covanis A, Levade T, Mengel E, et al. Commentary Recommendations on the diagnosis and management of Niemann-Pick disease type C. *Mol Genet Metab* [Internet]. 2009 [cited 2017 Nov 18];98:152–65. Available from: https://ac-els-cdn-com.zorac.aub.aau.dk/S1096719209001681/1-s2.0-S1096719209001681-main.pdf?_tid=4eba960a-cca0-11e7-a309-00000aacb35e&acdnat=1511037635_a54671bddaa6685f61a94c8262d07ecf
82. Beck M. Therapy for lysosomal storage disorders. *IUBMB Life* [Internet]. Wiley Subscription Services, Inc., a Wiley company; 2009 Jan 1 [cited 2017 Nov 18];62(1):n/a-n/a. Available from: <http://doi.wiley.com/10.1002/iub.284>
83. Palmieri M, Impey S, Kang H, di Ronza A, Pelz C, Sardiello M, et al. Characterization of the CLEAR network reveals an integrated control of cellular clearance pathways. *Hum Mol Genet* [Internet]. Oxford University Press; 2011 Oct 1 [cited 2017 Nov 18];20(19):3852–66. Available from: <https://academic.oup.com/hmg/article-lookup/doi/10.1093/hmg/ddr306>
84. Sardiello M, Palmieri M, di Ronza A, Medina DL, Valenza M, Gennarino VA, et al. A Gene Network Regulating Lysosomal Biogenesis and Function. *Science* (80-). 2009;325(5939).
85. Medina DL, Fraldi A, Bouche V, Annunziata F, Mansueto G, Spanpanato C, et al. Transcriptional activation of lysosomal exocytosis promotes cellular clearance. *Dev Cell* [Internet]. Elsevier; 2011 Sep 13 [cited 2017 Nov 18];21(3):421–30. Available from: <http://www.ncbi.nlm.nih.gov/pubmed/21889421>
86. Cianciola NL, Carlin CR. Adenovirus RID-alpha activates an autonomous cholesterol regulatory mechanism that rescues defects linked to Niemann-Pick disease type C. *J Cell Biol* [Internet]. Rockefeller University Press; 2009 Nov 16 [cited 2017 Dec 1];187(4):537–52. Available from: <http://www.ncbi.nlm.nih.gov/pubmed/19948501>
87. Patterson CM, Walkley US. Niemann-Pick disease, type C and Roscoe Brady. *Mol Genet Metab* [Internet]. Academic Press; 2017 Jan 1 [cited 2017 Nov 18];120(1–2):34–7. Available from: <http://www.sciencedirect.com.zorac.aub.aau.dk/science/article/pii/S1096719216303201>
88. Lim-Melia ER, Kronn DF. Current enzyme replacement therapy for the treatment of lysosomal storage diseases. *Pediatr Ann*. 2009;38(8):448–55.
89. Rohrbach M, Clarke JTR. Treatment of lysosomal storage disorders : progress with enzyme replacement therapy. *Drugs*. 2007;67(18):2697–716.
90. Frantantoni JC, Hall CW, Neufeld EF. Hurler and Hunter Syndromes: Mutual Correction of the Defect in Cultured Fibroblasts. *Source Sci New Ser* [Internet]. 1968 [cited 2017 Nov 18];162(3853):570–2. Available from: <http://www.jstor.org/stable/1724931>
91. Nielsen GK, Dagnaes-Hansen F, Holm IE, Meaney S, Symula D, Andersen NT, et al. Protein replacement therapy partially corrects the cholesterol-storage phenotype in a mouse model of Niemann-Pick type C2 disease. *PLoS One* [Internet]. Public Library of Science; 2011 [cited 2016 Sep 23];6(11):e27287. Available from: <http://www.ncbi.nlm.nih.gov/pubmed/22073306>
92. Friedland N, Liou H-L, Lobel P, Stock AM. Structure of a cholesterol-binding protein deficient in Niemann-Pick type C2 disease. *Proc Natl Acad Sci U S A* [Internet]. National Academy of Sciences; 2003 Mar 4 [cited 2017 May 16];100(5):2512–7. Available from:

<http://www.pubmedcentral.nih.gov/articlerender.fcgi?artid=151372&tool=pmcentrez&render type=abstract>

93. McCauliff LA, Xu Z, Li R, Kodukula S, Ko DC, Scott MP, et al. Multiple surface regions on the Niemann-pick C2 protein facilitate intracellular cholesterol transport. *J Biol Chem*. 2015;290(45):27321–31.
94. Howarth M, Takao K, Hayashi Y, Ting AY. Targeting quantum dots to surface proteins in living cells with biotin ligase. *Proc Natl Acad Sci U S A* [Internet]. National Academy of Sciences; 2005 May 24 [cited 2017 Nov 18];102(21):7583–8. Available from: <http://www.ncbi.nlm.nih.gov/pubmed/15897449>
95. Russell WC, Graham FL, Smiley J, Nairn R. Characteristics of a Human Cell Line Transformed by DNA from Human Adenovirus Type 5. *J Gen Virol* [Internet]. 1977 Jul 1 [cited 2017 Nov 23];36(1):59–72. Available from: <http://www.ncbi.nlm.nih.gov/pubmed/886304>
96. Host-range mutants of adenovirus type 5 defective for growth in HeLa cells. *Virology* [Internet]. Academic Press; 1977 Mar 1 [cited 2017 Nov 23];77(1):319–29. Available from: <http://www.sciencedirect.com.zorac.aub.aau.dk/science/article/pii/0042682277904287?via%3Dihub>
97. Southern PJ, Berg P. Transformation of mammalian cells to antibiotic resistance with a bacterial gene under control of the SV40 early region promoter. *J Mol Appl Genet* [Internet]. 1982 [cited 2017 Nov 23];1(4):327–41. Available from: <http://www.ncbi.nlm.nih.gov/pubmed/6286831>
98. Perrière N, Demeuse P, Garcia E, Regina A, Debray M, Andreux J-P, et al. Puromycin-based purification of rat brain capillary endothelial cell cultures. Effect on the expression of blood-brain barrier-specific properties. *J Neurochem* [Internet]. 2005 Apr [cited 2017 Nov 23];93(2):279–89. Available from: <http://doi.wiley.com/10.1111/j.1471-4159.2004.03020.x>
99. Gaillard PJ, Gerrit De Boer A. Relationship between permeability status of the blood–brain barrier and in vitro permeability coefficient of a drug. *Eur J Pharm Sci* [Internet]. 2000 [cited 2017 Nov 27];12:95–102. Available from: www.elsevier.nl
100. ThermoFisher Scientific. ViraPower™ Lentiviral Expression Systems [Internet]. 2010 [cited 2016 Oct 20]. Available from: <https://www.thermofisher.com/dk/en/home/references/protocols/proteins-expression-isolation-and-analysis/protein-expression-protocol/lentiviral-expression-systems.html>
101. Röder B, Frühwirth K, Vogl C, Wagner M, Rossmann P. Impact of long-term storage on stability of standard DNA for nucleic acid-based methods. *J Clin Microbiol* [Internet]. American Society for Microbiology (ASM); 2010 Nov [cited 2017 Nov 23];48(11):4260–2. Available from: <http://www.ncbi.nlm.nih.gov/pubmed/20810770>
102. Barczak W, Suchorska W, Rubiś B, Kulcenty K. Universal real-time PCR-based assay for lentiviral titration. *Mol Biotechnol* [Internet]. Springer; 2015 Feb [cited 2017 Nov 23];57(2):195–200. Available from: <http://www.ncbi.nlm.nih.gov/pubmed/25370825>
103. Chen P, Tian J, Kovesdi I, Bruder JT. Promoters influence the kinetics of transgene expression following adenovector gene delivery. *J Gene Med* [Internet]. 2008 Feb [cited 2017 Nov 22];10(2):123–31. Available from: <http://doi.wiley.com/10.1002/jgm.1127>
104. Damdindorj L, Karnan S, Ota A, Hossain E, Konishi Y, Hosokawa Y, et al. A Comparative Analysis of Constitutive Promoters Located in Adeno-Associated Viral Vectors. *PLoS One* [Internet]. 2014 [cited 2017 Nov 22];9(8). Available from: <http://journals.plos.org/plosone/article/file?id=10.1371/journal.pone.0106472&type=printable>
105. Smith RL, Traul DL, Schaack J, Clayton GH, Staley KJ, Wilcox ACL. Characterization of

- Promoter Function and Cell-Type-Specific Expression from Viral Vectors in the Nervous System. *J Virol* [Internet]. 2000 [cited 2017 Nov 22];74(23):11254–61. Available from: <http://jvi.asm.org.zorac.aub.aau.dk/content/74/23/11254.full.pdf>
106. Damdindorj L, Karnan S, Ota A, Takahashi M, Konishi Y, Hossain E, et al. Assessment of the long-term transcriptional activity of a 550-bp-long human β -actin promoter region. *Plasmid* [Internet]. 2012 Nov [cited 2017 Nov 22];68(3):195–200. Available from: <http://linkinghub.elsevier.com/retrieve/pii/S0147619X12000807>
 107. Liu M-L, Winther BL, Kay MA. Pseudotransduction of Hepatocytes by Using Concentrated Pseudotyped Vesicular Stomatitis Virus G Glycoprotein (VSV-G)–Moloney Murine Leukemia Virus-Derived Retrovirus Vectors: Comparison of VSV-G and Amphotropic Vectors for Hepatic Gene Transfer. *J Virol* [Internet]. 1996 [cited 2017 Nov 22];70(4):2497–502. Available from: <http://jvi.asm.org/content/70/4/2497.full.pdf>
 108. Naldini L, Blömer U, Gallay P, Ory D, Mulligan R, Gage FH, et al. In Vivo Gene Delivery and Stable Transduction of Nondividing Cells by a Lentiviral Vector. *Source Sci New Ser* [Internet]. 1996 [cited 2017 Nov 21];272(5259):263–7. Available from: <http://www.jstor.org/stable/2889637>
 109. Yee JK, Friedmann T. in *The Development of Human Gene Therapy*. Cold Spring Harb Lab Press Cold Spring Harb NY. 1999;21–45.
 110. Pariente N, Mao S-H, Morizono K, Chen ISY. Efficient targeted transduction of primary human endothelial cells with dual-targeted lentiviral vectors. *J Gene Med* [Internet]. John Wiley & Sons, Ltd.; 2008 Mar 1 [cited 2017 Nov 27];10(3):242–8. Available from: <http://doi.wiley.com/10.1002/jgm.1151>
 111. Abel T, Filali E El, Waern J, Schneider IC, Yuan Q, Unch RC, et al. Specific gene delivery to liver sinusoidal and artery endothelial cells. *Blood* [Internet]. 2013 [cited 2017 Nov 27];122(12):2030–8. Available from: <http://www.bloodjournal.org.zorac.aub.aau.dk/content/bloodjournal/122/12/2030.full.pdf?sso-checked=true>
 112. Sakoda T, Kasahara N, Kedes L, Ohyanagi M. Lentiviral Vector-Mediated Gene Transfer to Endothelial Cells Compared with Adenoviral and Retroviral Vectors. *Prep Biochem Biotechnol* [Internet]. Taylor & Francis Group ; 2007 Jan 18 [cited 2017 Nov 26];37(1):1–11. Available from: <http://www.tandfonline.com/doi/abs/10.1080/10826060601039345>
 113. Anliker B, Abel T, Kneissl S, Hlavaty J, Caputi A, Brynza J, et al. Specific gene transfer to neurons, endothelial cells and hematopoietic progenitors with lentiviral vectors. *Nat Methods* [Internet]. Nature Publishing Group; 2010 Nov 10 [cited 2017 Nov 27];7(11):929–35. Available from: <http://www.nature.com/doi/abs/10.1038/nmeth.1514>
 114. Glover DJ, Lipps HJ, Jans DA. Towards safe, non-viral therapeutic gene expression in humans. *Nat Rev Genet* [Internet]. Nature Publishing Group; 2005 Apr 10 [cited 2017 Nov 22];6(4):299–310. Available from: <http://www.nature.com/doi/abs/10.1038/nrg1577>
 115. Mao Y, Yan R, Li A, Zhang Y, Li J, Du H, et al. Lentiviral Vectors Mediate Long-Term and High Efficiency Transgene Expression in HEK 293T cells. *Int J Med Sci* [Internet]. Ivyspring International Publisher; 2015 [cited 2017 Nov 27];12(5):407–15. Available from: <http://www.ncbi.nlm.nih.gov/pubmed/26005375>
 116. Biffi A, Montini E, Lorioli L, Cesani M, Fumagalli F, Plati T, et al. Lentiviral hematopoietic stem cell gene therapy benefits metachromatic leukodystrophy. *Science* [Internet]. 2013 Aug 23 [cited 2017 Nov 27];341(6148):1233–158. Available from: <http://www.sciencemag.org/cgi/doi/10.1126/science.1233158>
 117. Blömer U, Naldini L, Kafri T, Trono D, Verma IM, Gage FH. Highly Efficient and Sustained Gene Transfer in Adult Neurons with a Lentivirus Vector. *J Virol* [Internet]. 1997 [cited

- 2017 Nov 21];71(9):6641–9. Available from:
<http://jvi.asm.org.zorac.aub.aau.dk/content/71/9/6641.full.pdf>
118. Hadaczek P, Eberling JL, Pivrotto P, Bringas J, Forsayeth J, Bankiewicz KS. Eight years of clinical improvement in MPTP-lesioned primates after gene therapy with AAV2-hAADC. *Mol Ther* [Internet]. Nature Publishing Group; 2010 Aug [cited 2016 Oct 3];18(8):1458–61. Available from: <http://www.ncbi.nlm.nih.gov/pubmed/20531394>
 119. Gray SJ, Woodard KT, Samulski RJ. Viral vectors and delivery strategies for CNS gene therapy. *Ther Deliv* [Internet]. 2010;1(4):517–34. Available from: <http://www.pubmedcentral.nih.gov/articlerender.fcgi?artid=4509525&tool=pmcentrez&rendertype=abstract>
 120. Pan D, Gunther R, Duan W, Wendell S, Kaemmerer W, Kafri T, et al. Biodistribution and Toxicity Studies of VSVG-Pseudotyped Lentiviral Vector after Intravenous Administration in Mice with the Observation of in Vivo Transduction of Bone Marrow. *Mol Ther* [Internet]. Elsevier; 2002 Jul 1 [cited 2017 Nov 26];6(1):19–29. Available from: <http://linkinghub.elsevier.com/retrieve/pii/S1525001602906301>
 121. Donsante A, Vogler C, Muzyczka N, Crawford J, Barker J, Flotte T, et al. Observed incidence of tumorigenesis in long-term rodent studies of rAAV vectors. *Gene Ther* [Internet]. 2001 Sep 11 [cited 2017 Nov 26];8(17):1343–6. Available from: <http://www.ncbi.nlm.nih.gov/pubmed/11571571>
 122. Münch RC, Janicki H, Völker I, Rasbach A, Hallek M, Büning H, et al. Displaying high-affinity ligands on adeno-associated viral vectors enables tumor cell-specific and safe gene transfer. *Mol Ther* [Internet]. American Society of Gene & Cell Therapy; 2013 Jan [cited 2017 Nov 26];21(1):109–18. Available from: <http://www.ncbi.nlm.nih.gov/pubmed/22968478>
 123. Michelfelder S, Kohlschütter J, Skorupa A, Pfennings S, Müller O, Kleinschmidt JA, et al. Successful expansion but not complete restriction of tropism of adeno-associated virus by in vivo biopanning of random virus display peptide libraries. *PLoS One* [Internet]. Public Library of Science; 2009 [cited 2017 Nov 26];4(4):e5122. Available from: <http://www.ncbi.nlm.nih.gov/pubmed/19357785>
 124. Sands MS, Haskins ME. CNS-directed gene therapy for lysosomal storage diseases. *Acta Paediatr* [Internet]. NIH Public Access; 2008 Apr [cited 2017 Nov 24];97(457):22–7. Available from: <http://www.ncbi.nlm.nih.gov/pubmed/18339183>

Appendix I

Calculated Multiplicity Of Infections

Transductions were done by addition of 400 μ L of viral stock to each well or filter containing RBECs or HeLa cells. Both cell types were seeded in filters or wells with a surface area of 1.9 cm^2 .

<i>RBECs</i>	<i>Density (cells/cm²)</i>	<i>Total cells</i>	<i>MOI</i>
	100,000	190,000	0.2
	100,000	190,000	0.3
	100,000	190,000	0.7
	100,000	190,000	0.1
Median			0.2

<i>HeLa cells</i>	<i>Density (cells/cm²)</i>	<i>Total cells</i>	<i>MOI</i>
	20,000	38,000	0.8
	20,000	38,000	1.6
	20,000	38,000	3.7
	20,000	38,000	0.4
Median			1.2

Appendix II

Initial comparisons of TEER measurements in non-modified RBEC co-cultures following medium change

The change in TEER, measured as the percentage of the start value, of RBECs with medium change was compared to the change in TEER, measured as the percentage of the start value, of RBECs without medium change after 24 and 48 hours with the Man-Whitney test. No significant differences were found after 24 or 48 hours.

TEER	Start	24 hours	% Change 24 hours	48 hours	% Change 48 hours
No medium change	325	231	70,95	169	52,12
	322	264	82,04	217	67,44
	309	253	81,98	211	68,32
	426	302	70,99	198	46,45
	376	335	88,98	225	59,98
	376	335	88,98	228	60,58
	505	246	48,82	212	41,94
	432	256	59,43	210	48,70
	477	279	58,50	231	48,47
Medium change	373	220	59,06	166	44,54
	297	175	58,87	151	50,82
	315	209	66,43	209	66,55
	290	190	65,64	155	53,54
	371	206	55,69	171	46,22
	316	197	62,41	180	56,97
	403	223	55,28	250	61,94
	401	229	57,22	197	49,11
	331	248	74,75	237	71,48